UNIVERSIDAD DE CHILE
FACULTAD DE CIENCIAS FíSICAS Y MATEMÁTICAS
DEPARTAMENTO DE INGENIERÍA ELÉCTRICA

DESIGN AND EVALUATION OF DISTRIBUTED CONTROLLERS FOR OPTIMAL DISPATCH AND CONGESTION MANAGEMENT OF MICROGRIDS

TESIS PARA OPTAR AL GRADO DE
DOCTORA EN INGENIERÍA ELÉCTRICA

JACQUELINE DEL ROSARIO LLANOS PROAÑO

PROFESORA GUÍA:
DRA. DORIS SÁEZ HUEICHAPAN

PROFESOR CO-GUÍA:
DR. DANIEL OLIVARES QUERO

MIEMBROS DE LA COMISIÓN:
DR. CESAR AZURDIA MEZA
DR. DANIEL SBÁRBARO HOFER
DR. MATÍAS NEGRETE PINCETIC

SANTIAGO DE CHILE
2020

RESUMEN DE LA TESIS PARA OPTAR
AL TÍTULO DE DOCTORA EN INGENIERÍA ELÉCTRICA
POR: JACQUELINE DEL ROSARIO LLANOS PROAÑO
FECHA: 2020
PROFESORA GUÍA: DRA. DORIS SÁEZ HUEICHAPAN

DESIGN AND EVALUATION OF DISTRIBUTED CONTROLLERS FOR OPTIMAL DISPATCH AND CONGESTION MANAGEMENT OF MICROGRIDS

El uso de micro-redes es una alternativa para la integración de unidades de generación distribuida (GD), incluidas las fuentes de energía renovables. Por lo que el diseño de sistemas de control que garanticen el funcionamiento confiable, seguro y económico de las micro-redes en modo aislado o conectado a la red son necesarios. En este contexto las tareas de control de una micro-red se pueden dividir en 3 niveles: 1) Control Primario que incluye el control de corriente, voltaje y frecuencia de los GDs, 2) Control Secundario, nivel encargado de restaurar frecuencia y voltaje a valores nominales, y 3) Control Terciario encargado del despacho óptimo de la micro-red, coordinación de la microrred con la red principal.

Estos tres niveles de control en un enfoque tradicional operan en diferentes escalas de tiempo, el control primario opera en el orden de los milisegundos, el control secundario en segundos, y el control terciario en minutos y horas. Respecto a los controladores secundario y terciario su arquitectura tradicional de control tiene un enfoque centralizado. Sin embargo, el enfoque centralizado es menos práctico frente a la operación plug-and-play de las unidades de generación distribuida, esto debido a que el algoritmo de control requiere ser modificado. Además, la constante variación de la generación y la demanda puede llevar a sobrecarga o congestión de las líneas, afectando la vida útil de las líneas de distribución y los transformadores en la micro-red, las congestiones provocan la activación de las protecciones eléctricas lo que podría conducir a tener demanda no suministrada. Otro desafío del control de micro-redes está relacionado a las topologías de la red de comunicación, que implica pérdidas de datos o retardos.

Con el objetivo de resolver las problemáticas descritas anteriormente, en esta tesis se propone novedosas estrategias de control distribuido usando algoritmos de consenso para la restauración de frecuencia, gestión de congestiones y el despacho óptimo de la micro-red. Estas estrategias mejoran el desempeño de la micro-red en cuanto a confiabilidad, robustez frente a fallas de comunicación, flexibilidad respecto a la operación plug-and-play de las unidades de generación.

Las estrategias de control propuestas resuelven las condiciones de Karush-Kuhn-Tucker (KKT) de una formulación lineal de flujo de potencia óptima basada en mediciones del sistema real, sin requerir un modelo matemático. La operación óptima de la micro-red se obtiene en la misma escala de tiempo que el control secundario, logrando el despacho óptimo para cambios rápidos de frecuencia. El problema de congestión se resuelve en los controladores basándose en el redespacho de las unidades de generación utilizando estrategias de control distribuido y consenso, sin requerir la incorporación de tecnología nueva y costosa o la resolución de problemas complejos de optimización. Resultados experimentales y por simulación validan la implementación de las propuestas.

Abstract

The microgrid is an alternative for the integration of distributed generation (DG), including renewable energy sources. Therefore, the control should ensure higher reliability, security and minimum operating cost in isolated or grid-connected mode of operation of the microgrid. In this context, the microgrid control tasks can be divided into 3 distinct levels: 1) Primary Control; which includes output current, voltage, and frequency control of DG units, 2) Secondary Control, at which level the frequency and voltage are restored to nominal values, and 3) Tertiary Control, at which level the optimal dispatch of the microgrid and coordination of the microgrid with the main grid are achieved.

Each control level traditionally operates on a different time scale. The primary control is performed within a shorter time scale (milliseconds), the secondary control in seconds, while the optimal dispatch requires several minutes or hours depending on the complexity of the optimization problem to be solved. Regarding the secondary and tertiary controllers, the centralized approach is the traditional control architecture used. However, the centralized approach is less practical because the DG units present a plug-and-play mode operation, which makes the electrical topology microgrid time-varying. Thus, the central controller needs to be modified. Also, in microgrids line overloading or congestion can occur. The congestion can significantly affect the lifetime of the distribution lines and transformers in the microgrid. Furthermore, the activation of thermal protections can lead to unsupplied demand. Another challenge of microgrid control is related to the topologies of the communication network, which implies loss of data or delays.

In order to solve the issues previously described, in this thesis a novel distributed control strategy is proposed, which is based on a consensus algorithm for frequency restoration, congestion management, and optimal operation of the microgrid. The strategy improves the performance of the microgrid regarding robustness and reliability in the event of communication failure and during plug-and-play operation. The strategy also provides the capacity to cope with rapid changes in demand.

The proposed control strategy solves Karush-Kuhn-Tucker (KKT) conditions of a linear optimal power flow formulation based on real system measurements, without requiring a mathematical power flow model. The distributed controller enables the optimal operation of the microgrid in the time-scale of the frequency restoration control. The congestion problem is solved based on re-dispatch of the generating units using distributed control strategies that do not require adding new and/or expensive technology or solving complex optimization problems. Experimental and simulation results validate the implementation of the proposals.

Este trabajo de tesis lo dedico a:

A mi esposo Dieguito.

A mis padres Isabel y Enrique.

A mis sobrinos Davity, Beto, Mate, Toñito, Manu y Davidcito.

Acknowledgements

Agradezco a Dios por sus innumerables bendiciones durante este período.

Extiendo mi más sincera gratitud a mi profesora guía Prof. Doris Sáez Hueichapan, que a mas de guiarme en mi tesis me apoyo en mi formación como investigadora, de quien he aprendido mucho, así como también por su confianza al permitirme trabajar en el Laboratorio de Control de Micro-redes que dirige. A mi profesor co-guía Prof. Daniel Olivares por su tiempo y dedicación durante el desarrollo de esta tesis. A los profesores, Prof. John Simpson y Prof. Mehrdad Kazerani por todos sus comentarios y aportes en este trabajo de tesis, y su colaboración durante mi estadía de investigación.

Agradezco a Dieguito, mi compañero de sueños por su apoyo incondicional y sus palabras de aliento en el momento preciso. A mi familia que pese a estar lejos con sus llamadas siempre me hicieron sentir cerca de ellos.

A mis grandes amigos con quienes compartimos inolvidables momentos: Luis, Juan, Panchito, Lis, Carlitos, Alex, Diego J, Dieguito M, Oscarin, Maury, Rubén, Eve, Dany, Mercedes, Andrés Ch., Gina y Leo. A mis herman@s por elección Rosy, Javy, Vane, Naty, Elenis, Andrecito. Gracias por su cariño.

Mil gracias a mis amigos del Laboratorio por cada almuerzo cada buen momento compartido durante nuestras largas jornadas de trabajo: Enrique, Felipito, Erwin, Manuel, Leonel, Claudio, Maury, Andrés, Mati U., Mati D., Felipe y Yanira. Gracias por hacer que el tiempo sea especial.

Agradezco al gobierno chileno, por la beca CONICYT/63140113 para Doctorado Nacional para Extranjeros. Además, agradezco al Instituto Sistemas Complejos de Ingeniería (ISCI) ANID PIA/BASAL AFB180003 y Solar Energy Research Center SERC-Chile (CONICYT/FONDAP/15110019). Finalmente, a los proyectos: FONDECYT 1170683 "Robust Distributed Predictive Control Strategies for the Coordination of Hybrid AC and DC Microgrids", FONDEQUIP EQM160122 "Equipment for the Emulation and Testing of Energy Storage Systems", FONDEQUIP EQM 130158 "Microgrid Emulator for the Design and Validation of Novel Control Strategies" y FONDECYT 1181517 que me apoyaron económicamente durante mis estudios doctorales.

Contents

List of Figures

List of Tables

Chapter 1

Introduction

1.1 Research Motivation

Nowadays, the electricity demand has increased around the world, where the distributed energy resources (DERs) allow this increment to be supported. In this context, governments and societies are promoting the use of DERs based on renewable energy (RE) that can help to decrease global warming and climate change. At the same time, tariff policies are being introduced so that electricity demand is satisfied [1].

With the increased of the electricity demand and the penetration of Distributed Generation (DG) units based on renewable energy resources and distributed energy storage (DES) units, microgrids have emerged as systems that allow the integration of these units. A microgrid is described as a cluster of DG units, DES units, and distributed loads, coordinated to supply electricity in order to fulfill economic, technical, and environmental requirements [2–4].

Microgrids can operate in a grid-connected mode using a Point of Common Coupling (PCC) or in an isolated mode [5, 6]. In microgrids, the DGs span from typical fossil-fuelled engines to renewable energy (RE) sources such as wind turbines (WT) and photovoltaic power (PV) [1, 5, 7].

Microgrids not only integrate the distributed generation units and take advantage of the renewable resources, but also allow electricity to be supplied to isolated communities where the electricity network is difficult to access. In these scenarios, microgrids can operate in isolated mode [8]. In order to achieve these tasks, the control and optimal management of the microgrid become highly important.

Currently, effort is going into designing control systems that ensure reliable, secure, and economical operation of microgrids in either grid-connected or isolated microgrid mode [5]. In this context, this thesis proposes two distributed control schemes for optimal dispatch of isolated microgrids considering congestion management. The proposed controllers are based on a decomposition of the optimal dispatch problem of a microgrid and rely on local voltage and frequency measurements, as well as global congestion alerts triggered by current measurements in distribution lines.

1.2 Problem Statement

The implementation of microgrids is an alternative for overcoming the challenges of inte grating distributed generator units, including renewable energy sources. Currently, efforts are being made to design control systems that ensure reliable, secure, and economical operation of microgrids in either grid-connected or isolated microgrid mode [5]. There are several issues to research in microgrid control. In this thesis the problems to solve are related to the following challenges:

- The control of isolated microgrids is more challenging than those that are grid-connected due to a more critical demand-supply balance and limited controllable assets for solving voltage and overload problems [5]. Line overload or congestion can significantly affect the lifetime of the distribution lines and transformers in the microgrid. Furthermore, the consequent activation of thermal protections could lead to unsupplied demand [9].

- Another challenge is that the topology of the smart grid is unknown not only because of the variety of configurations of the power grid and communication network topologies, but also because "plug-and-play" technologies will make the topology time-varying [10].

- Although centralized approaches have been effective up to now for conventional power systems, they may confront several implementation challenges when applied to a microgrid with penetration of renewable energies. The frequency of the microgrid may change rapidly and frequently due to the unexpected demand-supply imbalance, and the limited inertia present in the microgrid. There is an increasing need to develop fast, flexible, reliable, and cost-effective distributed solutions to meet the requirements of real-time applications in microgrids. Because of the intermittency of renewable resources, more frequent control updates are required [11].

1.3 Hypotheses

The hypotheses associated with this thesis are:

1. New distributed control techniques for frequency restoration, optimal dispatch, and congestion management of microgrids can improve microgrid performance both in terms of robustness in the event of communication failures, and reliability during plug-and-play operation compared to traditional centralized controllers.

2. The distributed optimal dispatch can be equivalent to that obtained with the linear optimal power flow of the microgrid.

3. Congestion management in the distribution power lines of microgrids can be achieved using distributed control strategies without knowledge of the network topology. These strategies can avoid the activation of thermal protection relays (overcurrent relays) as well as load disconnection.

4. Frequency restoration, optimal dispatch, and congestion management can be solved in the same time-frame.

1.4 Objectives

1.4.1 General Objective

The main goal of this research is to design and evaluate distributed control strategies for frequency restoration, optimal dispatch, and congestion management in an effort to achieve efficient, reliable and minimal cost operation.

1.4.2 Specific Objectives

1. To design a distributed control strategy for frequency restoration, optimal dispatch of isolated microgrids in order to improve microgrid performance in terms of robustness in the event of communication failures, and reliability during plug-and-play operation.

2. To demonstrate the optimality of the proposed control strategies.

3. To design a distributed control strategy to management the distribution power lines congestion of microgrids without knowledge of the network topology. These strategies can avoid the activation of thermal protection relays (overcurrent relays) as well as load disconnection.

4. To design a distributed control strategy for frequency restoration, optimal dispatch, and congestion management of an isolated microgrid in same time-frame.

5. To evaluate the performance of proposed control strategies, in normal operation and when the congestions occurs in the lines using simulation an experimental setup.

1.5 Contributions

The contributions of this research are the following:

- A novel distributed control strategy for frequency restoration, congestion management, and optimal operation of the microgrid are derived. The strategy improves the performance of the microgrid regarding robustness and reliability in the event of communication failure and during plug-and-play operation.

- The proposed control strategy solves Karush-Kuhn-Tucker (KKT) conditions of a linear optimal power flow formulation based on real system measurements and without requiring a mathematical power flow model. The distributed controller is able to restore the optimal operation of the microgrid in the time-scale of the frequency restoration control. Moreover, the equivalence of the controller steady-state and KKT conditions of a linear optimal power flow formulation is demonstrated.

- The congestion problem is solved based on re-dispatch of the generating units using distributed control strategies that do not require adding new and/or expensive technology or solving complex optimization problems.

1.6 Publications

1.6.1 Journal Publications

J. Llanos, D. E. Olivares, J. W. Simpson-Porco, M. Kazerani, and D. Saez. "A Novel Distributed Control Strategy for Optimal Dispatch of Isolated Microgrids Considering Congestion", *IEEE Transactions on Smart Grid*, vol. 10, no. 6, pp. 6595 – 6606, 28 March 2019. https://doi.org/10.1109/TSG.2019.2908128.

J. Llanos, R. Morales, A. Núñez, D. Sáez, M. Lacalle,R. Hernández, and F. Lanas. Load estimation for microgrid planning based on a self-organizing map methodology. *Applied Soft Computing*, vol. 53, no. 53, pp. 323-335, Jan. 2017.
https://doi.org/10.1016/j.asoc.2016.12.054.

C. Burgos-Mellado, **J. Llanos**, R. Cárdenas, D. Sáez, D. Olivares, M. Sumner, A. Costabeber, "Distributed Control Strategy Based on a Consensus Algorithm and on the Conservative Power Theory for Imbalances and Harmonics Sharing in 4-Wire Microgrids",*IEEE Transactions on Smart Grid*, vol. 11, no. 2, pp. 1604 - 1619, March 2020.
https://doi.org/10.1109/TSG.2019.2941117).

C. Burgos-Mellado, **J. LLanos**, R. Cárdenas, D. Sáez, D. Olivares, M. Sumner, A. Costabeber,"Single-Phase Consensus-Based Control for Regulating Voltage and Sharing Unbalanced Currents in 3-Wire Isolated AC Microgrids", *IEEE Access*, vol. 8, p. 164882-164898, 07 September 2020. https://ieeexplore.ieee.org/abstract/document/9187613.

E. Espina, **J. Llanos**, C. Burgos-Mellado, M. Martínez-Gómez, R. Cárdenas-Dobson, and D. Sáez-Hueichapan, "Distributed Control Strategies for Microgrids: An Overview", *Submitted to IEEE Access.*

J. Llanos, D. Saez, D. E. Olivares, J. W. Simpson-Porco, and M. Kazerani. "Distributed Control Strategy for Optimal Dispatch Considering the Coupling Between Active Power and Reactive Power for the Congestion Management". *Preparing for submission.*

1.6.2 Conference Publications

J. Llanos, J. Gomez, D. Saez, D. Olivares and John Simpson-Porco, "Economic Dispatch by Secondary Distributed Control in Microgrids", *21st European Conference on Power Electronics and Applications EPE '19 ECCE Europe*, Genova, Italy, 2019, pp. P.1-P.10, doi: 10.23919/EPE.2019.8915499. https://doi.org/10.23919/EPE.2019.8915499, Italy, September 2019.

E. Espina, C. Burgos-Mellado, R. Cárdenas, J.Gomez, **J. Llanos**, M. Martinez, A. Navas, E. Rute, D. Saez, "Experimental Hybrid ac/dc-Microgrid Prototype for Laboratory Research", *21st European Conference on Power Electronics and Applications*, *Accepted.*

V. Caquilpan, D. Sáez, R. Hernandez, **J. Llanos**, T. Roje and A. Nunez, "Load Estimation Based on Self-organizing Maps and Bayesian Networks for Microgrids Design in Rural Zones", *IEEE PES Innovative Smart Grid Technologies Latin America, Quito*, September 2017. https://doi.org/10.1109/ISGT-LA.2017.8126709.

J. Llanos, D Ortiz Villalba, D. Saez, D. Olivares, "Economic Dispatch for Optimal Management of Isolated Microgrids", *IEEE CONCAPAN XXXVI*, Costa Rica, June 2016. https://doi.org/10.1109/CONCAPAN.2016.7942382.

1.7 Thesis Outline

The rest of this thesis is structured as follows:

- **Chapter 2** presents the state of the art of the main topics related to control of microgrids, hierarchical control system, control architecture, and distributed control of microgrids. Finally, studies related to the Distributed Control in microgrids and congestion management are derived.

- **Chapter 3** develops a new distributed controller for optimal dispatch based on a consensus algorithm. Experimental results are shown and validate the good performance of the controller in the presence of sudden changes in the load, unit disconnection, and a communication link failure.

- **Chapter 4** presents the design of a new distributed control strategy for optimal dispatch, frequency restoration and congestion management. Also, distribution congestion control optimality mathematical demonstration is shown. Simulation and experimental results are shown and validate good performance of the controller in the presence of sudden changes in the load, unit disconnection, and communication link failure.

- **Chapter 5** describes the main conclusions of this PhD Project and presents an outlook on future research regarding these topics.

Chapter 2

Literature Review

This chapter presents the state-of-the-art of the main topics related to distributed controllers. First, the levels of microgrid control are studied. Next, the advantages and disadvantages of the control architectures are analyzed. Then, the most reported distributed control of microgrid are discussed, specifically the secondary and tertiary distributed control are studied. Finally, studies related to the congestion management are discussed.

2.1 Introduction

A microgrid has been defined as a cluster of Distributed Generation (DG) units, Energy Storage Systems (ESSs), and distributed loads, operated in coordination to reliably supply electricity [5, 12]. A main driver for the deployment of microgrids is to allow seamless integration of DG units.

A microgrid is capable of operating in grid-connected or stand-alone modes; and of handling the transitions between these two modes. In the grid-connected mode, a power deficit can be supplied by the main grid and excess power generated in the microgrid can be traded with the main grid. In the islanded mode of operation, a balance betweenthe demand of local loads and the real and reactive power within the microgrid must be achieved [5, 12, 13].

Microgrids can use alternate current (AC) or direct current energy (DC) or hybrid topology in which power sources and loads of both AC and DC nature can be integrated [14].

The AC microgrid is composed of AC-generators (e.g. wind turbine) with power converters, and AC-loads. An AC microgrid also includes DC-generators (e.g. PV, Energy Storage) and DC-loads, which can be connected to the AC microgrid using additional power electronics interfaces; however, a microgrid connected with additional interfaces may increase the power losses [15].

On the other hand, DC microgrids eliminate the power losses. This topology is becoming increasingly popular.DC microgrid integrates DC-load and DC-sources. These units are connected to the microgrid using power converters when required. Also, in a DC-microgrid it is possible to connect AC-loads and AC-sources using additional power electronics interfaces.

Recently, DC and AC dominated hybrid microgrids have gained popularity as they can maximize advantages of both AC and DC microgrids while providing improved compatibility characteristics [14]. Figure 2.1, shows a hybrid microgrid. This system requires proper power coordination control for bidirectional interlinking converters (BICs), which provide the required interconnect between the AC and DC subgrids [14].

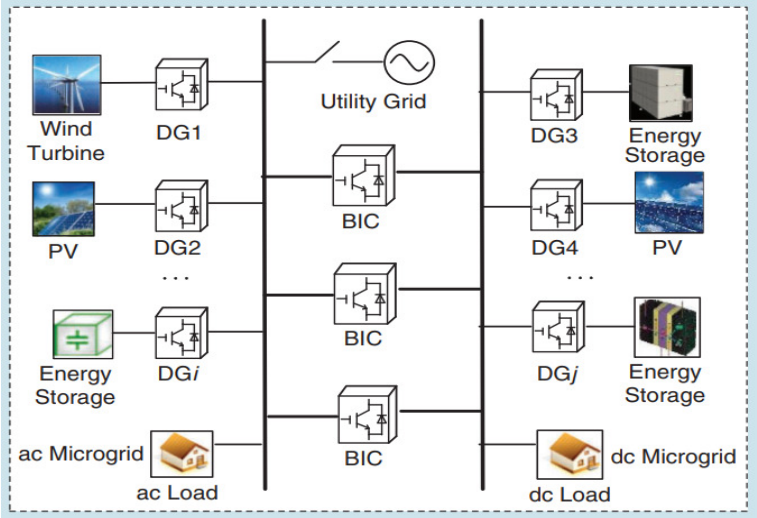

Figure 2.1: Hybrid Microgrid

The microgrid control tasks can be divided into three distinctive levels: 1) output current, voltage, and frequency control of DG units (Primary Control), 2) frequency and voltage restoration and (Secondary Control), and 3) optimal dispatch of the microgrid, coordination of the microgrid with the main grid (Tertiary Control) [16, 17]. Since most DG units require a DC-to-AC power electronic interface, the design of control schemes in the three levels that are applicable to inverter-interfaced units is required.

The secondary and tertiary levels are researched in this thesis. Frequency and voltage restoration in a microgrid are traditionally solved using a centralized or decentralized architecture approach. However, the distributed schemes can be used in this control level. Recently, there has been a rise in attention to distributed control and its applications in microgrids due to the need for higher reliability and security [18].

The optimal operation of a microgrid is typically obtained by solving an economic dispatch problem under a centralized approach. However, due to the advantages of distributed control approaches, recent works have proposed the use of distributed economic dispatch algorithms based on distributed control techniques. The multi-agent system (MAS) is a popular distributed control method, where a consensus algorithm is used for the coordination of agents [19].

The Energy Management System (EMS) solves an economic dispatch problem in order to achieve the optimal operation of the microgrid. In this context the EMS solves a optimization problem. This task can take from several minutes to hours to resolve.

The control of isolated microgrids is more challenging than in grid-connected mode due to a more critical demand-supply balance, and limited controllable assets to solve voltage and overloading problems [5]. Line overload, or congestion, can significantly affect the lifetime of the distribution lines and transformers in the microgrid. Congestion can also cause the activation of thermal protections, which can lead to unsupplied demand [9].

In bulk power systems, the congestion of transmission corridors is typically managed by re-dispatching generation units; however, more advanced control can also be achieved by phase shifters, line switching, FACTS/HVDC controllers, and even load curtailment [20]. In distribution networks, the problem of congestion management has been mostly approached using demand flexibility [9,21–23], or smart transformers [24] in which the proposed solutions require adding new expensive technology to existing systems or using distributed optimization techniques. In fact, congestion is a problem that can be produced in microgrids and which has not been thoroughly studied.

The scope of this chapter is to present an overview of the technical solutions regarding the implementation of control functionalities, specifically regard to frequency and voltage restoration and economic dispatch of an isolated microgrid.

2.2 Control of Microgrids

Microgrids have control capability, so they appear to the upstream network as a controlled, coordinated unit; their control and management capability distinguishes microgrids from distribution systems [17].

The microgrid generally assumes three critical functions: a) the control of the DGs, b) the energy management, and c) microgrid protection [25].

Also, in [5] the following desirable features of the control system are defined: a) output voltages and currents control of the various DG units, b) power balance, c) demand side management (DSM), d) economic dispatch and e) transition between modes of operation.

In this thesis, the control of the DG units and the energy management function are studied. These critical functions are separated in layers, where different tasks are solved in different time scales. In microgrids the traditionally hierarchical control is a control architecture used to control and to manage a microgrid.

2.2.1 Hierarchical Control System in Microgrid

The hierarchical control system shown in Figure 2.2 is typically utilised to control and manage an AC microgrid [12, 16, 26, 27]. This architecture is also applicable to a DC microgrid (eliminating frequency control) or a hybrid microgrid. In this structure, the control system is separated in three control layers: primary, secondary and tertiary control. Each control layer operates on a different time scale. Moreover, the lower layer control depends on the higher layer control.

The primary control is performed within a shorter time scale (0.2-1s) as compared to the

secondary control (2-10s), whereas the optimal dispatch requires several minutes depending on the complexity of the optimization problem to be solved [28].

In the hierarchical architecture, traditionally the secondary control (frequency and voltage restoration) and optimal dispatch are implemented using a centralized control approach.

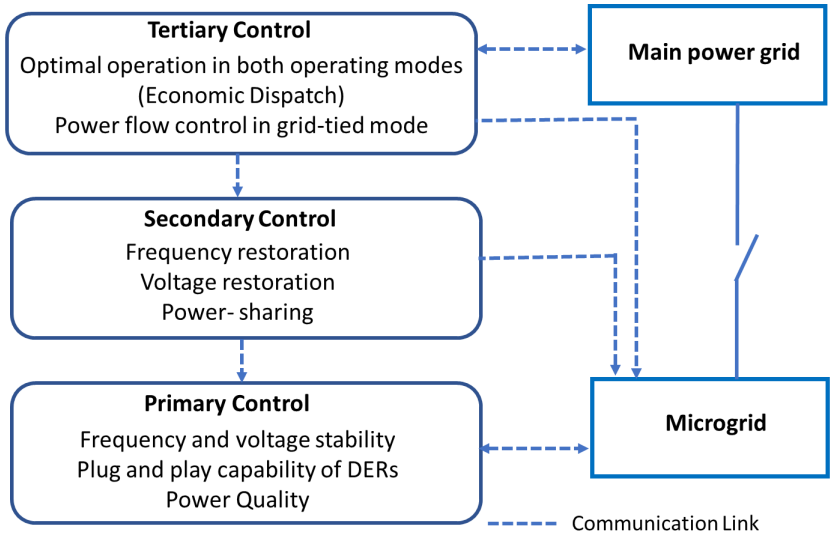

Figure 2.2: Control layers typically utilised for hierarchical control of microgrids

Primary Control

This layer is typically implemented using the following sub-layers: a) local or inner control loop which is usually implemented to regulate the currents and voltages of the power converters [29–31], b) droop control scheme, which emulates the behavior of a synchronous machine.

The local control has the fastest response. In microgrids based on voltage source inverters (VSIs), the controllers have voltage and current control loops with virtual impedance loops [16]. The first layer sends the set-points to local control, where the droop strategy is implemented to reach frequency and voltage stabilization, power balance, and proportional sharing of the load among DG units [32].

Equations (2.1) and (2.2) represent the droop control, where the frequency ω_{i} and the voltage E_{i} are obtained by the droop curve; ω^* is the nominal frequency; E_{i}^* is the nominal voltage; P_{i} is the active power injected by the inverter i; Q_{i} is the reactive power injected by the inverter i; P_{i}^* is the required active power i; Q_{i}^* is the required reactive power i; m_{i} is the P-W droop coefficient; and n_{i} is the Q-E droop coefficient [32, 33].

$$\omega_{\mathrm{i}} = \omega^* - m_{\mathrm{i}}(P_{\mathrm{i}} - P_{\mathrm{i}}^*) \tag{2.1}$$

$$E_{\mathrm{i}} = E^* - n_{\mathrm{i}}(Q_{\mathrm{i}} - Q_{\mathrm{i}}^*) \tag{2.2}$$

Secondary Control

The secondary control compensates the voltage and frequency deviation from their nominal values caused by the first layer. The equations (2.1) and (2.2) are modified. The terms Ω_i and e_i represent the control action for voltage and frequency compensation respectively (see (2.3) and (2.4))

$$\omega_i = \omega^* - m_i(P_i - P_i^*) + \Omega_i \tag{2.3}$$

$$E_i = E^* - n_i(Q_i - Q_i^*) + e_i \tag{2.4}$$

Tertiary control

The third layer achieves the optimal operation of the isolated microgrid, and it manages the power flow between the microgrid and the main grid in grid-connect mode. The tertiary control loop, which is typically the Energy Management System (EMS), is implemented with the purpose of achieving optimal operation in the microgrid.

The EMS is typically solved with a centralized control approach.Figure 2.3 shows the centralized control for tertiary and secondary control and the decentralized control approach for primary control [5] (See Figure 2.3).

The model predictive control (MPC) is the technique most used for the centralized approach. In general, the goal of the EMS is to manage the DERs economically to meet certain power quality standards. With the MPC approach, an optimisation problem is solved at each time step to determine a plan of action over a future time horizon. However, only the command for the next time-step is implemented [34–38]. This technique requires longer calculation times as compared with non-optimal controls, particularly when using nonlinear predictors. Therefore, when prediction models are not suitable for capturing the behaviour of the system or cannot be implemented in real-time, an alternative approach is to use a control with real-time decision-making [39].

2.3 Control Architectures

Centralized, decentralized or distributed control architectures can be used to control and manage a microgrid. In this section the features of these architectures are analyzed. The decentralized architecture is used in the primary layer control, and it is based on droop control. The centralized and distributed architectures are described with regards to secondary and tertiary control.

2.3.1 Centralized Control

This architecture requires a central controller, which can communicate with all the DGs in the microgrid. The central controller requires the capacity to process all the information transmitted from the other elements in the microgrid. A centralized controller is not considered robust against communication link failure, and plug&play operation of the DG units [5, 12, 40–42].

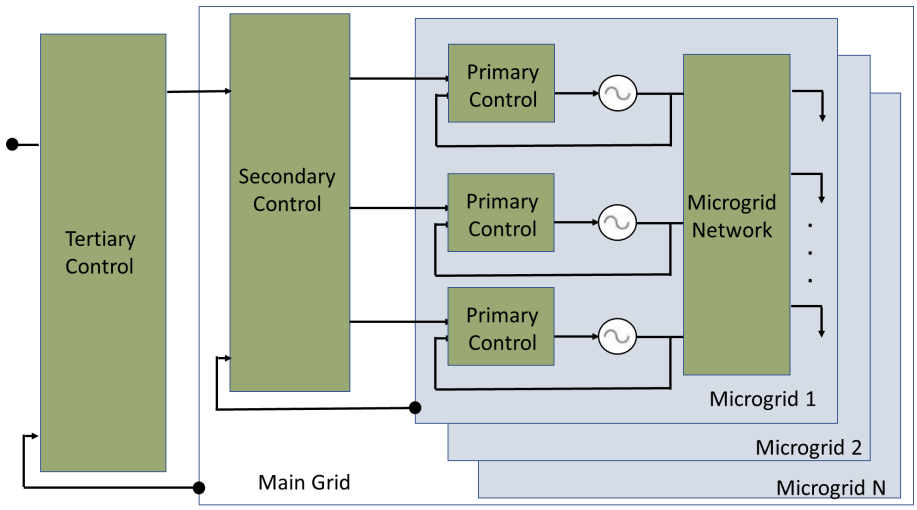

Figure 2.3: Hierarchical Control Levels for Microgrid Operation [5]

In the traditional hierarchical architecture, the secondary control (frequency and voltage restoration) and optimal dispatch are implemented using a centralized control approach (see Figure 2.4)

In this control approach, if the communication system fails, the microgrid will not be able to perform either economic dispatch or frequency/voltage restoration. The frequency and voltage are therefore maintained by primary droop controls.

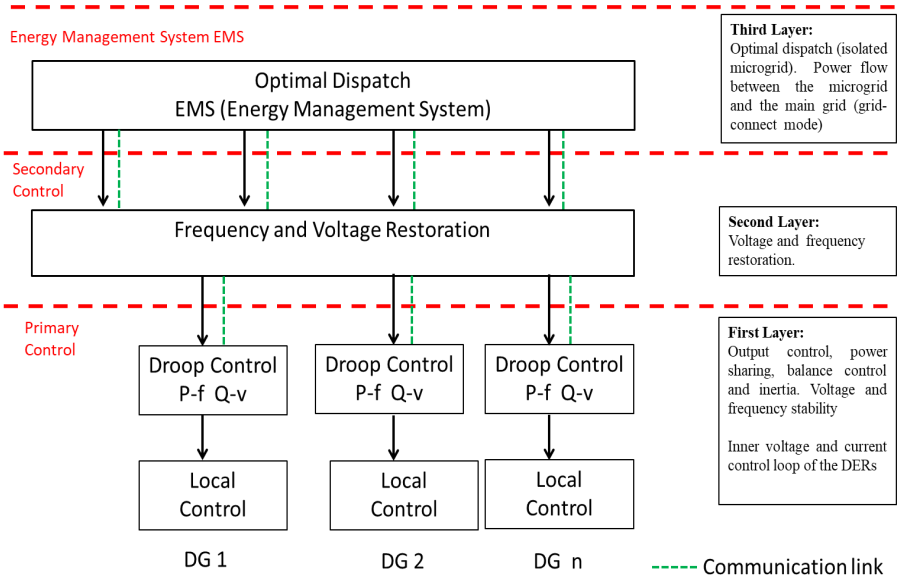

Figure 2.4: Hierarchical control architecture based on centralized control

2.3.2 Decentralized Control

In this case, the control system of each DG unit (agent) is implemented utilising local measurements only. The control methodologies are usually based on V-Q and f-P droops

[26,43,44]. In this control technique, the total load is shared between the DG units according to their power capabilities through a physical link [44].

The main problem of this architecture is that only local metering is considered. However, the decision or minimal cost of the microgrid is a global decision in which sharing information is necessary. For this reason, only centralized and distributed architectures are considered.

2.3.3 Distributed Control

In this case, the centralized controller is not necessary [see Figure 2.6b)] because the control effort is distributed along the microgrid, with "agents" working autonomously in a cooperative fashion to reach global objectives [41, 45, 46]. Distributed control systems enhance the scalability, and this method is more immune to single-point failures [42, 44].

The distributed control architecture in a microgrid is shown in Figure 2.5. Unlike within the typical hierarchical architecture based on centralized control (secondary and tertiary), in the distributed control architecture the secondary control (frequency and voltage regulation) and optimal dispatch are implemented with a distributed control approach. It is important to note that the secondary control and optimal operation have a similar time-scale.

The distributed controllers exchange information with their neighbors to achieve global goals. The controllers make decisions based on local measurements and the information available from each neighbor. The communication plays a dominant role in the coordination of various distributed resources to achieve a global operation goal. Any single point failure in the control system would not cause a cascading failure in the microgrid. It is flexible, making it easy to add DERs in the system without impacting the normal operation of the rest of the system. The controller also allows plug-and-play operation of DG units, which is very attractive for portable and remote microgrids [28].

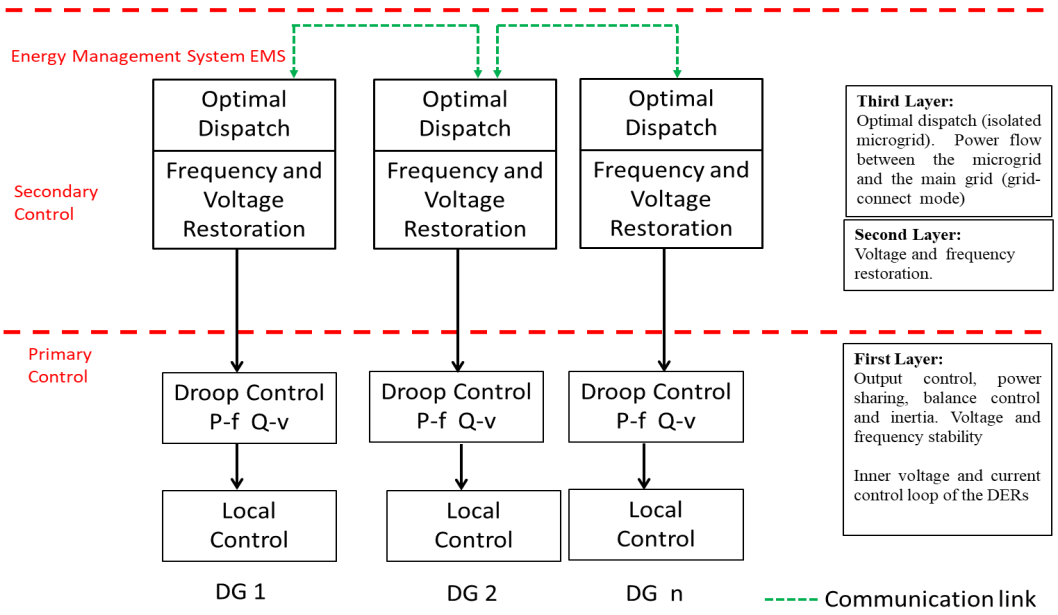

Figure 2.5: Hierarchical control architecture based on centralized control

According to [47], the communication system is important in both centralized control and distributed control. Even though the communication network is critical for both control approaches, the distributed control is more robust when a communication failure occurs. Notice that decentralized control lacks communication channels (See Figure 2.6(c)).

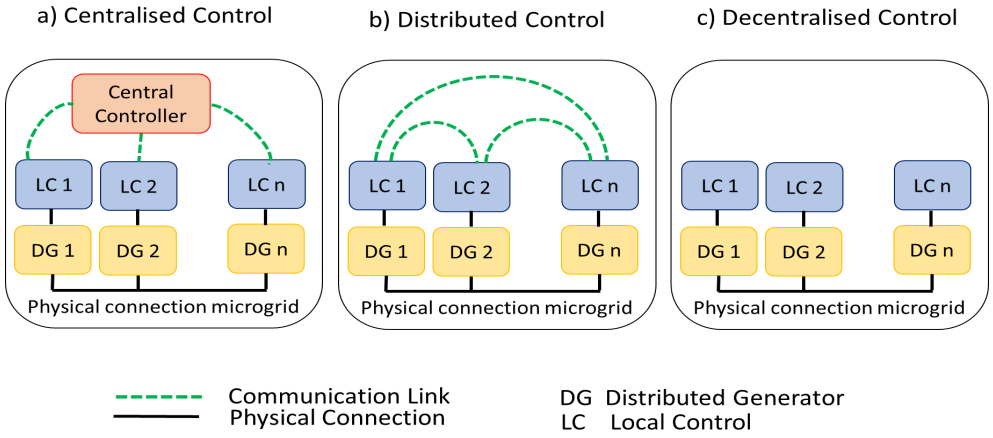

Figure 2.6: Hierarchical control architecture based on centralized control

A comparative summary of the characteristics of centralized and distributed control topologies is presented in Table 2.1. It is based on [18, 28, 42, 48–50].

Table 2.1: Comparison of hierarchical control and distributed control for microgrids.

Features	**Centralized control**	**Distributed control**
General features		
Computational cost	High	Low
Robust to single-point-failures	Low	High
Communication		
Communication complexity	Low	High
Communication robustness	Low	High
Bandwidth communication	Low-bandwidth	High-bandwidth
Operation		
Reliability	In case of a central control fault, the restoration and optimal operation of the microgrid are lost.	If a DER controller fails, the restoration and optimal operation are maintained.
Scalability of the control system	If a new DER unit is added to the microgrid, the centralised control has to be modified.	If a new unit is added to the microgrid, the distributed control does not need modification.
Flexibility	Low robustness under plug and play operation.	Plug and play capability.
Design and implementation		
Design complexity	Complex algorithms are required	Simple control algorithm e.g. based on proportional integral control (PI)
Hardware control	Powerful computer is required	An embedded controller is enough (economical)
Time-scales	Primary control, secondary control and optimal dispatch have different time-scale. The centralised optimal dispatch requires long computational times to solve the optimisation problem.	Secondary control and optimal dispatch have similar time-scale [51] The distributed optimal dispatch does not require solving an optimisation problem [52].
Implementation	Complex algorithms	Easy and simple to design and implement as it only handles local information

In this research, the distributed control approach is used to control and manage an isolated microgrid based on inverters. The previously mentioned main features regarding microgrid operation are summarized as follows:

- Robustness: If a fault is produced (e.g. in a controller or communication link) it would not cause cascading failure in the microgrid. On the other hand, in the centralized approach the central controller has a security vulnerability, because all control is in a common point [18, 28].

- Flexible control approach: It is simpler to realize changes in the microgrid, for instance DERs, loads, Battery Energy Storage Systems (BESS) can be added without impacting the normal operation of the rest of the system [28].

- Plug-and-play operation of DERs: This feature is very attractive for portable and remote microgrids [28].

The distributed controller is based on a communications network and consensus algorithm. In the next section, the communication structure and consensus algorithm are studied.

Communication Structure

The communication topology between agents (e.g. DERs) can be represented by a graph [53–55]. The graph can be expressed as $G = (V, E, A)$, where $V = \{v_1, v_2, \ldots, n\}$ represent the agents or nodes; $E = \{(v_\mathrm{i}, v_j)\}\,/(\mathrm{i}, j \in V)$ denotes the communication links; $A = [a_{\mathrm{i}j}]_{n\times n}$ is the adjacency matrix whose entry $a_{\mathrm{i}j}$ stands for a connection weight. The relationship $(v_\mathrm{i}, v_j) \in E \Leftrightarrow a_{\mathrm{i}j} > 0$ implies that nodes "i" and "j" can communicate with each other; otherwise, $a_{\mathrm{i}j} = 0$. The set of neighbours of the i-th node is given by $\mathcal{N}_\mathrm{i} = \{(\mathrm{i}, j) \in E\}$ where j are communicated agents. An example of a graph and its adjacency matrix for four agents is presented in Figure (2.7).

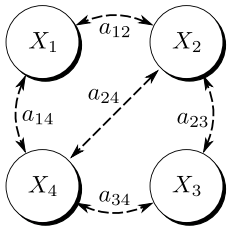

$$A = \begin{pmatrix} 0 & a_{12} & 0 & a_{14} \\ a_{12} & 0 & a_{23} & a_{24} \\ 0 & a_{23} & 0 & a_{34} \\ a_{14} & a_{24} & a_{34} & 0 \end{pmatrix}$$

Figure 2.7: Example of a graph of four agents and its adjacency matrix

The adjacency matrix is useful for analyzing the communication topology; its weight coefficients, $a_{\mathrm{i}j}$, can be used to determine the system stability. Furthermore, techniques have been developed based on the adaptive assignment of weights to improve convergence and stability of the graph [56]. In order to analyse the graphs, the Laplacian matrix is defined as $L = D - A$, with matrix D defined as $D = \mathrm{diag}\,\{\mathrm{d}_1, \mathrm{d}_2, \ldots, \mathrm{d}_n\} \in \mathbb{R}^{n\times n}/\,\mathrm{d}_\mathrm{i} = \sum_{j=1}^{n} a_{\mathrm{i}j}$. The addition of the elements located in each row of L are equal to zero and, when the graph has bidirectional flow of information between agents (i.e. G is balanced), the addition of all the elements located in each column of L is also equal to zero.

A necessary condition for stability is that the A matrix has to have a spanning tree, i.e.

there is a directed path from one node to any other node in the graph. The convergence speed of the states is related to the eigenvalues of the Laplacian matrix and depends, at the same time, on the algorithms (or protocols) used by each agent [54, 55]. The next subsection will introduce some basic concepts related to the algorithms typically used to achieve convergence in distributed control systems.

Remark 1 (Communication Requirements)

The communications network through which the DG units exchange information, defined by the adjacency matrix A (see Figure 2.7), does not necessarily have the same topology as the electric network of the microgrid. In this work, in order to ensure the optimal dispatch, power sharing, and congestion management, the communications network must allow bidirectional exchange of information. Also an ideal communication (without delays) is assumed. Notice that the use of the adjacency matrix can be extended to discrete, asynchronous and synchronous communication with delays [32, 57].

Consensus Algorithm

A communications network is required for the implementation of the proposed distributed control scheme. The bidirectional network is modelled as an undirected graph $\mathbb{G} = (\mathcal{N}, \mathcal{E}, A)$ between the DG units $\mathcal{N} = \{1, \ldots, N\}$, where $\mathcal{E}$ is the set of communication links and A is the nonnegative $N \times N$ weighted adjacency matrix. The elements of A are $a_{ij} = a_{ji} \geq 0$, with $a_{ij} > 0$ if and only if $\{i, j\} \in \mathcal{E}$ [32, 57].

Let $x_i \in \mathbb{R}$ denote the value of some quantity of interest at bus i; in our specific context, x_i will be an internal controller variable. The variables x_i should achieve consensus if $x_i(t) - x_j(t) \to 0$ as $t \to \infty$. Consensus can be achieved via the following algorithm [55]:

$$\dot{x}_i = -\sum\nolimits_{j \in \mathcal{N}(i)} a_{ij}(x_i - x_j)$$

which is distributed according to the topology of the communication network.

2.4 Distributed Control of Microgrids

2.4.1 Distributed Secondary Control for AC microgrid

As mentioned above, the primary control causes frequency and voltage deviations, and the secondary control restores these variables. The primary and secondary controls implemented in inverters are shown in Figure 2.8 . The secondary control (green lines) moves the droop curve (red lines) to frequency and voltage restoration. The droop equations (2.1), and (2.2) are modified by (2.3) and (2.4), where Ω_i and e_i are the secondary control actions [26, 32].

The existing secondary control strategies can be classified into three control approaches: centralized [12, 26, 58–60], decentralized [61, 62], and distributed control.

Figure 2.9 shows the most common strategies for secondary control. In the centralized approach, the central controller gathers measurements. These variables are compared with the references in order to compensate for secondary control, and the control actions (Ω_i

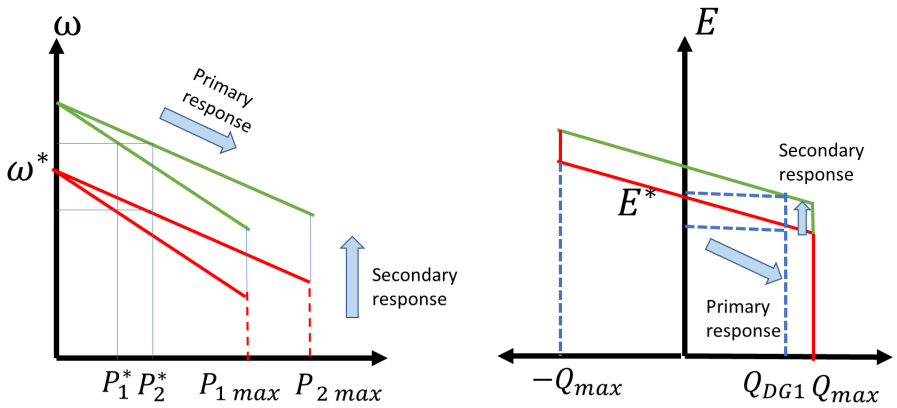

Figure 2.8: Secondary Control Action a) P-w droop and secondary control b) Q-E droop and secondary control [32]

and e_i) are sent through the communications channel to each DG control unit [12]. These controls are based on PI-type strategy [26, 58] or predictive control [59]. The centralized secondary control can include additional aspects, such as voltage unbalance compensation and harmonics [60].

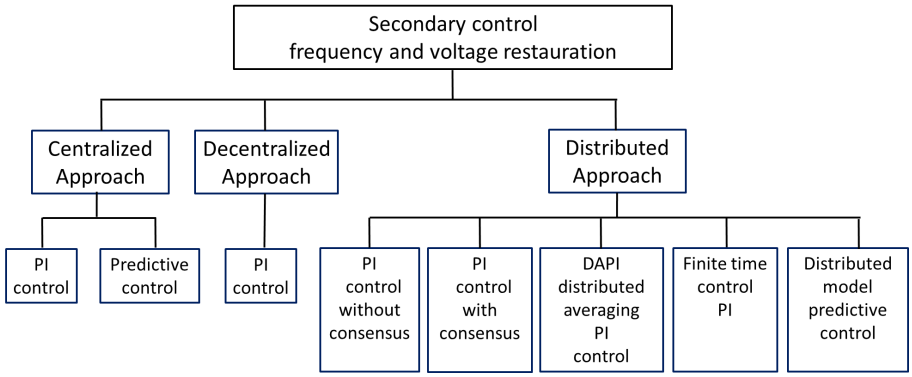

Figure 2.9: Approaches used for secondary control

On the other hand, in isolated microgrids, the distributed secondary control approach is adopted to increase reliability and security [18]. The distributed controls are usually based on the PI controller.

In [58] a distributed PI without a consensus approach is presented in which the frequency, voltage, and reactive power sharing controls are proposed separately. Each distributed PI controller considers the average frequency, average voltage, and reactive power measured, respectively, using the shared information. This proposal does not include the consensus approach. It assumes that the measurements are gathered at the same time. The authors extend this work in [63] considering three controllers: frequency/active power control, voltage restoration control, and reactive power sharing control. Unlike in previous work, the frequency restoration control does not require frequency measurement; it uses active power measurements to synchronize frequencies across the microgrid.

The secondary control can be implemented using two controllers: the first for frequency restoration and active power sharing, and the second for voltage restoration and reactive power sharing. In this context a distributed-average-proportion-integral control (DAPI) for frequency and active power sharing is shown in [32,64,65]. The distributed frequency restoration Ω_{i} in (2.5) is obtained from (2.6):

$$\omega_{\mathrm{i}} = \omega^* - m_{\mathrm{i}} P_{\mathrm{i}} + \Omega_{\mathrm{i}} \tag{2.5}$$

$$k_{\mathrm{i}} \dot{\Omega}_{\mathrm{i}} = -\left(\omega_{\mathrm{i}} - \omega^*\right) - \sum\nolimits_{j \in \mathcal{N}, j \neq \mathrm{i}} a_{\mathrm{i}j} (\Omega_{\mathrm{i}} - \Omega_j) \tag{2.6}$$

In (2.5), the first term on the right-hand side corresponds to the frequency error, whereas the second term is introduced to ensure that the frequency power mismatch is shared in a pre-specified proportion among all the DG units. Term $a_{\mathrm{i}}j$ represents the element of the adjacency matrix. In [32] a DAPI voltage restoration and reactive power sharing control is shown, represented by Equation(2.8), where ($\mathrm{e_i}$) is the voltage restoration control; E^* is the nominal voltage of the microgrid; Q^*_{i} is the reactive power rating of unit i. β_{i} and k_{i} are positive gains, and $a_{\mathrm{i}}j$ is an element of the adjacency matrix of communication between DG units. This control establishes a trade-off between voltage regulation and reactive power sharing.

$$E_{\mathrm{i}} = E^* - n_{\mathrm{i}} Q_{\mathrm{i}} + \mathrm{e_i} \tag{2.7}$$

$$\mathbf{k_i} \dot{\mathrm{e}}_{\mathrm{i}} = -\beta_{\mathrm{i}} \left(E_{\mathrm{i}} - E^*\right) - b_{\mathrm{i}} \sum\nolimits_{j \in \mathcal{N},, j \neq \mathrm{i}} a_{\mathrm{i}j} \left(\frac{Q_{\mathrm{i}}}{Q^*_{\mathrm{i}}} - \frac{Q_j}{Q^*_j} \right) \tag{2.8}$$

Other distributed secondary control strategies use finite-time control PI, such that all the DG units converge to the reference value in finite time [66, 67]. Recently, in [68, 69], it has been proposed that the voltage control is carried out with a consensus and distributed model predictive control approaches. The main problem regarding distributed control is the difficulty meeting requirements related to high-bandwidth communication. Nevertheless, this issue is solved using new technologies and a suitable design of the network communication as analyzed in [59] and [70].

2.4.2 Distributed Tertiary Control

The tertiary control level typically optimises the operation of an isolated microgrid by managing the power flow between the dispatchable units. If the MG is working in the grid-connected mode, the power flow between the MG and the main grid is optimised.

The optimal operation cost of a microgrid is achieved by solving an economic dispatch problem (ED). The ED solves an optimization problem where the goal is to achieve the minimum operating cost of the microgrid, subject to some operating constraints. It is worth mentioning that the ED can be implemented using centralized, decentralized [71–75] and distributed control approaches [52, 76–85].

The ED performed using the decentralized control approach, unlike with centralised and distributed approaches, does not need a communications network. In this context, the droop

adaptive method is the most common technique used to achieve the minimum operating cost. In [71–74, 86] a droop control scheme with dynamic modification is discussed. This scheme maintains all the advantages of the traditional droop technique, with a low generating-cost. A nonlinear droop is proposed in [71, 72, 74]. Meanwhile, in [73], a lineal droop function is proposed, which is easier to tune and implement to produce a cost reduction. In [75], some constraints, such as voltage, and frequency limits, are included in the optimisation problem. On the other hand, in [71], an adaptive droop has been proposed, with the droop coefficients being based on the maximum generating cost of each DER unit.

In all of these works, the overall minimum operation cost is not achieved because the power outputs of the DER units are tuned locally, according to their own generating cost, without information of the microgrid's total generating cost. These issues can be solved by using a distributed approach, where a communications network and cooperative decisions among the DER units are added. In this context, the distributed optimal dispatch of isolated microgrids has been studied for AC microgrids, DC microgrids, and hybrid AC/DC microgrids. The main reported works in this area are discussed in the following subsections.

Distributed Economic Dispatch of AC-microgrids

The conventional centralised dispatch problem can be solved in a distributed manner. In this sense, it should be highlighted that in contrast with the centralised approach, the distributed approach implies less cost by considering the communication between distributed generation units (see Figure 2.10).

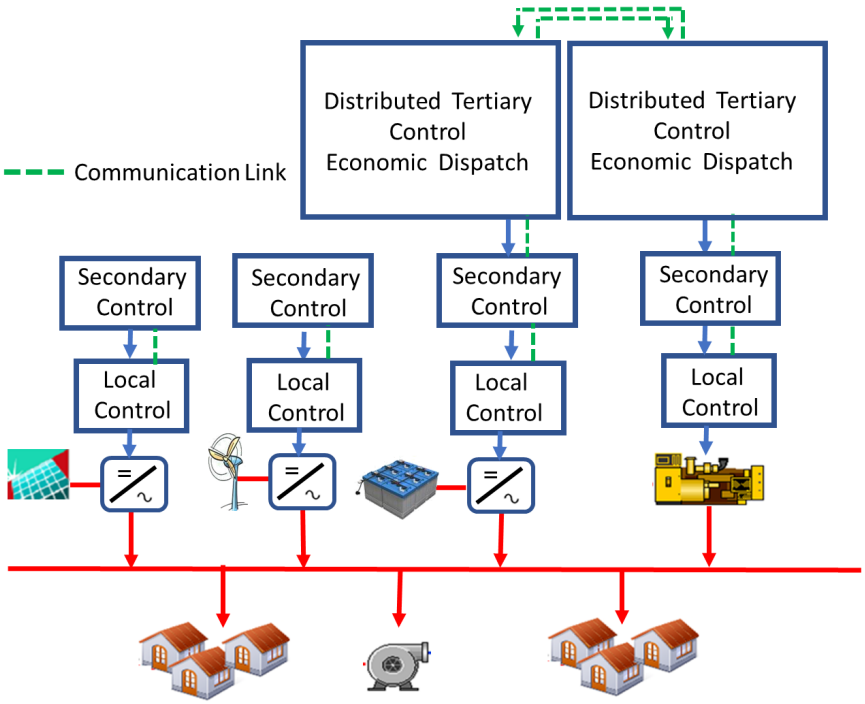

Figure 2.10: Implementation of a distributed tertiary control approach for economic dispatch

In terms of implementation, to achieve the distributed economic dispatch in microgrids,

the literature distinguishes between two main approaches, which depend on how the consensus variables are obtained. The first uses the Incremental Cost Consensus (ICC) concept in which the incremental cost (IC) is estimated [87–90], whereas the second employs the Distributed Gradient method [49, 89, 91, 92], which directly calculates a global incremental cost through a consensus algorithm. Both approaches are discussed below.

The ICC approach is based on a consensus algorithm of incremental costs (IC). In this sense, the ICC proposed in [87–90] is defined in (2.9),in this approach $\lambda_{\mathrm{i}}[k+1]$ is the estimation of the IC for each generator; P_{i} is the active power injected by each DER. β_{i} and α_{i} are the values of the quadratic cost function associated to the ith generator. $P_{D,\mathrm{i}}$ is the power demand of the system. $P_{D,\mathrm{i}}[t+1]$ is the estimation of the global supply-demand mismatch and ε is a positive scalar, which represents the convergence coefficient and controls the convergence speed [10, 88].

$$\lambda_{\mathrm{i}}[k+1] = \sum_{j=1}^{n} a_{\mathrm{i}j}\lambda_j[k] + \varepsilon P_{D,\mathrm{i}}[t] \tag{2.9a}$$

$$P_{\mathrm{i}}[t+1] = \frac{\lambda_{\mathrm{i}}[k+1] - \beta_{\mathrm{i}}}{2\alpha_{\mathrm{i}}} \tag{2.9b}$$

$$\hat{P}_{D,\mathrm{i}}[t+1] = P_{D,\mathrm{i}}[t] - (P_{\mathrm{i}}[t+1] - P_{\mathrm{i}}[t]) \tag{2.9c}$$

$$P_{D,\mathrm{i}} = \sum_{\mathrm{i}=1} a_{\mathrm{i}j}\hat{P}_{D,j}[t] \tag{2.9d}$$

In (2.9a) and (2.9d), terms $a_{\mathrm{i}j}$ represent the elements of the adjacency matrix (see section 2.1). In (2.9a) the consensus variable corresponds to the incremental cost λ, whereas in (2.9d), the estimation of the demand $\hat{P}_{D,j}$ is the consensus variable. The incremental cost, λ_{i}, in (2.9a) and (2.9b) is usually obtained by a constrained optimization problem. Under optimal operating conditions, the incremental cost of all DER units should be equal to the optimal Lagrange multiplier [87].

The formulation of the optimization problem assumes that the generating units have a quadratic cost function [see (2.10a)], where $C_{\mathrm{i}}(P_{\mathrm{i}})$ is the operating cost associated with the ith DER unit; α_{i}, β_{i} and γ_{i} are the coefficients related to the local cost function, as in (2.9). P_{i} is the active power injected by the ith DER. The total cost is obtained from (2.10b) (where n corresponds to the number of generation units in the MG). The power balance constraint is defined by (2.10c) where P_D is the demanded power of the microgrid. Finally, the IC for the ith DER units is given by (2.10d) [88].

$$C_{\mathrm{i}}(P_{\mathrm{i}}) = \alpha_{\mathrm{i}}P_{\mathrm{i}}^2 + \beta_{\mathrm{i}}P_{\mathrm{i}} + \gamma_{\mathrm{i}} \tag{2.10a}$$

$$C_{total} = \sum_{\mathrm{i}=1}^{n} C_{\mathrm{i}}(P_{\mathrm{i}}) \tag{2.10b}$$

$$P_D - \sum_{\mathrm{i}=1}^{n} P_{\mathrm{i}} = 0 \tag{2.10c}$$

$$IC_{\mathrm{i}} = \frac{\partial C_{\mathrm{i}}(P_{\mathrm{i}})}{\partial P_{\mathrm{i}}} = \lambda_{\mathrm{i}} \quad \mathrm{i} = 1, 2, .., n \tag{2.10d}$$

In [88], the ICC algorithm is implemented considering two different communication topologies. In [10,93], the minimization cost is achieved by implementing the ICC algorithm based on multi-agent systems (MAS) in which, each DER agent regulates the injected power by using a frequency droop strategy. The implementation of this proposal is shown in Fig. 2.11a. The convergence analysis considering different values of ε is also presented in [93].

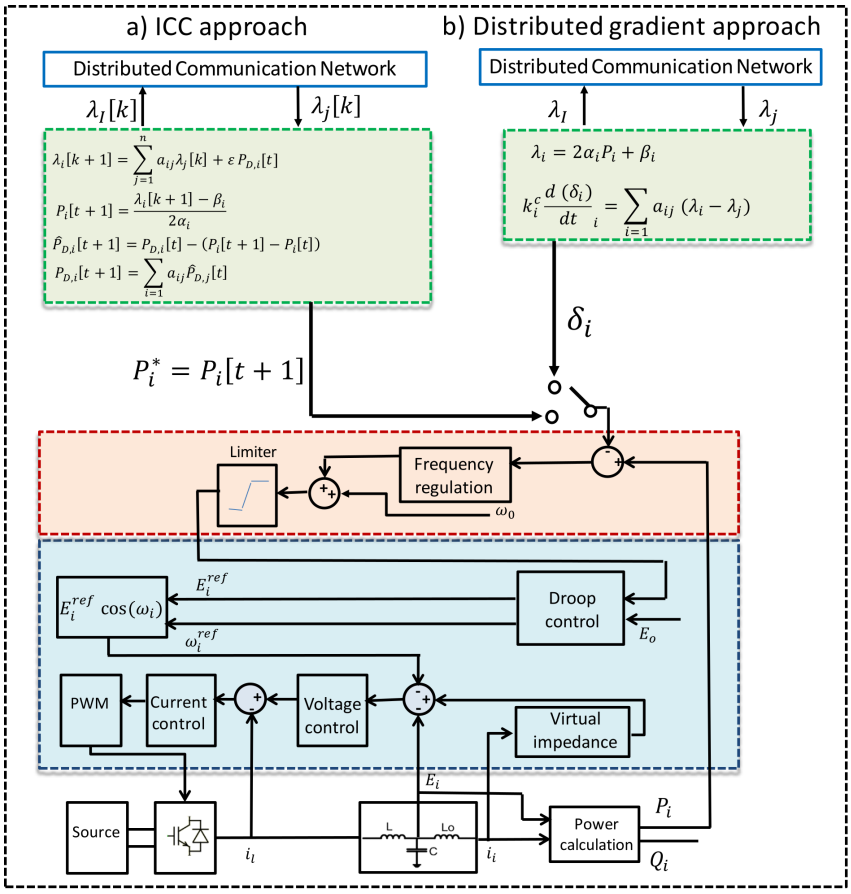

Figure 2.11: a) Control scheme of ICC [10,68] b) Control scheme of distributed gradient approach [49]

The studies described above implement the ICC algorithm to obtain the optimal operating cost of the microgrid. Nevertheless, these works do not consider power generation limits. To include the inequality constraint ($P_{\mathrm{i}}^{min} \leq P_{\mathrm{i}} \leq P_{\mathrm{i}}^{max}$), the equation set of (2.11) are included (see [11, 78, 79, 90]) where P_{i}^{min} and P_{i}^{max} denote the upper and lower limits of the active power for each generation unit.

$$\frac{\partial C_{\mathrm{i}}(P_{\mathrm{i}})}{\partial P_{\mathrm{i}}} = \lambda_{\mathrm{i}} \qquad for \quad P_{\mathrm{i}}^{min} \leq P_{\mathrm{i}} \leq P_{\mathrm{i}}^{max} \tag{2.11a}$$

$$\frac{\partial C_{\mathrm{i}}(P_{\mathrm{i}})}{\partial P_{\mathrm{i}}} < \lambda_{\mathrm{i}} \qquad for \quad P_{\mathrm{i}} = P_{\mathrm{i}}^{max} \tag{2.11b}$$

$$\frac{\partial C_{\mathrm{i}}(P_{\mathrm{i}})}{\partial P_{\mathrm{i}}} > \lambda_{\mathrm{i}} \qquad for \quad P_{\mathrm{i}} = P_{\mathrm{i}}^{min} \tag{2.11c}$$

In [11, 90], (2.9a)-(2.9d) are used to implement a distributed optimal dispatch scheme,

where two controllers are required: an upper controller that corresponds to the ICC and a lower controller that includes the power limits given by (2.11).

Note that in (2.10), renewable generation units are not included, because these can be considered with zero operating cost. However, in [94], the operating cost of a conventional generator and renewable generation units are considered. In order to achieve that, the authors define a pseudo renewable generation cost, where the objective of the power dispatch for renewable generation units is to minimize the curtailment of renewable energy (a subgradient algorithm is used). In [94] a two-stage method is presented. In the first stage, a distributed subgradient algorithm (algorithm for minimising a non-differentiable convex function) is utilised to rapidly recover the frequency. However, frequency measurement errors may prevent the first-stage iteration process from achieving steady-state convergence. In the second stage, an average consensus algorithm is applied to solve frequency oscillations caused by measurement errors. Thus, when frequency deviation lies below a certain threshold ε, the second stage algorithm will be activated.

In [78, 80], the network topology, transmission losses, and ICC consensus are included to achieve the optimal power flow inside the MG.

Unlike ICC, in the distributed gradient approach (see Fig. 2.11b), λ_{i} is not estimated, it is calculated using (2.10d) as shown in (2.12).

$$\lambda_{\mathrm{i}} = 2\alpha_{\mathrm{i}} P_{\mathrm{i}} + \beta_{\mathrm{i}} \qquad \mathrm{i} = 1, 2, 3, ..., n \tag{2.12}$$

To achieve identical λ_{i} in all the DER units, the consensus algorithm shown in (2.13) is implemented. In this expression λ_{i}, is the gradient for the neigbouring DERs i and j. The value of λ_{i} is calculated, not estimated, therefore the power balance can be defined by (2.14).

$$k_{\mathrm{i}}^{c} \frac{\mathrm{d}(\delta_{\mathrm{i}})}{\mathrm{d}t} = \sum_{j \in \mathcal{N}_{\mathrm{i}}} a_{\mathrm{i}j} (\lambda_{\mathrm{i}} - \lambda_j) \tag{2.13}$$

$$P_{\mathrm{i}} = \sum_{k=1}^{m} \mathrm{d}_{\mathrm{i}_k} P L_k \tag{2.14}$$

Here k is the load and PL_k is the demand of the kth load; $\mathrm{d}_{\mathrm{i}k} = 1$ if the load kth is in the neighborhood of the generator ith, otherwise $\mathrm{d}_{\mathrm{i}k} = 0$. The implementation of the distributed gradient approach is shown in Fig. 2.11b.

The distributed gradient λ_{i} approach is utilized in [49, 89, 91, 92]. In [49], the frequency restoration is implemented to optimize the power sharing. The same authors published in [89] a distributed control scheme where the active power limits are considered. The proposal has two stages: the first one calculates the optimal unconstrained incremental cost in the same manner as in [49], whereas the second one checks power generation constraint violations: if the constraint is activated, power injected from that DER unit is set to its maximum power limit (see (2.11)). On the other hand, the authors in [91] and [92] consider the same approach, but analyse the effects of communication delays in the consensus algorithm.

The authors in [81] analyze the convergence of distributed ED algorithms based on a simulation approach. On the other hand, in [82] a fully distributed dynamic ED method with second-order convergence is introduced, which is based on a parallel primal–dual interior-point algorithm with a matrix-splitting technique. In [83], authors prove the convergence of the algorithm using multi-parameter matrix perturbation and graph theory, and it is shown that the convergent values are the optimal solution of the proposed distributed ED control scheme. On the other hand, it is worth mentioning that the centralized ED is achieved if the KKT conditions of a linear optimal power flow (OPF) formulation are satisfied. In this context, in [52], the optimally operation of the proposal is demonstrated by showing that the KKT conditions are satisfied in the proposed distributed ED scheme.

Distributed Economic Dispatch of DC-microgrids

The ICC approach for *AC* microgrids discussed in the previous section can be extended to *DC* microgrids, where a consensus algorithm is used to achieve equal IC in all the generating units. The distributed ED of *DC* microgrids, unlike the distributed ED of *AC* microgrids, modifies the voltage droop control scheme. In this context, the ED is solved at the time that the global average voltage is restored [84, 85].

In [84], the ED is achieved by modifying the voltage reference from the droop control for *DC* microgrids through a PI controller $(K_p(P^*_{G,\mathrm{i}} - P_{G,\mathrm{i}}) + K_\mathrm{i}\int(P^*_{G,\mathrm{i}} - P_{G,\mathrm{i}})$, which modifies the output power of the ith DER ($P_{G,\mathrm{i}}$) to be equal to the optimal output power ($P^*_{G,\mathrm{i}}$). $P^*_{G,\mathrm{i}}$ is obtained from the ICC shown in (2.9). However, in this work the power limits for DERs are not considered. Moreover, this strategy only regulates the local output voltage of each DER instead of the global voltage of the microgrid, and for this reason, cannot guarantee optimal operation.

In [85], the global voltage regulation issue is covered, and the distributed consensus technique is used for ED and voltage control of the microgrid. The voltage reference for the local control is modified by adding the voltage deviations $\delta E_{\mathrm{i},1}$ and $\delta E_{\mathrm{i},2}$ to the reference voltage. The term $\delta E_{\mathrm{i},1}$ is added to achieve the ED of the *DC* microgrid, which is based on an ICC approach (2.9). The term $\delta E_{\mathrm{i},2}$ is obtained from a a PI controller, which removes the bus voltage deviation through distributed cooperation with the DER neighbours. Finally, unlike [84], the works reported in [85, 95] include the limits of the active power as depicted in (2.11).

In [96], a distributed adaptive droop control algorithm is proposed for optimal dispatch and secondary current regulation, by applying a consensus algorithm. The droop voltage controller $E_{ref\mathrm{i}}$ is obtained by (2.15); where E_{nom} denotes global nominal voltage of the *DC* microgid, m is the droop coefficient, $\mathrm{i}_{out\mathrm{i}}$ is the ith converter output current, $\mathrm{i}_{ref\mathrm{i}}$ is the current reference obtained from the distributed ED model, and ΔE_i is the voltage correction. The latter term is added to cancel out the effect of line impedance. The droop controller receives the current reference $\mathrm{i}_{ref\mathrm{i}}$ from the economical regulator (ER). The ER uses the consensus algorithm to estimate the system incremental cost IC (λ). The voltage correction ΔE_i is obtained from the secondary current regulator; this is used to distribute the current imbalance among converters, which is produced by a different line impedance.

$$E_{ref\mathrm{i}} = E_{nom} + \Delta E_\mathrm{i} - m(\mathrm{i}_{out\mathrm{i}} - \mathrm{i}_{ref\mathrm{i}}) \tag{2.15}$$

Unlike the distributed EDs reported in [84,85] (for *DC* microgrids) in [96], the centralised ED problem expressed in (2.10) is used to obtain λ considering power losses, where a penalty term is added into the cost function (2.10), as shown in (2.16). The amount of transmission losses is approximated by the square of the output power of each generating unit ($\mathrm{d_i}P_\mathrm{i}^2$). Although a penalty term is added for considering the transmission losses in the cost function, the power-losses are not modeled.

$$C_\mathrm{i}(P_\mathrm{i}) = \alpha_\mathrm{i}P_\mathrm{i}^2 + \beta_\mathrm{i}P_\mathrm{i} + \gamma_\mathrm{i} + \mathrm{d_i}P_\mathrm{i}^2 \tag{2.16}$$

Reference [97] solves an ED problem applying the distributed λ approach to achieve equal incremental cost in all the generating units. The proposal also includes a regulation of the average DER output voltage to take care of the generation–demand. The centralised ED implemented to obtain λ considers the total power losses (P_{loss}); however, the (P_{loss}) are assumed constant.

Several works include time delay analysis in their proposed consensus algorithms to evaluate their performance in this scenario. As reported in [98] time delays affect the convergence and performance of consensus algorithms. Thus, in [50, 84, 91, 99], the effects of a constant communication delay on the ED problem are studied using simulation work, whilst in [98], time-varying delays are analysed. Finally, in [98], the effects of the communication delay on the system stability is studied by using a linear matrix inequality.

Distributed Economic Dispatch of Hybrid AC/DC-microgrids

The economic dispatch in hybrid *AC*/*DC* microgrids has been addressed using the centralized approach which solves an optimisation problem. The optimization problem can be solved under market price uncertainties [100], by considering generation and load uncertainties [101] or energy storage losses [102].

Although these approaches are viable, it is worth noting that the centralized ED approach has a lower reliability under communication link faults and single point of failures. In a decentralized approach, the minimisation cost can be achieved when the distributed generating units have the same incremental cost. Notice that in Hybrid *AC*/*DC* microgrids, with the synchronisation of the *AC* frequency and *DC* voltage, the ICs in *AC* microgid and *DC* microgrid will be equalised. However, the droop control will inevitably cause deviations of the *AC* frequency and *DC* voltage [77].

In [77], a distributed control architecture is proposed for economic dispatch of hybrid *AC*/*DC* microgrids. The proposal has two levels. In the first level, the ED problem for an *AC* sub-microgrid (frequency droop) and ED problem for a *DC* sub-microgrid (voltage droop) are solved by using the incremental cost based on droop approach (IC) (2.10). The ILC does not need any information from the neighbors because the ICs of all *AC* DER units are forced to be identical with the synchronisation of the *AC* frequency (for *DC* sub-microgrids a similar approach could be used). In the second level, a distributed control canonical form is proposed to eliminate the deviation between *AC* frequency and *DC* voltage caused by droop control. However, because the fluctuations in *AC* frequency and *DC* voltage are removed, the sub-grid loading conditions are not visible. In order to extract the loading conditions

of the sub-grids, the authors propose a relative loading index (RLI). The references of the interlink converter power flow can be defined in base to this RLI.

The researches shown before achieve the optimal distributed dispatch. However, the following issues were not considered: Congestion management and Voltage control coupled with reactive power sharing. The studies that included power flow require estimators [78,80], and need the electrical network topology.

2.5 Congestion Management

Congestion is produced when the power flow from the line exceeds the limits of power of the sources that supply the electrical demand. Congestion in microgrids is caused by distributed energy resources, increasing demand, plug&play operation, intermittent energy sources, and changing microgrid topology. The congestion can induce voltage and overloading problems. Voltage problems occur when the bus voltage is close to or exceeds the limits of $+/-$ 10%. Overloading occurs when the loading is close to or exceeds the thermal limit of the power components [20]. Thermal overloading is produced in lines or transformers. In this work, congestion in the distribution lines is studied. Thermal overloading affects the lifetime of the lines and distribution transformers. Furthermore, thermal protection could be activated, which could lead to unsupplied demand [9]. It should also be noted that the control of isolated microgrids is more challenging than in connected microgrids because of the power balance necessary to assure that inadequate improper operation will not lead to a relatively high circulating current in the distribution lines [16]

The congestion problem is a problem that is beginning to be studied in microgrids. The congestion problem in transmission lines can be solved by: 1) Installation of new lines, 2) Dynamic line rating, 3) Use of storage, 4) use of controllable loads, 5) control of electrical vehicle load, 6) Demand response and 7) Inverter-control of DG units, which is cheaper and has shorter lead times for installing DG units [103]. Congestion in transmission lines for bulk power systems has been managed by: 1) A re-dispatch of active power from the sources, 2) Controllable loads, 3) Line switching, 4) Flexible Alternating Current Transmission System/High Voltage Direct Current (FACTS/HVDC) [20].

The voltage control in a distributed system is solved by implementing: 1) New lines, 2) Dedicated devices (FACTS) which are limited for LV grids, 3) Smart transformer OLTCs, 4) Storage, and 5) Inverter-control of DG units [103]. On the other hand, the thermal overloading in a distribution system can be mitigated by load control methods [21–23]. This approach includes direct and indirect methods. The direct method involves using network control of household appliances or other types of controllable loads. These controllers use centralized control architecture. Indirect methods are based on motivating end-users to shift their consumption, and in this way removing the congestion from the lines [9, 22].

Distribution system operators (DSO) can change the total active and reactive power at buses by installing new local distributed generators and FACTS devices, such as the static VAR compensator SVC, or by motivating the customers to change P_{i} and Q_{i} via market methods, or directly controlling P_{i} and Q_{i} under pre-agreement with customers. In [103] the DSO sends appropriate set points to the wind turbines in order to solve the congestion

problem. The most common solutions used in distribution networks are load control or demand flexibility, [21–23], and smart transformers [104, 105]; these solutions require adding new expensive technology to existing systems or solving more complex optimization problems. In this work, in order to avoid having to acquire these new technologies, the re-dispatch of active power from the DG is implemented to resolve the congestion using inverter control.

The re-dispatch of active power from the DG to remove congestion can be achieved by modifying the droop control of frequency regulation. For instance a modified frequency droop control for voltage source inverters, which applies state-dependent weights to the line power flow values is proposed in [106]. This controller does not require a communications network, and frequency restoration is not considered. On the other hand, in [107] the use of a distributed approach for regulation and restoration of frequency and congestion management is shown. This proposal depends on the topology system, requires voltage magnitudes and virtual phase angles in each bus, and considers only synchronous generator units. The inverters are not considered, and this control is compared with Automatic Generation Control (AGC) [107].

Unlike previous research, in this thesis the congestion management, frequency and voltage restoration, and optimal operation of the microgrid are all achieved in the same time scale. The proposals are for inverters in an isolated microgrid.

2.6 Analysis and Discussion

This section presents a review of current developments in economic dispatch using a dis- tributed control systems approach applied to isolated AC, DC, and hybrid microgrids. For each type of MGs, the main distributed control schemes proposed in the literature are described and discussed.

Also, a brief comparison of centralized and distributed controllers for microgrids is shown in Table 2.1. Based on this comparison table, in this research the distributed control approach is applied to secondary and tertiary controllers of an isolated microgrid based on inverters. The following are the main advantages applied to microgrids regarding the distributed control approach: i) Robustness: If a fault is produced (e.g. in a controller or communication link) it would not cause cascading failure in the microgrid. On the contrary, the centralized approach has a security vulnerability of the central controller as a common point of failure, ii) Flexibility: For the management of the microgrid when the DG units or local loads are added, the distributed control does not require changes in the controller. Again, on the contrary, in the centralized approach programming changes are required. Also, the distributed approach is flexible regarding changes in the electrical topology. iii) It allows plug-and-play operation of DERs, which is very attractive for remote microgrids.

In the previous studies regarding distributed economic dispatch, the optimal distributed dispatch has been achieved. However, the congestion issues in the electrical lines in microgrids were not considered. Also, in these works, the economic dispatch relies on the electrical network topology. These aspects are considered to identify the requirements design of the controllers proposed. In the next sections, novel distributed controllers are proposed.

The following are the control requirements identified: frequency and voltage restoration, congestion management, optimal dispatch (OD) of isolated microgrids in the same time scale, where the previous knowledge of electrical network topology is not necessary. The controller must show good performance against sudden changes in the load, congested lines, plug-and-play operation of DG units in the microgrid. It must also be able to successfully drive the system to optimal economic operation.

In order to design the distributed control, two stages are planned. The first stage consists of the design of a novel distributed control strategy for frequency restoration and optimal dispatch in isolated microgrids at the same time scale. The second stage consists of the design of a novel distributed control strategy for frequency restoration and optimal dispatch considering congestion management in isolated microgrids in the same time scale. The controllers proposed are studied in chapters 3 and 4 respectively.

Chapter 3

Distributed Control Strategy for Optimal Dispatch and Frequency Restoration

In this chapter, a distributed controller to achieve the economic dispatch (ED) and the frequency restoration of a micro-grid is proposed, which complies with the Karush-Kuhn-Tucker optimality conditions for a linear optimal power flow formulation. The consensus over the Lagrange multipliers allows an optimal dispatch without considering an electrical microgrid model. Next, the proposal is explained in detail.

3.1 Introduction

In this section a distributed controller in order to achieve the ED of a microgrid is proposed, which complies with the Karush-Kuhn-Tucker (KKT) optimality conditions for a linear optimal power flow formulation. The consensus over the Lagrange multipliers allows an optimal dispatch without considering an electrical microgrid model, preserving the frequency and voltage restoration into the secondary control level for isolated microgrids.

As mentioned in the chapter 2, the existing secondary control strategies can be classified into three control approaches: centralized, decentralized, and distributed control. In the first approach, the central controller uses measurements from the whole microgrid to compensate the frequency and voltage deviations, however if the central controller fails the frequency/voltage restoration are not achieved.

The decentralized and distributed approaches are usually based on PI controllers in order to restore the frequency and the voltage [12] [58]. Decentralized approach uses just local measurements to achieve the regulation, whereas distributed approach uses information from neighbors DG units, requiring a communication network and increasing reliability and security in isolated microgrids [16] [18]. Nowadays a consensus algorithm is included to the distributed approach improving the real and reactive power sharing [28], [32].

The optimal operation is usually a tertiary control level task, and it is achieved by solving an economic dispatch problem. This controller is often formulated under a centralized

approach, and requires several minutes to solve an optimization problem. However, in microgrids, the disturbances can be produced at seconds, then the optimal dispatch is not updated for this time scale. In order to solve the optimal dispatch at shorter times, it can be analyzed with decentralized or distributed control approaches.

The adaptive droop controller is a common technique used to achieve minimal operation cost based on decentralized schemes [74, 86]. In this scheme, the DGs controllers are tuned according to its generation cost. However, due the DGs do not share information, the global minimum generation cost is not achieved in the microgrid.

Some techniques used for minimal cost based on distributed control approach are the following: incremental cost consensus estimated (ICC) [10, 93], and gradient consensus [49], [108]. The ICC is used in Multi-Agent System (MAS) [10], and it is based on consensus algorithm and incremental cost (IC). IC and global supply-demand mismatch are estimated for each generator [109], however, these works do not consider the generating power limits. In [10, 93, 110] external controllers are added in order to consider the power generating limits applying ICC approach, in these cases a pseudo generating cost for DG neighbors is estimated. Unlike ICC, the distributed gradient approach computes the incremental cost [49, 92]. All these works include the IC as the consensus variable. The experimental results validate the adequate performance of the controller against sudden changes in the load and communication failures, the microgrid performance when a DG unit is disconnected is tested as well.

The contributions of this proposal, shown in this chapter, are as follow: i) the optimal dispatch and frequency restoration are considered in the same time scale in order to archive the optimal dispatch when fast disturbances occur, ii) the KKT optimality conditions of the linear centralized OPF problem are satisfied, iii) the microgrid topology is not required for achieve the optimal dispatch, iv) the proposed controller was tested in a experimental microgrid. This section presents a formulation of the network-constrained optimal dispatch problem in isolated microgrids. The formulation is then used to derive a distributed frequency that drives the system to a solution of the optimal dispatch problem. The proposed controller assumes the availability of current measurements to local DG controllers, all of which are shared through a communications network that allows bidirectional exchange of information.

The design of the proposed distributed controller is based on a centralized optimal economic dispatch formulation and the KKT optimal conditions. A consensus algorithm over the Lagrange multipliers related to real power balance is considered as well. The proposed approach is described in detail below.

3.1.1 Communication Structure

It was explained in chapter 2, a communication network is required for the implementation the distributed control scheme. A connected communication topology is necessary, in Figure 3.1 the connected and non-connected communication topology are shown.

The bidirectional network is modelled as an undirected graph $\mathbb{G} = (\mathcal{N}, \mathcal{E}, A)$ between the DG units $\mathcal{N} = \{1, \ldots, N\}$, where $\mathcal{E}$ is the set of communication links and A is the nonnegative $N \times N$ weighted adjacency matrix. The elements of A are $a_{\mathrm{i}j} = a_{j\mathrm{i}} \geq 0$, with $a_{\mathrm{i}j} > 0$ if and only if $\{\mathrm{i}, j\} \in \mathcal{E}$ [32, 57]. Let $x_{\mathrm{i}} \in \mathbb{R}$ denote the value of some quantity of

interest at bus i; in our specific context, x_{i} will be an internal controller variable. It is said the variables x_{i} achieve consensus if $x_{\mathrm{i}}(t) - x_j(t) \to 0$ as $t \to \infty$. Consensus can be achieved via the following algorithm [55]:

$$\dot{x}_{\mathrm{i}} = -\sum\nolimits_{j \in \mathcal{N}(\mathrm{i})} a_{\mathrm{i}j}(x_{\mathrm{i}} - x_j) \tag{3.1}$$

which is distributed according to the topology of the communication network.

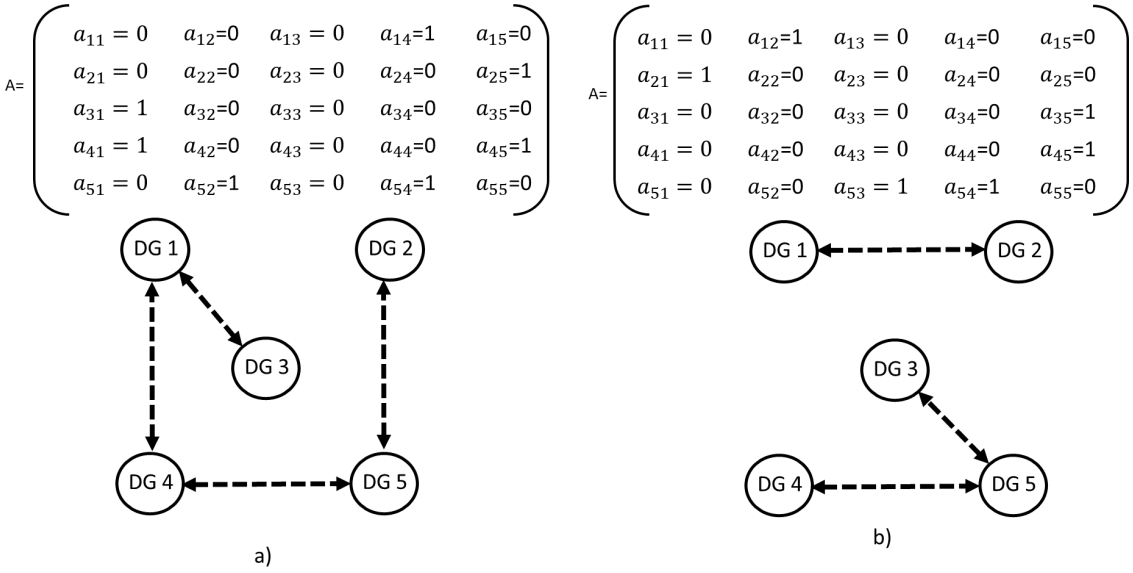

Figure 3.1: a) Connected communication topology b) Non-connected communication topology.

Remark 1 (Communication Requirements)

The communications network through which the DG units exchange information, defined by the adjacency matrix A (see Figure 3.1), does not necessarily have the same topology as the electric network of the microgrid. In this work, in order to ensure the optimal dispatch, power sharing, and congestion management, the communications network must allow bidirectional exchange of information. Also an ideal communication (without delays) is assumed. Notice that the use of the adjacency matrix can be extended to discrete, asynchronous and synchronous communication with delays [32, 57].

3.1.2 Centralized Optimal Dispatch

Prior to the distributed controller proposal design, a centralized optimal economic dispatch and its KKT optimality conditions are presented, which are used in the design of the controller proposed.

Let's consider a balanced three-phase isolated microgrid, with a set of buses $\mathcal{J} = \{1, \ldots, J\}$, a set of DGs $\mathcal{N} = \{1, \ldots, N\}$ Each bus is equipped with either a generation unit, a load, or both.

Generation units inject real power P_i to the microgrid, which is constrained within minimum and maximum limits.

The optimal dispatch problem considered in this work determines the least-cost dispatch of controllable DG units in a microgrid. The formulation is based on a single-bus system.

$$\begin{aligned} \underset{\mathbf{P}}{\text{minimize}} \quad & \sum\nolimits_{\mathrm{i}\in\mathcal{N}} C_\mathrm{i}(P_\mathrm{i}) && && \text{(3.2a)} \\ \text{subject to} \quad & P_D = \sum\nolimits_{\mathrm{i}\in\mathcal{N}} P_\mathrm{i} && && \text{(3.2b)} \\ & P_\mathrm{i}^{\min} \le P_\mathrm{i} \le P_\mathrm{i}^{\max} && \forall\, \mathrm{i}\in\mathcal{N} && \text{(3.2c)} \end{aligned}$$

where $\mathcal{N}$ is the sets of DGs, P_i is the real power dispatch of generator i, $C_\mathrm{i}(P_\mathrm{i})$ is a convex cost function, $\mathbf{P} = \{P_\mathrm{i} : \mathrm{i}\in\mathcal{N}\}$, P_D is the total microgrid demand.

It is assumed that Slater's constraint qualification condition holds, implying strong duality, and that the problem may be studied through its Lagrange dual. The Lagrangian function of the optimal dispatch problem (3.2a), (3.2b), and (3.2c), is shown in (3.3).

$$\begin{aligned} \mathbb{L}(P_\mathrm{i},\lambda,\gamma_\ell,\sigma_\mathrm{i}^+,\sigma_\mathrm{i}^-) = & \sum\nolimits_{\mathrm{i}\in\mathcal{N}} C_\mathrm{i}(P_\mathrm{i}) \\ & + \lambda\left(P_D - \sum\nolimits_{\mathrm{i}\in\mathcal{N}} P_\mathrm{i}\right) \\ & + \sum\nolimits_{\mathrm{i}\in\mathcal{N}} \sigma_\mathrm{i}^+(P_\mathrm{i} - P_\mathrm{i}^{\max}) \\ & + \sum\nolimits_{\mathrm{i}\in\mathcal{N}} \sigma_\mathrm{i}^-(P_\mathrm{i}^{\min} - P_\mathrm{i}) \end{aligned} \tag{3.3}$$

where the Lagrange multiplier λ is associated with the power balance constraint (3.2b), $\{\sigma_\mathrm{i}^+, \sigma_\mathrm{i}^-\}$ with the maximum and minimum power outputs of DGs in equation (3.2c), respectively. The KKT optimality conditions of the problem are:

Stationarity condition:

$$\frac{\partial\mathbb{L}}{\partial P_\mathrm{i}} = \nabla C_\mathrm{i}(P_\mathrm{i}) - \lambda + \sigma_\mathrm{i}^+ - \sigma_\mathrm{i}^- = 0 \qquad \mathrm{i}\in\mathcal{N} \tag{3.4a}$$

Complementary slackness:

$$\sigma_\mathrm{i}^+(P_\mathrm{i} - P_\mathrm{i}^{\max}) = 0 \qquad \mathrm{i}\in\mathcal{N} \tag{3.4b}$$

$$\sigma_\mathrm{i}^-(P_\mathrm{i}^{\min} - P_\mathrm{i}) = 0 \qquad \mathrm{i}\in\mathcal{N} \tag{3.4c}$$

Primal feasibility:

(3.2b)(3.2c)

Dual feasibility:

$$\sigma_\mathrm{i}^+,\ \sigma_\mathrm{i}^- \ge 0 \qquad \mathrm{i}\in\mathcal{N} \tag{3.4d}$$

From (3.4a), it follows that at the optimal point, it must be true that

$$\lambda = \nabla C_\mathrm{i}(P_\mathrm{i}) + \sigma_\mathrm{i}^+ - \sigma_\mathrm{i}^- \qquad \mathrm{i}\in\mathcal{N} \tag{3.5}$$

Based on the optimality conditions of the centralized optimal dispatch problem, a new distributed control strategy is designed with the objective of providing frequency regulation, while driving the microgrid to an optimal dispatch that complies with the KKT conditions (3.4a) - (3.4d).

Previously to show the Distributed Optimal Dispatch Proposed, the distributed-averaging proportional-integral (DAPI) approach presented in [32] is studied. DAPI controller is modified in order to achieve the optimal dispatch, as will be shown in Section 3.1.4.

3.1.3 Distributed Frequency and Voltage Restorator Control

The distributed-averaging proportional-integral (DAPI) approach presented in [32] is used in this work for frequency regulation, it is shown in (3.6) (3.7) where m_i is $P-\omega$ droop coefficient, P_i is the real power injection, ω^* is the nominal frequency and ω_i corresponds to frequency regulated in the ith DG.

The DAPI secondary control action Ω_i in is obtained from (3.7), where the terms $a_{\mathrm{i}j}$ are the entries of the adjacency matrix; thus, the control action Ω_j is shared with generator i only if $a_{\mathrm{i}j}$ is nonzero.

$$\omega_\mathrm{i} = \omega^* - m_\mathrm{i} P_\mathrm{i} + \Omega_\mathrm{i} \tag{3.6}$$

$$k_\mathrm{i}\dot{\Omega}_\mathrm{i} = -\left(\omega_\mathrm{i} - \omega^*\right) - \sum\nolimits_{j\in\mathcal{N}, j\neq\mathrm{i}} a_{\mathrm{i}j}(\Omega_\mathrm{i} - \Omega_j) \tag{3.7}$$

Also, DAPI voltage-regulation and reactive-power-sharing controllers are implemented based on [111]. The control law of this controller is represented by equations (3.8) and (3.9), where $\mathrm{e_i}$ is the control action for voltage regulation, E_i is the voltage of the ith DG, n_i represents the Q-E droop coefficient, E^* is the microgrid nominal voltage, Q_i^* is the reactive power rating of unit i, β_i and k_i are positive gains, and $a_{\mathrm{i}j}$ is an element of the adjacency matrix of communication between DGs. In this case $\mathrm{e_i}$ establishes a trade-off between voltage regulation and reactive power sharing.

$$E_\mathrm{i} = E^* - n_\mathrm{i} Q_\mathrm{i} + \mathrm{e_i} \tag{3.8}$$

$$\mathbf{k_i}\dot{\mathrm{e}}_\mathrm{i} = -\beta_\mathrm{i}\left(E_\mathrm{i} - E^*\right) - b_\mathrm{i}\sum\nolimits_{j\in\mathcal{N},,j\neq\mathrm{i}} a_{\mathrm{i}j}\left(\frac{Q_\mathrm{i}}{Q_\mathrm{i}^*} - \frac{Q_j}{Q_j^*}\right) \tag{3.9}$$

3.1.4 Proposed Distributed Optimal Dispatch

The proposed distributed controllers have the following features: i) The secondary control and the optimal economic dispatch are solved in the same time scale, ii) The distributed control approach is used, iii) The optimal dispatch is achieved using PI controllers, iv) The real-time measurements are used in order to obtain the economic optimal dispatch, v) The control actions for frequency regulation and optimal dispatch are added to the droop controller, vi) The communication network is connected, bidirectional and ideal (without large time-delays). vii) The communication topology is different from the electrical network topology.

Secondary control and the optimal economic dispatch need to be solved in the same time scale. The first stage comprises the design of secondary control for frequency and voltage

restoration, then in the second stage a new term is added in order to achieve the economic dispatch.

The distributed controller is based on communication network, and consensus algorithm. These topics was described previously in chapter 2. However, before studying the algorithm design the consensus algorithm is shown.

This section presents a distributed secondary control including optimal dispatch, this proposal is shown in (3.10). These two objectives of control are achieve in the same time scale.

The proposed controller aims at driving the system to an optimal dispatch that complies with the KKT conditions of the problem. For this purpose, equation (3.6) is modified as (3.10a), where the additional term ρ_{i} is a control action to drive the units to their optimal dispatch level.

In particular, control actions ρ_{i} changes the dispatch of DGs until all units reach the same value of λ. The condition of $\lambda_{\mathrm{i}} = \lambda_j = \lambda$ in steady-state is enforced by equation (3.10c), it is achieved because the consensus algorithm is applied, the consensus algorithm was explained in the Section 2.3.3 . In (3.10c), $a_{\mathrm{i}j}$ is the element of the adjacency matrix A, and j represents the neighboring, k_{i}^1 is a positive gains of the controller. .

λ, corresponds to the (unique) dual variable associated with the demand-supply balance equation of the microgrid's optimal dispatch problem, (3.5). Based on equation (3.5), the λ_{i} of each DG that complies with the stationarity condition can be calculated from (3.11).

$$\omega_{\mathrm{i}} = \omega^* - m_{\mathrm{i}}(P_{\mathrm{i}}) + \Omega_{\mathrm{i}} + \rho_{\mathrm{i}} \tag{3.10a}$$

$$k_{\mathrm{i}}\dot{\Omega}_{\mathrm{i}} = -(\omega_{\mathrm{i}} - \omega^*) - \sum\nolimits_{j\in\mathcal{N}(\mathrm{i})} a_{\mathrm{i}j}(\Omega_{\mathrm{i}} - \Omega_j) \tag{3.10b}$$

$$k_{\mathrm{i}}^1\dot{\rho}_{\mathrm{i}} = -\sum\nolimits_{j\in\mathcal{N}(\mathrm{i})} a_{\mathrm{i}j}(\lambda_{\mathrm{i}} - \lambda_j) \tag{3.10c}$$

$$k_{\mathrm{i}}^4\dot{\sigma}_{\mathrm{i}}^+ = \mu_{\mathrm{i}}^2 \max\left\{P_{\mathrm{i}} + \frac{1}{\mu_{\mathrm{i}}^2}k_{\mathrm{i}}^5\sigma_{\mathrm{i}}^+ - P_{\mathrm{i}}^{\max}, 0\right\} - k_{\mathrm{i}}^5\sigma_{\mathrm{i}}^+ \tag{3.10d}$$

$$k_{\mathrm{i}}^6\dot{\sigma}_{\mathrm{i}}^- = \mu_{\mathrm{i}}^3 \max\left\{P_{\mathrm{i}}^{\min} + \frac{1}{\mu_{\mathrm{i}}^3}k_{\mathrm{i}}^7\sigma_{\mathrm{i}}^- - P_{\mathrm{i}}, 0\right\} - k_{\mathrm{i}}^7\sigma_{\mathrm{i}}^- \tag{3.10e}$$

$$\lambda_{\mathrm{i}} = \nabla C_{\mathrm{i}}(P_{\mathrm{i}}) + \sigma_{\mathrm{i}}^+ - \sigma_{\mathrm{i}}^- \tag{3.11}$$

The Lagrange multipliers σ_{i}^+, σ_{i}^- from the centralized optimal economic dispatch are represented as control actions in the proposed distributed controllers. In this context, σ_{i}^+ and σ_{i}^- are local control actions to keep the active power dispatch of DG units within limits, which in equilibrium correspond to the dual variables associated with maximum and minimum active power limits, respectively.

The equations (3.10d) and (3.10e) induce increases in the values of σ_{i}^+ and σ_{i}^- whenever unit i goes beyond its maximum or minimum active power dispatch levels, respectively. Also, control actions σ_{i}^+ and σ_{i}^- are driven down to zero by the second term of the controller if the

active power dispatch of unit i is strictly within limits, where k_{i}^4, k_{i}^5, k_{i}^6, k_{i}^7, μ_{i}^2 and μ_{i}^3 are positive gains of the controllers.

The stationarity centralized KKT condition (3.4a) is satisfied through (3.10c) and (3.11) in the distributed controller, the complementary slackness constraints (3.4b) and (3.4c) are satisfied by (3.10d) and (3.10e) respectively. The dual feasibility constraints (3.4d) are satisfied by (3.10d) and (3.10e). Finally the primal feasibility condition defined by (3.2b) is satisfied by (3.10a), and the primal feasibility condition defined by (3.2c) is satisfied by (3.10d) and(3.10e).

The design and proper operation of the proposed distributed controller (3.10a) to (3.10e) and (3.11) relies on the following assumptions:

(i) Each DG in the microgrid is able to communicate Ω_{i}, λ_{i} to neighboring DGs through a connected and bidirectional communication network.

(ii) The communication topology is connected which means that all the nodes have at least one connection with another node.

Figure 3.2 shows the architecture of the local controller implemented in each DG that enables the distributed control strategy. The first layer corresponds to voltage and current control, also a virtual impedance is added for microgrids with resistive lines [112]. The second layer correspond to primary control droop, where the terms of the equations (3.6) and (3.8) are calculated using local measurements.

The proposed layer includes the distributed controllers for frequency and voltage restoration and economic dispatch. We added the term Ω_{i} from (3.10b) in order to achieve frequency restoration, and ρ_{i} in order to achieve the economic dispatch of the microgrid, this is obtained from (3.11), (3.10c), (3.10d) and (3.10e). The proposed controller receives from each neighbor j the following information: Ω_j, λ_j, Q_j and Q_j^*, while it sends $\Omega_{\mathrm{i}}, \lambda_{\mathrm{i}}, Q_{\mathrm{i}}$ and Q_{i}^*. The exchange of information between local DG controllers occurs through the communication network.

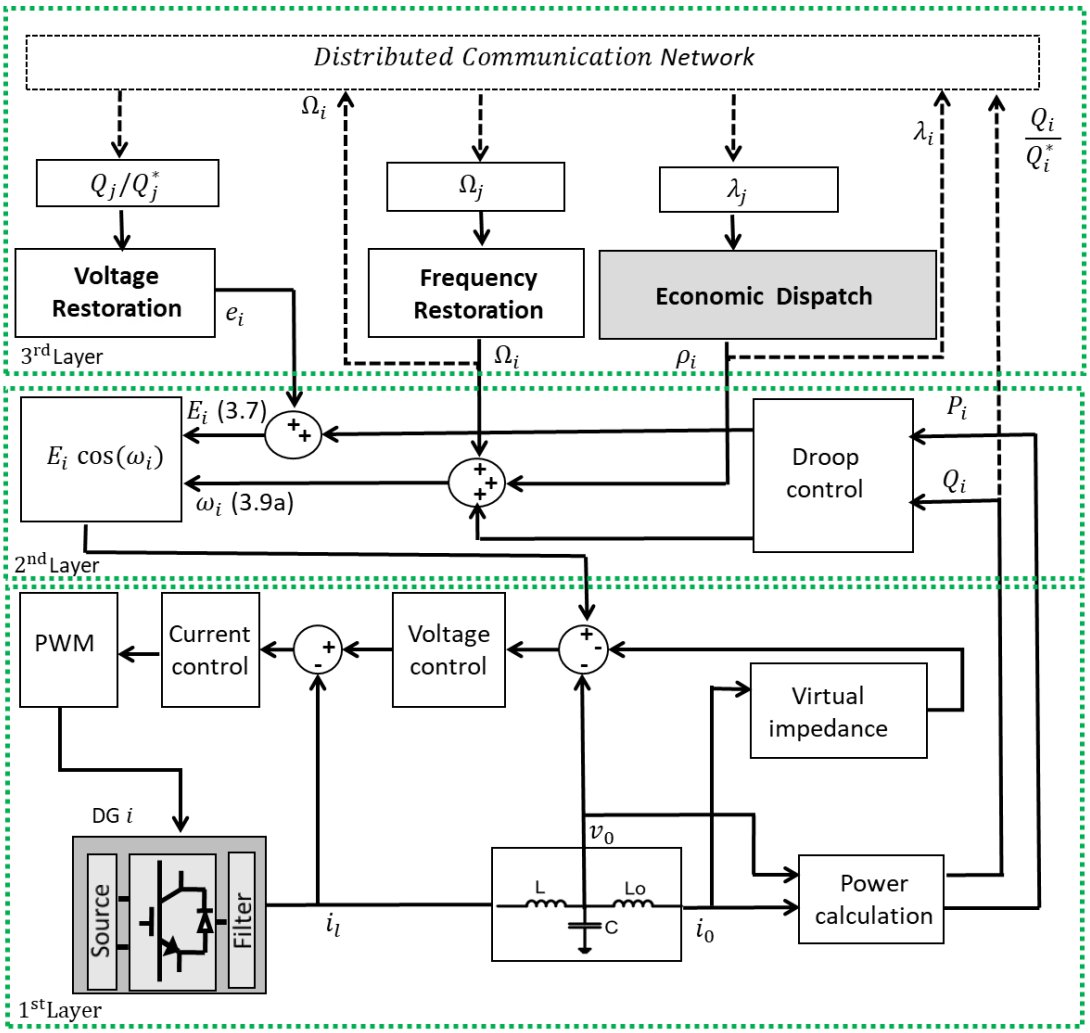

Figure 3.2: Distributed control scheme

3.2 Experimental Results

In order to validate the proposed controllers, experimental tests were performed in the Laboratory of Microgrids Control at the University of Chile shown in Figure 3.3. The microgrid topology is composed of three converters, two local loads and two power lines. The characteristics of DG units and network parameters are given in Table 3.1 and Table 3.2, respectively. Ethernet communication network is implemented to share information among DGs, as is shown at left side of Figure 3.3, and it is able to emulate a communication failure. The topologies, as well as the adjacency matrix A, with and without failure, are shown in Figure 3.4.

In this work different operating costs of each DG are considered, DG 2 has the lowest operating cost and DG 3 is the more expensive, the generating cost function (3.12) of each DG unit is assumed quadratic, the parameters used in this work are shown in Table 3.3.

$$C_i(P_i) = a_i P_i^2 + b_i P_i + c_i \tag{3.12}$$

Three operating scenarios are evaluated. i) Load impacts scenario. ii) Communication links failures scenario, where a failure of the communication link between DG 1 and DG 3 is produced (See Figure3.4b). iii) Controller performance when the DG 3 is disconnected of the microgrid.

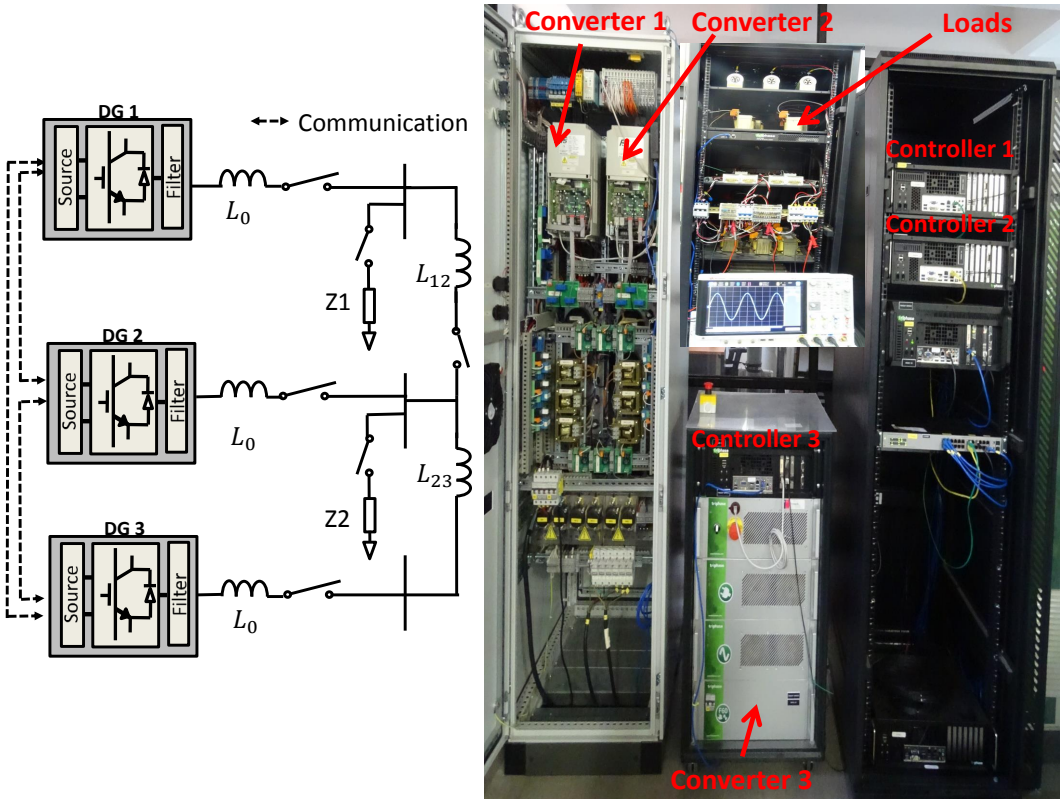

Figure 3.3: Microgrid experimental setup

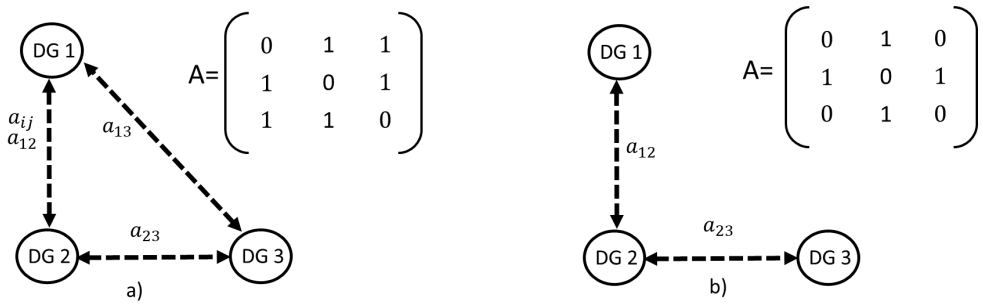

Figure 3.4: Microgrid communication topology a) Original topology b) Topology with communication links failure

Table 3.1: DG characteristics

Parameter	**Symbol**	**DG1-DG3**
Max Active Power	P_{i}^{max}	2kW
Min Active Power	P_{i}^{min}	0kW
P-W Droop Coefficient	m_{i}	$2.5{\cdot}10^{-3}\frac{\mathrm{rad}}{\mathrm{W}\cdot\mathrm{s}}$
Q-E Droop Coefficient	n_{i}	$1.5{\cdot}10^{-3}\frac{\mathrm{V}}{\mathrm{var}}$
Frequency Control Gain	k_{i}	0.5s
Voltage Control Gain	$\mathbf{k_i}$	1s
OD Control Gain	k_{i}^1	0.5s
Max Power Control Gain	k_{i}^2	0.1s
Min Power Control Gain	k_{i}^4	0.1s
Return to Zero Gain	$\frac{k_{\mathrm{i}}^3}{u_{\mathrm{i}}^2}, \frac{k_{\mathrm{i}}^5}{u_{\mathrm{i}}^3}$	0.01s

Table 3.2: Microgrid parameters

Parameter	**Symbol**	**Value**
Nominal Frequency	$\omega^*/2\pi$	50 Hz
Nominal Voltage	E^*	150 V
Filter Capacitance	C	25μF
Filter Inductance	L_f	1.8mH
Coupling Inductance	L_o	2.5mH
Sampling Period	T_{SP}	1/16E3 S
Load 1	L_1	11Ω
Load 2	L_2	22Ω
Line Impedance	$L_{\mathrm{i}}j$	2.5mH
Cutoff f−Droop filter	ω_c	1*2π rad/S

Table 3.3: DG Cost parameters

Parameter	**DG1**	**DG2**	**DG3**
$\mathrm{a_i}$ [\$/kW^2]	0.444	0.264	0.5
$\mathrm{b_i}$ [\$/kW]	0.111	0.067	0.125
$\mathrm{c_i}$ [\$]	0	0	0

3.2.1 Dynamic Performance

Figure 3.5 and Figure 3.6 show the experimental results when the load changes. At time-frame 1, the load 1 and the distributed control for frequency and voltage restoration are activated (equations (3.7) and (3.9)). At time-frame 2, the distributed proposed controller for economic dispatch is also activated (equations (3.11), (3.10c), (3.10d) and (3.10e)). At time-frame 3 the load 2 is added, finally at time-frame 4 the load 2 is removed.

As it can be seen in Figure 3.5a the frequency remains in the nominal value, when the proposed controller is activated (time-frame 2-4) and also when the load changes occurs

(time-frame 3 and 4). Figure 3.5b shows the voltage at the output of the three converters, as it can be seen the voltage remains in the nominal value in steady-state.

Figure 3.6 shows the real power generated by each DG unit, at time-frame 1 the real power is sharing by the units because only the frequency and voltage restorators are activated, also the power injected to the microgrid is equal in all DG units because their characteristics are the same. At time-frames 1 and 2 the load does not change, as it can be seen at time-frame 2 the DG units are re-dispatched considering the operating cost of each unit in order to archive the economic dispatch of the microgrid, the DG 2 generates more real power than the other units because its operating cost is the lowest, while DG 3 injects less real power than the other DG units because this is more expensive. The good performance of the proposed controller is shown with an increment and decrement of load at time-frame 3 and time-frame 4 respectively.

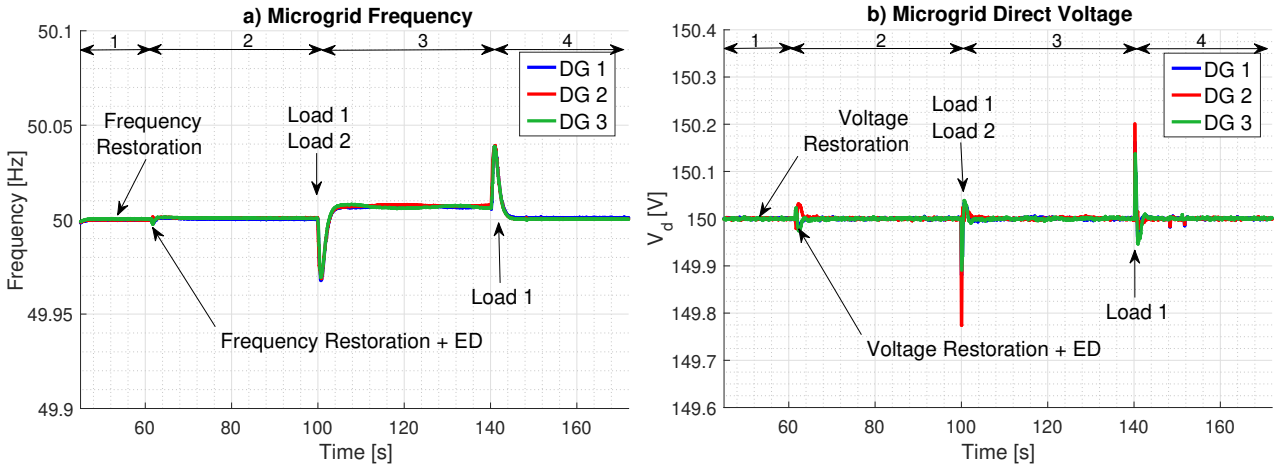

Figure 3.5: Distributed control response a) Frequency b) Voltage

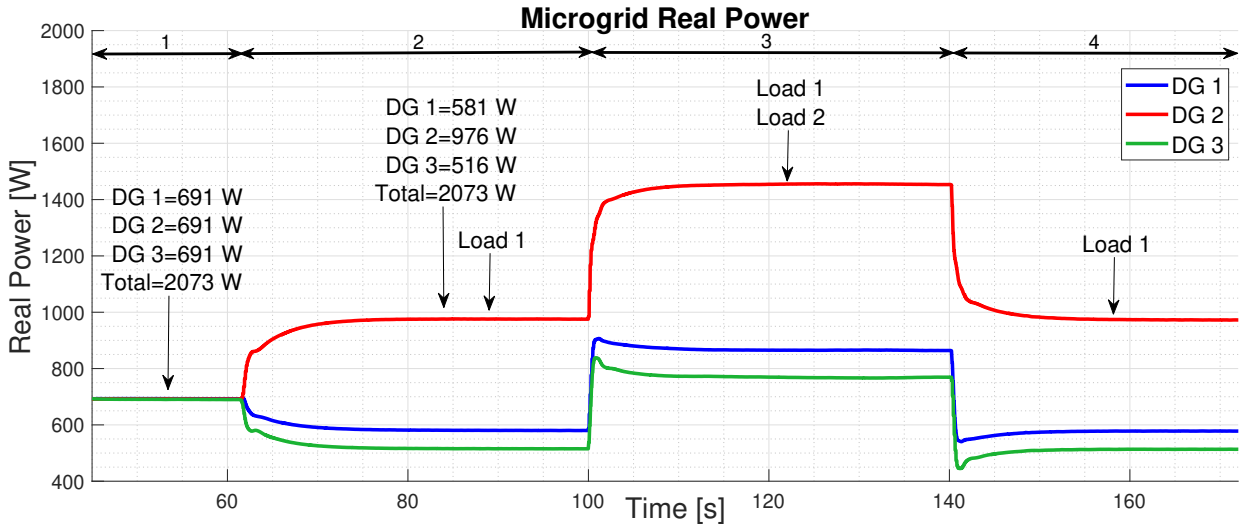

Figure 3.6: Distributed control response - Real Power

Figure 3.7 shows the total operating cost of the microgrid at the time-frame under study. The analysis includes two approaches. The blue line shows the total cost for the proposed distributed controller. The red line shows the total operating cost obtained from an optimal centralized dispatch performed off-line for each operating point, this approach might be on-line solved, however, a high computationally burden is involved. As it can be see the total cost of our proposal is the same as the total cost obtained by optimal centralized dispatch approach. Our proposal solves the optimal economic dispatch using PI controllers and achieves the same results obtained by the centralized approach. It is worth mentioning that the centralized optimal dispatch was performed off-line for the three operation points shown in Figure 3.7 with the aim to evaluate the economic performance of our proposal.

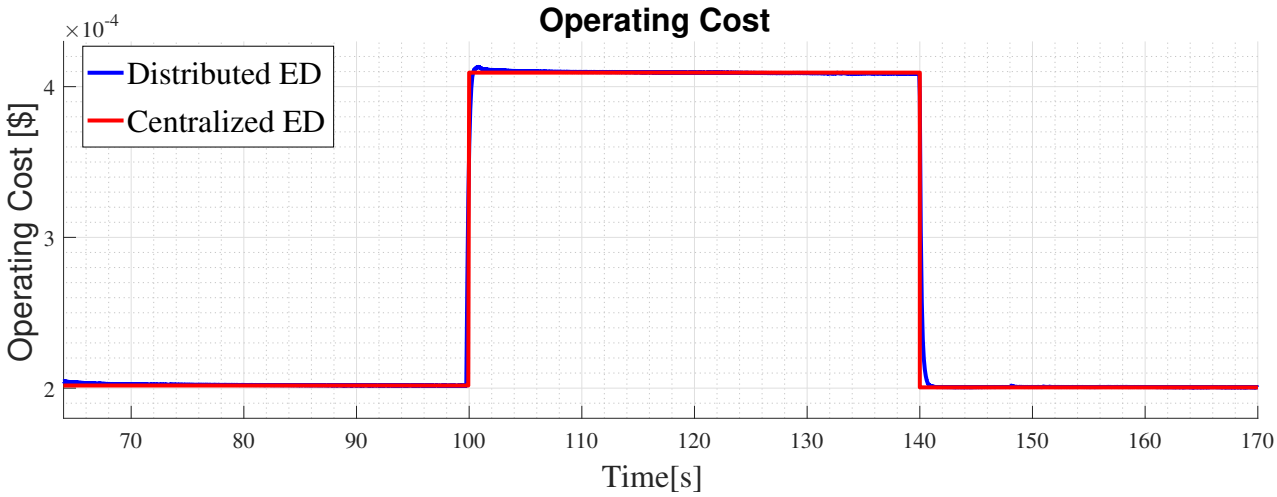

Figure 3.7: Operating cost

3.2.2 Performance Against the Sudden Loss of a DG Unit

In this scenario the DG 3 is disconnected, the results are shown in Figure 3.8 and Figure 3.9. During the time-frame 1 the proposed controllers (frequency and voltage restoration and economic dispatch) are activated, at time-frame 2 the DG 3 is disconnected, finally at time-frame 3 the load is increased.

In Figure 3.8a and Figure 3.8b the frequency and voltage are restored respectively to the nominal value when the disconnection of DG 3 is produced (time-frame 2 and time-frame 3). Figure 3.9 shows the results of the real power injected, at time-frame 2 when the DG 3 is disconnected the real power is re-dispatched considering the operating cost of each DG, thus the DG 2 supplies more real power than DG 1 because the operating cost of DG 2 unit is lower. In order to validate the controller performance when a DG unit is disconnected an incremental load is produced (time-frame 3). As it can be seen the frequency and voltage are restored to their nominal values, at the same time the operating cost of DG units are considered.

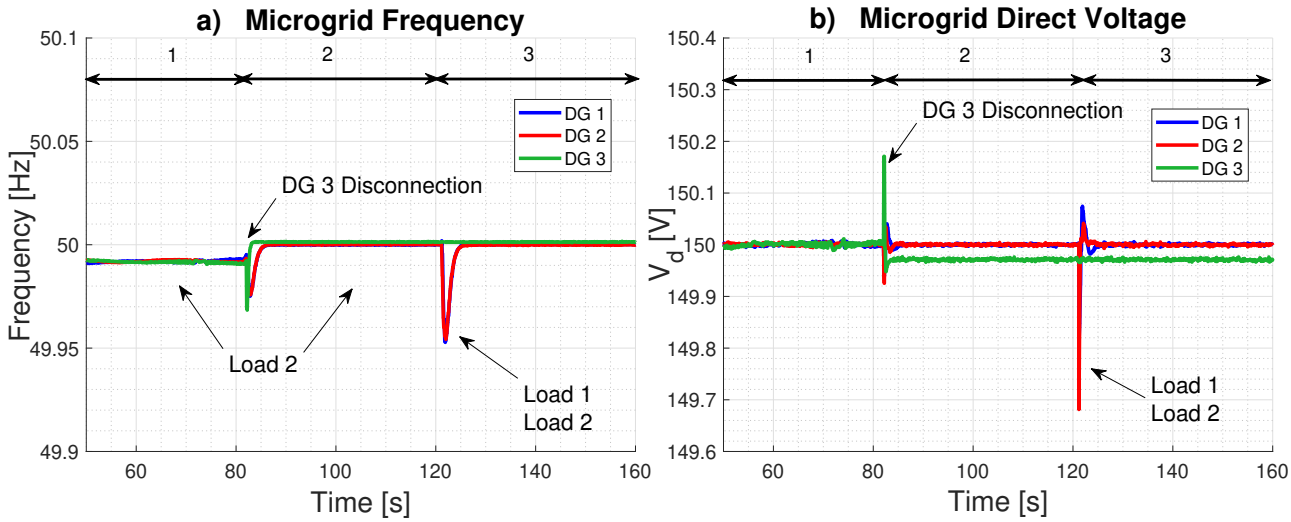

Figure 3.8: Distributed control response test by disconnecting DG3 a) Frequency b) Voltage

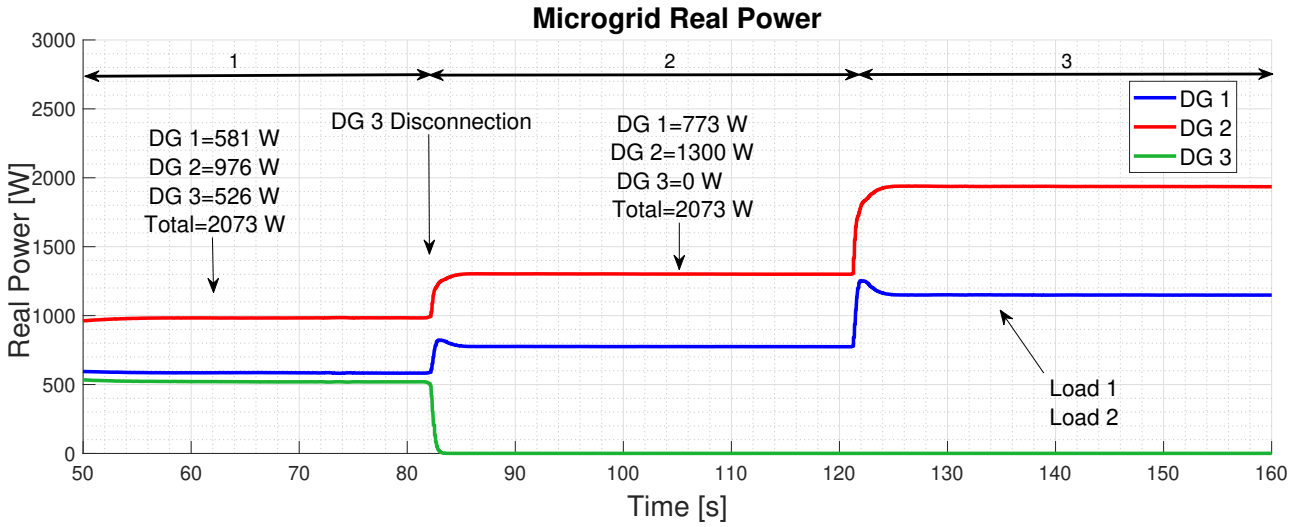

Figure 3.9: Distributed control response test by disconnecting DG3 - Real Power

3.2.3 Performance Against Communication Link Failures

Figure 3.10 and Figure 3.11 show the performance of the proposed distributed controller when a communication link failure occurs. At time-frame 1, load 1, and all controller proposed (frequency and voltage restoration and economic dispatch) are activated, at time-frame 2 the communication link between DG 1 and DG 2 fails (Figure 3.4b). Finally at time-frame 3 an incremental of load is produced (load 1 and load 2). As it can be seen the frequency (Figure 3.10a) and voltage (Figure 3.10b) remain in the nominal value when the communication link failure is produced.

In Figure 3.11, the real power does not change when a communication link failure is produced (time-frame 2), because the controller detects the change in the communication

network topology through the adjacency matrix, which is included in the consensus algorithm of the controller. Notice that the communication network topology is connected when the fail is produced.

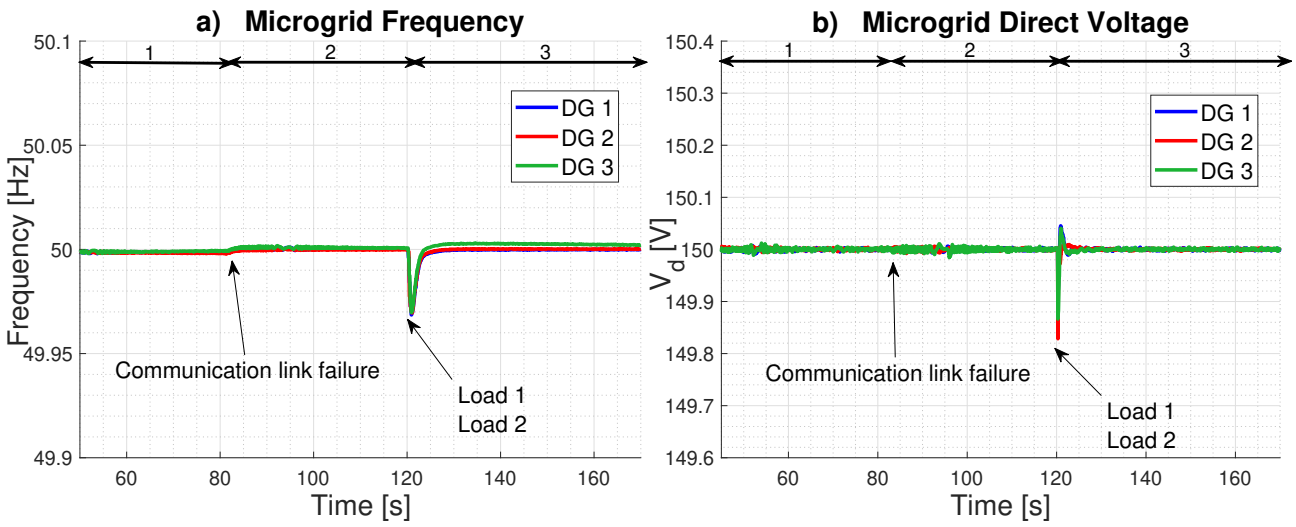

Figure 3.10: Distributed control response test by communication link failure a) Frequency b) Voltage

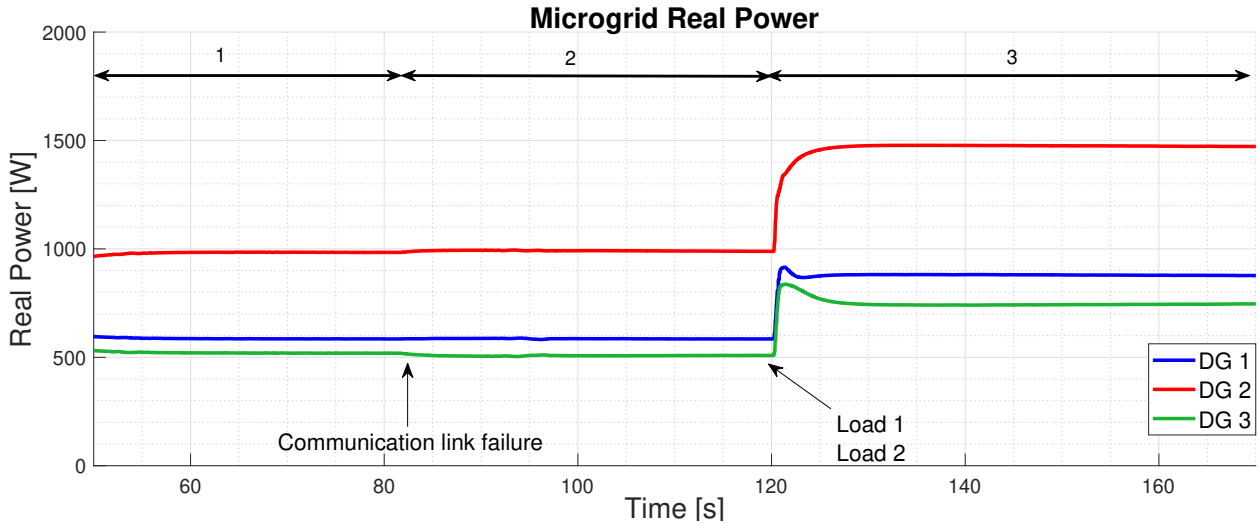

Figure 3.11: Distributed control response test by communication link failure - Real Power

3.3 Analysis and Discussion

The distributed controller proposed achieves the minimum operating cost when restoring frequency and voltage. The controller uses its local measurements and information exchanged among neighboring DG units through a communication network. In order to address economic dispatch, the controller includes the first KKT condition in the formulation, and it

does not need to know the topology of the microgrid, the minimum and maximum power limits of the generating units are considered. The experimental results validate the distributed controller's good performance against sudden changes in the load, failures in the communications links, and plug-and-play operation of DG.

The controller proposed in this chapter considers the following technical and economic tasks: minimum operating cost considering power limits of DG units, frequency, and voltage restoration in a distributed approach. To achieve these tasks, measurements and information exchanged among neighboring DG units through a communication network and consensus algorithm are required. The assumption of this proposal is that a communication network does not include delays, packet loss, connect network, and high bandwidth. However, the congestion from the electrical lines in the microgrid is not considered. It is worth mentioning that in a distributed approach this task has a challenge. In the next section, a novel distributed controller that solves the congestion from the electrical lines will be proposed.

Chapter 4

Distributed Control Strategy for Optimal Dispatch and Congestion Management

This chapter presents a novel distributed control strategy for frequency control, congestion management, and optimal dispatch (OD) in isolated microgrids. The proposed strategy drives the distributed generators (DGs) within the microgrid to a dispatch that complies with the Karush-Kuhn-Tucker (KKT) conditions of a linear optimal power flow (OPF) formulation. The controller relies on local power and frequency measurements, information from neighbouring DGs, and line-flow measurements transmitted through a communications network. Extensive simulations and experimental results show a good performance of the controller against sudden changes in the load, congested lines and availability of DGs in the microgrid, being able to successfully drive the system to an optimal economic operation.

4.1 Introduction

The optimal operation of a microgrid is typically obtained by solving an economic dispatch problem under a centralized approach. However, due to the advantages of distributed control approaches, recent works have proposed the use of distributed economic dispatch algorithms based on the decomposition techniques. On the other hand, the congestion in the electrical lines is a present issue in microgrid, because the DG units presents a plug&play operation, causing congestion along the lines. This problem can be addressed by control systems that manage congestion.

The multi-agent system (MAS) is a popular distributed control method, where a consensus algorithm is used for the coordination of agents. For instance, in [78] a MAS has been proposed for the optimal resource management in an isolated microgrid. In [94], frequency regulation and optimal dispatch controls are proposed based on MAS. The incremental cost consensus is frequently used when transmission losses are considered in optimal management [11, 78, 80]. In [78] an Energy Management System (EMS) based on an incremental cost consensus strategy is presented for optimal dispatch DG units and demand response. The strategy proposed in [80] reaches consensus of lagrangian multipliers using a correction term that ensures demand-supply balance.

The optimal distributed control schemes have also been used in bulk power systems. Some applications are presented in [79,113–115]. In [113] a decentralized optimal frequency control with controllable loads is described. In [114] a distributed optimal frequency control for a power system is proposed, achieving automatic congestion control.

The control of isolated microgrids is more challenging than in grid-connected ones due to a more critical demand-supply balance, and limited controllable assets to solve voltage and overloading problems [5]. Lines overloading, or congestion, can significantly affect the lifetime of the distribution lines and transformers in the microgrid, and the activation of thermal protections could can lead to unsupplied demand [9].

In bulk power systems, the congestion of transmission corridors is typically managed by re-dispatching generation units; however, more a advanced control can also be achieved by phase shifters, line switching, FACTS/HVDC controllers, and even load curtailment [20]. In distribution networks, the problem of congestion management has been mostly approached using demand flexibility [9,21–23], or smart transformers [104]; where the proposed solutions require adding new expensive technology to existing systems, or using distributed optimization techniques.

Recently, in [24], a consensus-based algorithm for frequency regulation in isolated microgrid has been proposed, taking into account the congestion of distribution lines. This work addresses the problem of congestion using a hierarchical approach where the Distribution Network Operator (DNO) sends optimal set points of generation, and a lower-level control changes these set point values for congestion management; therefore, the new set points are not optimal. To the best of the authors' knowledge, the problem of combined congestion management and optimal dispatch in microgrids has not been thoroughly studied in the existing literature.

In [116], a distributed control approach is proposed for frequency control and congestion management; however, the optimal economic operation is not considered. On the other hand, [114] present a distributed controller for cost-minimizing frequency regulation with consideration of capacity constraints and tie-line congestion in bulk power systems. This distributed control assumes a base economic dispatch and minimizes the cost of deviation to solve capacity violations, considering the use of virtual phase estimators to identify limit violations.

This thesis proposes a distributed inverter-control scheme for optimal dispatch of isolated microgrids considering congestion. Control rules are based on a decomposition of the optimal dispatch problem of a microgrid, and relies on local voltage and frequency measurements, as well as global congestion alerts triggered by current measurements in selected distribution lines. The contributions of this paper are as follows:

(i) A novel distributed control architecture for frequency control, congestion management, and optimal operation of the microgrid is proposed.

(ii) The proposed control strategy solves KKT conditions of a linear OPF formulation based on real system measurements, without requiring a mathematical power flow model.

(iii) We provide strong evidence via simulations that the controller is able to restore the optimal operation of the microgrid in the time-scale of the secondary frequency control. Moreover, the equivalence of the controller steady-state and KKT conditions of a linear OPF formulation is demonstrated.

This section shows a formulation of the network-constrained optimal dispatch problem in isolated microgrids. The formulation is then used to derive a distributed frequency and congestion controller that drives the system to a solution of the optimal dispatch problem. The proposed controller assumes the availability of current measurements from distribution lines and local DG controllers, all of which are shared through a communications network that allows bidirectional exchange of information.

4.2 Centralized Optimal Dispatch

Let's consider a balanced three-phase isolated microgrid, with a set of buses $\mathcal{J} = \{1, \dots, J\}$, a set of DGs $\mathcal{N} = \{1, \dots, N\}$ and a set of distribution lines $\mathcal{L} = \{1, \dots, L\}$. Each bus is equipped with either a generation unit, a load, or both.

Inductive lines of reactance X_{ij} connect buses i and j. Generation units inject real power P_i to the microgrid, which is constrained within minimum and maximum limits.

The optimal dispatch problem considered in this work determines the least-cost dispatch of controllable DG units in a microgrid while maintaining line currents within limits. The formulation is based on a single-bus system representation without losses; however, line capacity limits are imposed by additional constraints on DG power injections, as follows:

$$\underset{\mathbf{P}}{\text{minimize}} \quad \sum\nolimits_{\mathrm{i}\in\mathcal{N}} C_\mathrm{i}(P_\mathrm{i}) \tag{4.1a}$$

$$\text{subject to} \quad P_D = \sum\nolimits_{\mathrm{i}\in\mathcal{N}} P_\mathrm{i} \tag{4.1b}$$

$$I_\ell(\mathbf{P}) \le I_\ell^{\max} \qquad \forall\ \ell \in \mathcal{L} \tag{4.1c}$$

$$P_\mathrm{i}^{\min} \le P_\mathrm{i} \le P_\mathrm{i}^{\max} \qquad \forall\, \mathrm{i} \in \mathcal{N} \tag{4.1d}$$

where $\mathcal{N}$ and $\mathcal{L}$ are the sets of DGs and distribution lines in the microgrid, respectively, P_i is the real power dispatch of generator i, $C_\mathrm{i}(P_\mathrm{i})$ is a convex cost function, $\mathbf{P} = \{P_\mathrm{i} : \mathrm{i} \in \mathcal{N}\}$, P_D is the total microgrid demand, and $I_\ell^{\max}$ is the current limit of line ℓ.

The function $I_\ell(\mathbf{P})$ represents the magnitude of the current in distribution line ℓ in terms of the real power dispatch of DGs. In general, $I_\ell(\mathbf{P})$ is a non-linear function [117], and hence the optimization problem (4.1) is non-convex.

By considering the following linear approximation of $I_\ell(\mathbf{P})$ at a particular operating point I_ℓ^0:

$$I_\ell(\mathbf{P}) \approx I_\ell^0 + \sum\nolimits_{\mathrm{i}=1}^{n} P_\mathrm{i} G_{\mathrm{i}\ell} \tag{4.2}$$

, equation (4.1c) can be replaced by:

$$I_\ell^0 + \sum\nolimits_{\mathrm{i}\in\mathcal{N}} P_\mathrm{i} G_{\mathrm{i}\ell} \le I_\ell^{\max} \qquad \forall\ \ell \in \mathcal{L}\,, \tag{4.3}$$

where $G_{i\ell}$ corresponds to the participation factor of generator i in the current of distribution line ℓ. For a particular operating point $G_{i\ell}$ includes the sign of the current; thus lower limits on line currents are not required. It is assumed that participation factors $G_{i\ell}$ can be externally provided by, for example, an online estimator. The $G_{i\ell}$ estimation methodology used in this work is described in detail in subsection II-B.

The non-convex inequality constraints (4.1c) are replaced by (4.3); then, the problem (4.1) becomes convex. It is assumed that Slater's constraint qualification condition holds, implying strong duality, and that the problem may be studied through its Lagrange dual. The Lagrangian function of the optimal dispatch problem (4.1a), (4.1b), and (4.1d), using the linear approximation of functions $I_\ell(\mathbf{P})$ (4.3) is:

$$\begin{aligned}\mathbb{L}(P_{\mathrm{i}},\lambda,\gamma_\ell,\sigma_{\mathrm{i}}^+,\sigma_{\mathrm{i}}^-) &= \sum\nolimits_{\mathrm{i}\in\mathcal{N}} C_{\mathrm{i}}(P_{\mathrm{i}}) \\ &+ \lambda\left(P_D - \sum\nolimits_{\mathrm{i}\in\mathcal{N}} P_{\mathrm{i}}\right) \\ &+ \sum\nolimits_{\ell\in\mathcal{L}} \gamma_\ell\left(I_\ell^0 + \sum\nolimits_{\mathrm{i}\in\mathcal{N}} P_{\mathrm{i}} G_{i\ell} - I_\ell^{\max}\right) \\ &+ \sum\nolimits_{\mathrm{i}\in\mathcal{N}} \sigma_{\mathrm{i}}^+(P_{\mathrm{i}} - P_{\mathrm{i}}^{\max}) \\ &+ \sum\nolimits_{\mathrm{i}\in\mathcal{N}} \sigma_{\mathrm{i}}^-(P_{\mathrm{i}}^{\min} - P_{\mathrm{i}})\end{aligned} \tag{4.4}$$

where the Lagrange multiplier λ is associated with the power balance constraint (4.1b), $\{\gamma_\ell\}$ with line capacity limits (4.3), and $\{\sigma_{\mathrm{i}}^+, \sigma_{\mathrm{i}}^-\}$ with the maximum and minimum power outputs of DGs in equation (4.1d), respectively. The KKT optimality conditions of the problem are:
Stationarity condition:

$$\frac{\partial \mathbb{L}}{\partial P_{\mathrm{i}}} = \nabla C_{\mathrm{i}}(P_{\mathrm{i}}) - \lambda + \sum\nolimits_{\ell\in\mathcal{L}} \gamma_\ell G_{i\ell} + \sigma_{\mathrm{i}}^+ - \sigma_{\mathrm{i}}^- = 0 \qquad \mathrm{i}\in\mathcal{N} \tag{4.5a}$$

Complementary slackness:

$$\gamma_\ell\left(I_\ell^0 + \sum\nolimits_{\mathrm{i}\in\mathcal{N}} P_{\mathrm{i}} G_{i\ell} - I_\ell^{\max}\right) = 0 \qquad \ell\in L \tag{4.5b}$$

$$\sigma_{\mathrm{i}}^+(P_{\mathrm{i}} - P_{\mathrm{i}}^{\max}) = 0 \qquad \mathrm{i}\in\mathcal{N} \tag{4.5c}$$

$$\sigma_{\mathrm{i}}^-(P_{\mathrm{i}}^{\min} - P_{\mathrm{i}}) = 0 \qquad \mathrm{i}\in\mathcal{N} \tag{4.5d}$$

Primal feasibility:

(4.1b), (4.1d) and (4.2)

Dual feasibility:

$$\gamma_\ell,\ \sigma_{\mathrm{i}}^+,\ \sigma_{\mathrm{i}}^-\ \geq 0 \qquad \mathrm{i}\in\mathcal{N}\ \ \ell\in L \tag{4.5e}$$

From (4.5a), it follows that at the optimal point, it must be true that

$$\lambda = \nabla C_{\mathrm{i}}(P_{\mathrm{i}}) + \sum\nolimits_{\ell\in\mathcal{L}} \gamma_\ell G_{i\ell} + \sigma_{\mathrm{i}}^+ - \sigma_{\mathrm{i}}^- \qquad \mathrm{i}\in\mathcal{N} \tag{4.6}$$

Based on the optimality conditions of the centralized optimal dispatch problem, a new distributed control strategy is designed with the objective of providing frequency regulation,

while driving the microgrid to an optimal dispatch that complies with the KKT conditions (4.5).

Note that the formulation of the optimization problem does not include the coupling between line-currents and reactive power injections, since it is assumed the DAPI voltage control described in [32], and implemented in our case studies, controls reactive power injections to maintain voltages in their nominal values at all nodes. Thus, this work focuses on frequency control and congestion control by means of optimally dispatching of real power of DG units.

4.3 Online Estimator of Participation Factors

The online estimation methodology considers an event-based update of participation factors $G_{\mathrm{i}\ell}$, summarized as follows:

(i) Instantaneous participation factors $G^{*}_{\mathrm{i}\ell}(t)$ are continuously calculated as $G^{*}_{\mathrm{i}\ell}(t) = \Delta I_{\ell}(t)/\Delta P_{\mathrm{i}}(t)$, $\forall \ell$, where $\Delta P_{\mathrm{i}}(t) = P_{\mathrm{i}}(t) - P_{\mathrm{i}}^{ref}$ and $\Delta I_{\ell}(t) = I_{\ell}(t) - I_{\ell}^{ref}$. Parameters P_{i}^{ref} and I_{ℓ}^{ref} correspond to a previous operating point of the microgrid for which the current participation factors are deemed valid.

(ii) Variables $P_{\mathrm{i}}(t)$ are monitored for changes beyond a pre-defined threshold with respect to P_{i}^{ref} (e.g., 5% changes). Let us call t^{*} the time for which such condition is verified.

(iii) Parameters $G_{\mathrm{i}\ell}$ are updated after a pre-defined deadband period δ, as $G_{\mathrm{i}\ell} = G^{*}_{\mathrm{i}\ell}(t^{*}+\delta)$, and parameters P_{i}^{ref} and I_{ℓ}^{ref} are updated as $P_{\mathrm{i}}^{ref} = P_{\mathrm{i}}(t^{*}+\delta)$, $I_{\ell}^{ref} = I_{\ell}(t^{*}+\delta)$. Parameter δ is necessary to allow the instantaneous participation factors to arrive to a steady-state value after a disturbance in the system, in order to avoid unnecessary oscillations in the congestion controller. In particular, we use a value of $\delta = 0.5s$ in our case studies.

4.4 Distributed Control Scheme

Figure 4.1 shows the architecture of local controllers of each DG that enables the distributed control strategy. Three control layers are distinguished. The first layer corresponds to the output voltage and current controls, which rely only on local measurements. The second control layer corresponds to the primary droop, which determines the reference of frequency (ω_{i}) and voltage (E_{i}), used in the first control layer. Finally, the third control layer is related to voltage and frequency regulation, and the proposed congestion control. The voltage regulation control maintains the voltage at its nominal value, whereas the frequency regulation and proposed congestion control change the reference of the frequency droop controllers in order to maintain the frequency at its nominal value, remove the overloading of distribution lines, and drive the system to an optimal dispatch. In order to achieve the objectives of the third layer, local DG controllers minimize the terms of the lagrangian function in (4.4) associated with their local variables for given values of lagrangian multipliers. Then, by using a distributed averaging strategy, the controllers converge to unique global values of such multipliers. The exchange of information between local DG controllers occurs through the communication network shown in Figure 4.1. The required communication network, fre-

quency regulation control and congestion control strategies are explained in more detail in the following sections.

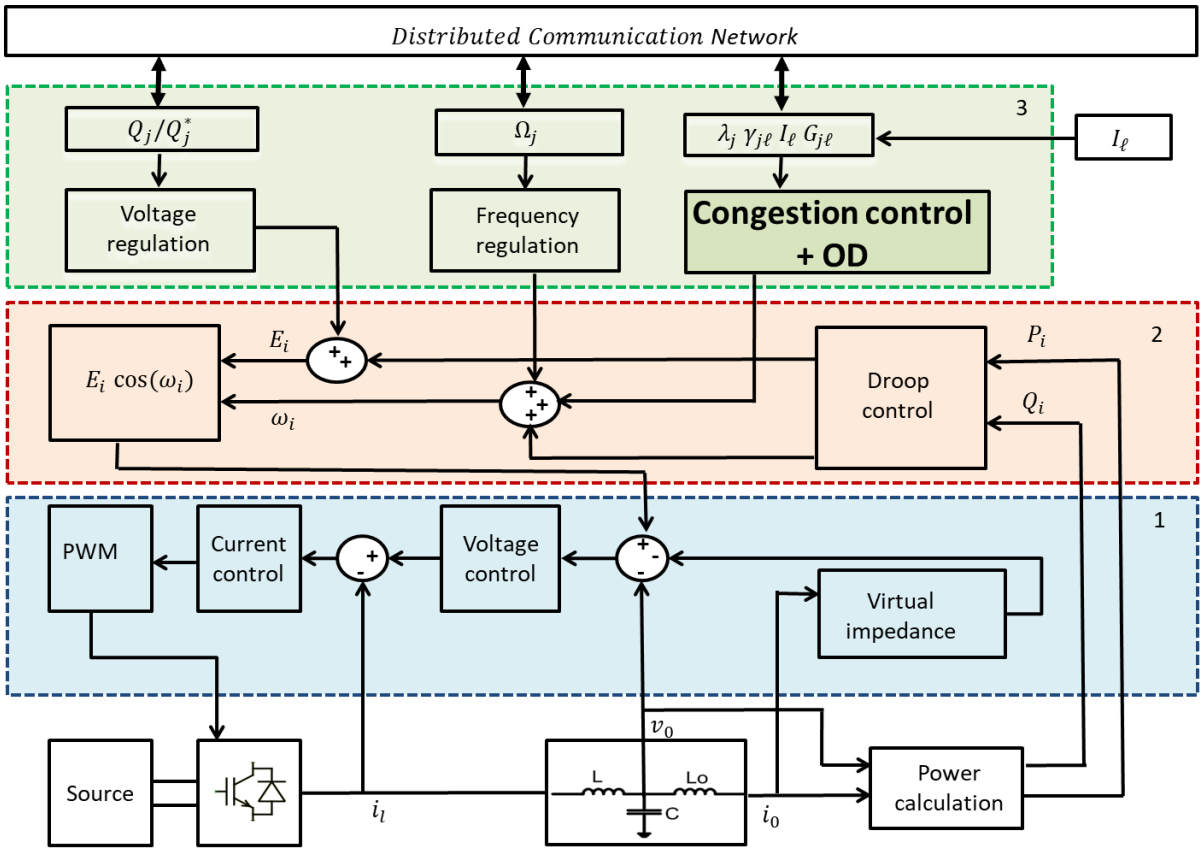

Figure 4.1: Distributed control architecture for each DG

4.4.1 Communication Structure

A communication network is required for the implementation of the proposed distributed control scheme. The bidirectional network is modelled as an undirected graph $\mathbb{G} = (\mathcal{N}, \mathcal{E}, A)$ between the DG units $\mathcal{N} = \{1, \ldots, N\}$, where $\mathcal{E}$ is the set of communication links and A is the nonnegative $N \times N$ weighted adjacency matrix. The elements of A are $a_{ij} = a_{ji} \geq 0$, with $a_{ij} > 0$ if and only if $\{i, j\} \in \mathcal{E}$ [32,57]. Let $x_i \in \mathbb{R}$ denote the value of some quantity of interest at bus i; in our specific context, x_i will be an internal controller variable. It is said the variables x_i achieve consensus if $x_i(t) - x_j(t) \to 0$ as $t \to \infty$. Consensus can be achieved via the following algorithm [55]:

$$\dot{x}_i = -\sum\nolimits_{j \in \mathcal{N}(i)} a_{ij}(x_i - x_j)$$

which is distributed according to the topology of the communication network.

Remark 1 (Communication Requirements)

The communications network through which the DG units exchange information, defined by the adjacency matrix A (see Figure 4.2), does not necessarily have the same topology as

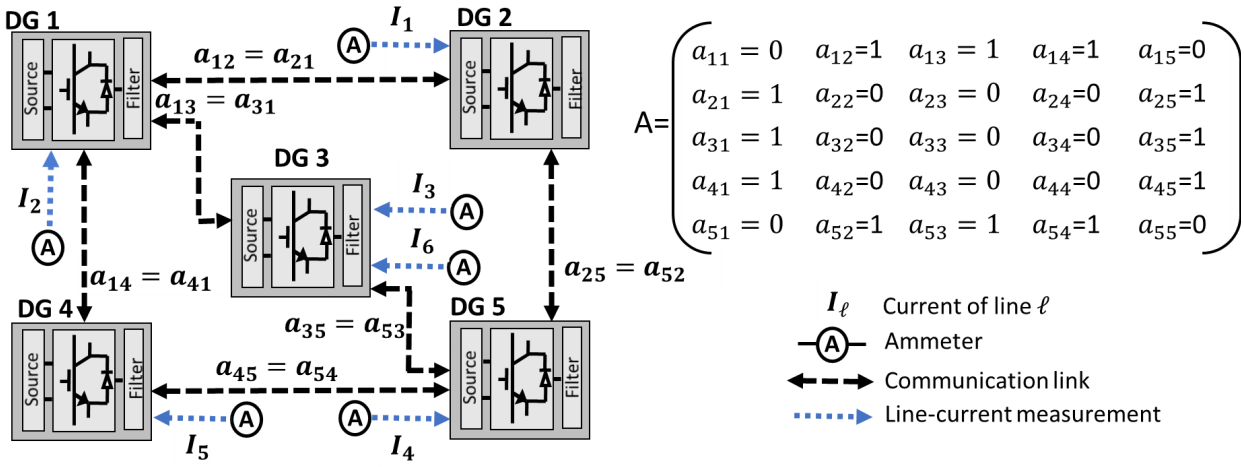

Figure 4.2: Communication topology and adjacency matrix.

the electric network of the microgrid. In this work, in order to ensure the optimal dispatch, power sharing, and congestion management, the communications network must allow bidirectional exchange of information. Also an ideal communication (without delays) is assumed. Notice that the use of the adjacency matrix can be extended to discrete, asynchronous and synchronous communication with delays [32, 57].

4.5 Congestion Control and Optimal Operation

This section presents a novel distributed congestion control to eliminate overloading in distribution lines of microgrids while maintaining optimality of dispatch (4.7). The design is based on the convex optimization problem (4.1a), (4.1b), (4.1d) and (4.3) presented in Section 4.2.

$$\omega_{\mathrm{i}} = \omega^* - m_{\mathrm{i}}(P_{\mathrm{i}}) + \Omega_{\mathrm{i}} + \rho_{\mathrm{i}} \tag{4.7a}$$

$$k_{\mathrm{i}}\dot{\Omega}_{\mathrm{i}} = -(\omega_{\mathrm{i}} - \omega^*) - \sum\nolimits_{j\in\mathcal{N}(\mathrm{i})} a_{\mathrm{i}j}(\Omega_{\mathrm{i}} - \Omega_j) \tag{4.7b}$$

$$k_{\mathrm{i}}^1\dot{\rho}_{\mathrm{i}} = -\sum\nolimits_{j\in\mathcal{N}(\mathrm{i})} a_{\mathrm{i}j}(\lambda_{\mathrm{i}} - \lambda_j) \tag{4.7c}$$

$$\begin{aligned} k_{\mathrm{i}}^2\dot{\gamma}_{\mathrm{i}\ell} = &-\sum\nolimits_{j\in\mathcal{N}(\mathrm{i})} a_{\mathrm{i}j}(\gamma_{\mathrm{i}\ell} - \gamma_{j\ell}) \\ &+ \mu_{\mathrm{i}}^1 \max\left\{I_\ell + \frac{1}{\mu_{\mathrm{i}}^1}k_{\mathrm{i}}^3\gamma_{\mathrm{i}\ell} - I_\ell^{\max}, 0\right\} - k_{\mathrm{i}}^3\gamma_{\mathrm{i}\ell} \end{aligned} \tag{4.7d}$$

$$k_{\mathrm{i}}^4\dot{\sigma}_{\mathrm{i}}^+ = \mu_{\mathrm{i}}^2 \max\left\{P_{\mathrm{i}} + \frac{1}{\mu_{\mathrm{i}}^2}k_{\mathrm{i}}^5\sigma_{\mathrm{i}}^+ - P_{\mathrm{i}}^{\max}, 0\right\} - k_{\mathrm{i}}^5\sigma_{\mathrm{i}}^+ \tag{4.7e}$$

$$k_{\mathrm{i}}^6\dot{\sigma}_{\mathrm{i}}^- = \mu_{\mathrm{i}}^3 \max\left\{P_{\mathrm{i}}^{\min} + \frac{1}{\mu_{\mathrm{i}}^3}k_{\mathrm{i}}^7\sigma_{\mathrm{i}}^- - P_{\mathrm{i}}, 0\right\} - k_{\mathrm{i}}^7\sigma_{\mathrm{i}}^- \tag{4.7f}$$

$$\lambda_{\mathrm{i}} = \nabla C_{\mathrm{i}}(P_{\mathrm{i}}) + \sum\nolimits_{\ell\in\mathcal{L}} \gamma_{\mathrm{i}\ell}G_{\mathrm{i}\ell} + \sigma_{\mathrm{i}}^+ - \sigma_{\mathrm{i}}^- \tag{4.8}$$

The proposed controller aims at driving the system to an optimal dispatch that complies with the KKT conditions of the problem. For this purpose, equation (3.7) is modified as (4.7a), where the additional term ρ_{i} is a secondary control action to drive the units to their optimal dispatch level considering congestion in the lines, and k_{i}^1 is a positive gain of the controller. In particular, control actions ρ_{i} will introduce a perturbation to the frequency droop controller in (4.7a) that changes the dispatch of DGs until all units reach the same value of λ, which corresponds to the (unique) dual variable associated with the demand-supply balance equation of the microgrid's optimal dispatch problem, (1b). The condition of $\lambda_{\mathrm{i}} = \lambda_j = \lambda$ in steady-state is enforced by equation (4.7c).

As in (4.3), $G_{\mathrm{i}\ell}$ represents the participation factor of unit i in the current of line ℓ, and it is obtained from an external online estimator.

Based on equation (4.6), the λ_{i} of each DG that complies with the stationarity condition can be calculated from (4.8). Variable $\gamma_{\mathrm{i}\ell}$ is a distributed congestion control action; $\gamma_{\mathrm{i}\ell}$ in equilibrium corresponds to the dual variable γ_ℓ in (4.5b). Finally, σ_{i}^+ and σ_{i}^- are local control actions to keep the active power dispatch of DG units within limits, which in equilibrium correspond to the dual variables associated with maximum and minimum active power limits, respectively.

The control action $\gamma_{\mathrm{i}\ell}$ is obtained from equation (4.7d), where the first term on the right-hand-side introduces a perturbation whenever there is a mismatch between the $\gamma_{\mathrm{i}\ell}$'s observed by neighbouring DGs. This is necessary in order to obtain unique γ_ℓ actions in steady state, which can then be interpreted as dual variables of line-current limit equations (4.3). The second and third terms induce an increase in the value of $\gamma_{\mathrm{i}\ell}$ in case of overloading of line ℓ, and a decrease down to zero when the overloading is (strictly) resolved. This is consistent with the fact that, if line ℓ is overloaded, the value of γ_ℓ is being underestimated by the controller; hence, it must be increased. Similarly, if the line-current limit is non-binding, the value of γ_ℓ must decrease down to zero. Finally, k_{i}^2, k_{i}^3, and μ_{i}^1 are positive gains of the controller. It is assumed throughout the paper that $k_{\mathrm{i}}^3/\mu_{\mathrm{i}}^1 = \kappa > 0$ for all $\mathrm{i} \in \mathcal{N}$.

Likewise, equations (4.7e) and (4.7f) induce increases in the values of σ_{i}^+ and σ_{i}^- whenever unit i goes beyond its maximum or minimum active power dispatch levels, respectively. Also, control actions σ_{i}^+ and σ_{i}^- are driven down to zero by the second term of the controller if the active power dispatch of unit i is strictly within limits, where k_{i}^4, k_{i}^5, k_{i}^6, k_{i}^7, μ_{i}^2 and μ_{i}^3 are positive gains of the controllers.

The design and proper operation of the proposed distributed controller relies on the following assumptions:

(i) Each DG in the microgrid is able to communicate Ω_{i}, λ_{i}, $\gamma_{\mathrm{i}\ell}$, I_ℓ to neighboring DGs through a connected and bidirectional communication network.

(ii) Each DG has information of $\gamma_{\mathrm{i}\ell}$ for all distribution lines of the microgrid, and each line subject to congestion has at least one DG with non-zero participation factor associated.

(iii) Current measurements of all distribution lines are available to the local controllers of all DGs in the microgrid.

(iv) Participation factors $G_{i\ell}$ are calculated with reasonable accuracy by an external online estimator and are available to each DG.

(v) Reactive power is only used for voltage control, and it is not available for solving overloading problems.

(vi) There is no conflict between control actions of congestion controllers of the different lines.

4.6 Distributed Congestion Control Optimality Demostration

Figure 4.3 shows the closed-loop microgrid system. The network model is defined by (4.9), where $p_\ell(\theta)$ in (4.9a) is the power flow from the line ℓ, B_{ij} is the line susceptance, and V_i and V_j are the voltages at i and j nodes. In (4.9b) the active power in the DG i is defined, where P_{Di} is the demand at the node i.

$$p_\ell(\theta) = V_i V_j B_{ij}(\theta_i - \theta_j) \qquad \ell = \{i, j\} \tag{4.9a}$$

$$P_i(\theta) = P_{Di} - \sum\nolimits_{j\in\mathcal{N}} V_i V_j B_{ij}(\theta_i - \theta_j) \qquad i \in \mathcal{N} \tag{4.9b}$$

Using also the proposed distributed control (4.7) and (4.8), the closed-loop microgrid system is given by the following equations (4.10)

$$\dot{\theta}_i = \omega^* - \omega_i \tag{4.10a}$$

$$\dot{\theta}_i = -m_i(P_i) + \Omega_i + \rho_i \tag{4.10b}$$

$$k_i\dot{\Omega}_i = m_i(P_i) - \Omega_i - \rho_i - \sum\nolimits_{j\in\mathcal{N}(i)} a_{ij}(\Omega_i - \Omega_j) \tag{4.10c}$$

$$\begin{aligned} k_i^1\dot{\rho}_i = &-\sum\nolimits_{j\in\mathcal{N}(i)}(\nabla C_i(P_i) + \sum\nolimits_{\ell\in\mathcal{L}} \gamma_{i\ell}G_{i\ell} + \sigma_i^+ - \sigma_i^-) \\ &- (\nabla C_j(P_j) + \sum\nolimits_{\ell\in\mathcal{L}} \gamma_{j\ell}G_{j\ell} + \sigma_j^+ - \sigma_j^-) \end{aligned} \tag{4.10d}$$

$$\begin{aligned} k_i^2\dot{\gamma}_{i\ell} = &-\sum\nolimits_{j\in\mathcal{N}(i)} a_{ij}(\gamma_{i\ell} - \gamma_{j\ell}) \\ &+ \mu_i^1 \max\left\{I_\ell + \frac{1}{\mu_i^1}k_i^3\gamma_{i\ell} - I_\ell^{\max}, 0\right\} - k_i^3\gamma_{i\ell} \end{aligned} \tag{4.10e}$$

$$k_i^4\dot{\sigma}_i^+ = \mu_i^2 \max\left\{P_i + \frac{1}{\mu_i^2}k_i^5\sigma_i^+ - P_i^{\max}, 0\right\} - k_i^5\sigma_i^+ \tag{4.10f}$$

$$k_i^6\dot{\sigma}_i^- = \mu_i^3 \max\left\{P_i^{\min} + \frac{1}{\mu_i^3}k_i^7\sigma_i^- - P_i, 0\right\} - k_i^7\sigma_i^- \tag{4.10g}$$

4.6.1 Distributed Congestion Control Optimality

This subsection discusses the optimality of the stationary points of the proposed distributed controller.

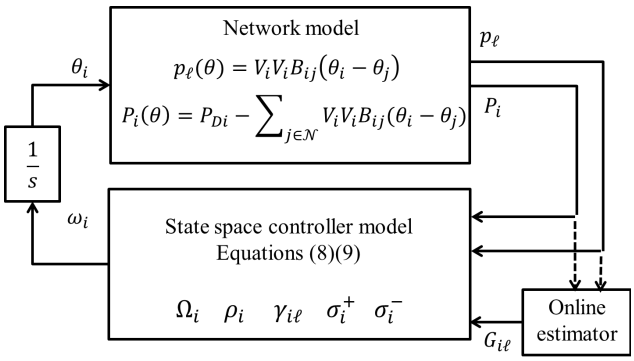

Figure 4.3: Close-loop microgrid system.

The optimum solution of the optimization problem described by (4.1a), (4.1b), (4.1d), and (4.3), must comply with the KKT conditions. Thus, in the following, an equilibrium point of the closed-loop system (4.10) also verifies the KKT conditions in (4.5a)-(4.5e).

Theorem 1 Distributed Optimal Dispatch. Consider the optimal dispatch problem (4.1a), (4.1b), (4.1d), and (4.3), and the closed-loop microgrid system (4.10). Assume that the dispatch problem has a strictly feasible point. Let
$(\theta_{\mathrm{i}}^*, \Omega_{\mathrm{i}}^*, \rho_{\mathrm{i}}^*, \gamma_{\mathrm{i}\ell}^*, (\sigma_{\mathrm{i}}^+)^*, (\sigma_{\mathrm{i}}^-)^*)$ be an equilibrium point of the closed-loop microgrid, and let

$$P_{\mathrm{i}}^* := P_{D\mathrm{i}} - \sum\nolimits_{j\in\mathcal{N}(\mathrm{i})} V_{\mathrm{i}} V_j B_{\mathrm{i}j}(\theta_{\mathrm{i}}^* - \theta_j^*), \qquad \mathrm{i}\in\mathcal{N}$$
$$\lambda_{\mathrm{i}}^* := \nabla C_{\mathrm{i}}(P_{\mathrm{i}}^*) + \sum\nolimits_{\ell\in\mathcal{L}} \gamma_{\mathrm{i}\ell}^* G_{\mathrm{i}\ell} + (\sigma_{\mathrm{i}}^+)^* - (\sigma_{\mathrm{i}}^-)^*$$

be the real power injections of each DG unit, and their lagrangian multipliers associated with the demand-supply balance equation. The following statements hold:

(i) for each $\ell \in \{1, \ldots, L\}$, there is a constant $\gamma_\ell^* \geq 0$ such that

$$\gamma_{\mathrm{i}\ell}^* = \gamma_\ell^* \quad \text{for all} \quad \mathrm{i}\in\mathcal{N};$$

(ii) there is a constant λ^* such that

$$\lambda_{\mathrm{i}} = \lambda^* \quad \text{for all} \quad \mathrm{i}\in\mathcal{N};$$

(iii) $(P_{\mathrm{i}}^*, \lambda^*, \gamma_\ell^*, (\sigma_{\mathrm{i}}^+)^*, (\sigma_{\mathrm{i}}^-)^*)$ is an optimal point of the optimization problem (4.1a), (4.1b), (4.1d), and (4.3) .

The proof of Theorem 1 is presented in following section.

Proof of Theorem 1

Theorem 1 states that any equilibrium point of the closed loop system under the proposed controller is also a KKT point. We proceed by showing that any equilibrium of the closed-loop microgrid yields a solution of the KKT condition.

Stationarity condition: We begin with (4.7c). Since the communication graph $\mathbb{G}$ is connected, it follows from (4.7c) that $\lambda_{\mathrm{i}} = \lambda_j = \lambda$ for some constant λ for all i, j [55]. Equation (4.8) then immediately yields the KKT stationarity condition (4.6).

Primal feasibility of power balance (4.1b)**:**

Equation (4.1b) corresponds to physical constraints of energy balance that is always satisfied in the system. From equation (4.10) of the closed-loop microgrid system, it is directly deductible (4.10a) that at equilibrium, $\omega_{\mathrm{i}} = \omega^*$, this equality is satisfied when the power balance is achieved.

Complementary slackness of DG active power limits:

The equations (4.7e) and (4.7f) in equilibrium yield

$$0 = \mu_{\mathrm{i}}^2 \cdot \max\left\{P_{\mathrm{i}} + \frac{1}{\mu_{\mathrm{i}}^2} k_{\mathrm{i}}^5 \sigma_{\mathrm{i}}^+ - P_{\mathrm{i}}^{\max}, 0\right\} - k_{\mathrm{i}}^5 \sigma_{\mathrm{i}}^+ \tag{4.11a}$$

$$0 = \mu_{\mathrm{i}}^3 \cdot \max\left\{P_{\mathrm{i}}^{\min} + \frac{1}{\mu_{\mathrm{i}}^3} k_{\mathrm{i}}^7 \sigma_{\mathrm{i}}^+ - P_{\mathrm{i}}, 0\right\} - k_{\mathrm{i}}^7 \sigma_{\mathrm{i}}^- \tag{4.11b}$$

for all $\mathrm{i} \in \{1, \ldots, n\}$. We will prove that complementarity condition (4.5c) holds in equilibrium, using equation (4.11a). In light of (4.11a), the set of buses can be partitioned into two disjoint sets $U, V \subset \{1, \ldots, n\}$ such that

$$P_{\mathrm{i}} + \frac{1}{\mu_{\mathrm{i}}^2} k_{\mathrm{i}}^5 \sigma_{\mathrm{i}}^+ - P_{\mathrm{i}}^{\max} \leq 0\,, \qquad \mathrm{i} \in U\,, \tag{4.12a}$$

$$P_{\mathrm{i}} + \frac{1}{\mu_{\mathrm{i}}^2} k_{\mathrm{i}}^5 \sigma_{\mathrm{i}}^+ - P_{\mathrm{i}}^{\max} > 0\,, \qquad \mathrm{i} \in V\,. \tag{4.12b}$$

Then equation (4.11a) can be reduced to

$$\begin{aligned} 0 &= -k_{\mathrm{i}}^5 \sigma_{\mathrm{i}}^+\,, && \mathrm{i} \in U\,, \\ 0 &= \mu_{\mathrm{i}}^2 (P_{\mathrm{i}} - P_{\mathrm{i}}^{\max})\,, && \mathrm{i} \in V\,, \end{aligned}$$

from which we conclude that $\sigma_{\mathrm{i}}^+ = 0$ for all $\mathrm{i} \in U$ and $P_{\mathrm{i}} = P_{\mathrm{i}}^{\max}$ for all $\mathrm{i} \in V$. In either case, we conclude that $\sigma_{\mathrm{i}}^+ (P_{\mathrm{i}} - P_{\mathrm{i}}^{\max}) = 0$. For $\mathrm{i} \in U$, substitution of $\sigma_{\mathrm{i}}^+ = 0$ into (4.12a) immediately shows that $P_{\mathrm{i}} \leq P_{\mathrm{i}}^{\max}$ and for $\mathrm{i} \in V$, substitution of $P_{\mathrm{i}} = P_{\mathrm{i}}^{\max}$ into (4.12b) implies that $\sigma_{\mathrm{i}}^+ > 0$. We conclude that the complementary slackness condition (4.5c) holds, that the upper bound in (4.1d) is primal feasible, and that the multipliers σ_{i}^+ are dual feasible. Analogous arguments using (4.11b) show complementary slackness for σ_{i}^-, primal feasibility of the lower bound in (4.1d), and dual feasibility of σ_{i}^-.

Complementarity condition of line current limits: The equation (4.7d) at equilibrium yields

$$\begin{aligned} 0 = &- \sum\nolimits_{j \in \mathcal{N}(\mathrm{i})} a_{\mathrm{i}j} (\gamma_{\mathrm{i}\ell} - \gamma_{j\ell}) \\ &+ \mu_{\mathrm{i}}^1 \max\left\{I_\ell + \frac{1}{\mu_{\mathrm{i}}^1} k_{\mathrm{i}}^3 \gamma_{\mathrm{i}\ell} - I_\ell^{\max}, 0\right\} - k_{\mathrm{i}}^3 \gamma_{\mathrm{i}\ell} \end{aligned} \tag{4.13}$$

for all $\ell \in \{1, \ldots, L\}$. We will show that the complementarity condition (4.5b) holds. For each line ℓ, we partition the set of DGs into two disjoint subsets $R, S \subset \{1, \ldots, n\}$

$$I_\ell + \frac{1}{\mu_{\mathrm{i}}^1} k_{\mathrm{i}}^3 \gamma_{\mathrm{i}\ell} - I_\ell^{\max} \leq 0\,, \quad \mathrm{i} \in R\,, \tag{4.14a}$$

$$I_\ell + \frac{1}{\mu_{\mathrm{i}}^1} k_{\mathrm{i}}^3 \gamma_{\mathrm{i}\ell} - I_\ell^{\max} > 0\,, \quad \mathrm{i} \in S\,. \tag{4.14b}$$

With these definitions, equation (4.13) reduces to

$$\sum\nolimits_{j \in \mathcal{N}(\mathrm{i})} a_{\mathrm{i}j} (\gamma_{\mathrm{i}\ell} - \gamma_{j\ell}) = -k_{\mathrm{i}}^3 \gamma_{\mathrm{i}\ell}\,, \quad \mathrm{i} \in R\,, \tag{4.15a}$$

$$\sum\nolimits_{j \in \mathcal{N}(\mathrm{i})} a_{\mathrm{i}j} (\gamma_{\mathrm{i}\ell} - \gamma_{j\ell}) = \mu_{\mathrm{i}}^1 (I_\ell - I_\ell^{\max})\,, \quad \mathrm{i} \in S\,. \tag{4.15b}$$

The rest of the demonstration is separated in 3 cases:

- *Case I:* $S = \emptyset$ (i.e., $\mathrm{i} \in R,\ \forall \mathrm{i}$)
- *Case II:* $R = \emptyset$ (i.e., $\mathrm{i} \in S,\ \forall \mathrm{i}$)
- *Case III:* Both R and S are non-empty.

Case I

When S is empty, it follows from (4.15a) that

$$0 = -\sum\nolimits_{j \in \mathcal{N}(\mathrm{i})} a_{\mathrm{i}j} (\gamma_{\mathrm{i}\ell} - \gamma_{j\ell}) - k_{\mathrm{i}}^3 \gamma_{\mathrm{i}\ell}$$

for all $\mathrm{i} \in \{1, \ldots, n\}$. Letting $\boldsymbol{\gamma}_\ell = (\gamma_{1\ell}, \gamma_{2\ell}, \ldots, \gamma_{n\ell})^\mathsf{T}$, this equation may be written in matrix form as $M\boldsymbol{\gamma}_\ell = 0$, where

$$M_{\mathrm{i}j} = \begin{cases} -a_{\mathrm{i}j} & \text{if} \quad \mathrm{i} \neq j \\ \sum_{j \in \mathcal{N}(\mathrm{i})} a_{\mathrm{i}j} + k_{\mathrm{i}}^3 & \text{if} \quad \mathrm{i} = j \end{cases}$$

Since $k_{\mathrm{i}}^3 > 0$ for all $\mathrm{i} \in \{1, \ldots, n\}$, the symmetric matrix M has strictly positive diagonal entries and is strictly diagonally dominant; it is therefore positive definite, and we conclude that $\boldsymbol{\gamma}_\ell = 0$. We may therefore take $\gamma_\ell^* = 0$ in statement (i) of the Theorem. From (4.14a) then, we conclude that $I_\ell - I_\ell^{\max} \leq 0$. Therefore, the primal feasibility condition (4.3) is satisfied, the complementary slackness condition (4.5b) is satisfied, and the multipliers are dual feasible.

Case II

When the set R is empty, it follows from (4.15b) that

$$\sum\nolimits_{j \in \mathcal{N}(\mathrm{i})} a_{\mathrm{i}j} (\gamma_{\mathrm{i}\ell} - \gamma_{j\ell}) = \mu_{\mathrm{i}}^1 (I_\ell - I_\ell^{\max})\,,$$

for all $\mathrm{i} \in \{1, \dots, n\}$. Summing all these equations, we obtain

$$\sum\nolimits_{\mathrm{i}\in\mathcal{N}} \sum\nolimits_{j\in\mathcal{N}(\mathrm{i})} a_{\mathrm{i}j}(\gamma_{\mathrm{i}\ell} - \gamma_{j\ell}) = \sum\nolimits_{\mathrm{i}\in\mathcal{N}(\mathrm{i})} \mu_{\mathrm{i}}^1 (I_\ell - I_\ell^{\max}) \quad \forall \mathrm{i}, \ell$$

Since the communication graph $\mathbb{G}$ is undirected, the sum on the left is zero and we find that $\sum_{\mathrm{i}=1}^n \mu_{\mathrm{i}}^1 (I_\ell - I_\ell^{max})$, which implies that $I_\ell = I_\ell^{\max}$. Substituting $I_\ell = I_\ell^{\max}$ into (4.14b), we find that $\gamma_{\mathrm{i}\ell} > 0$. Substituting $I_\ell = I_\ell^{\max}$ into (4.15b), we find that

$$\sum\nolimits_{j\in\mathcal{N}(\mathrm{i})} a_{\mathrm{i}j}(\gamma_{\mathrm{i}\ell} - \gamma_{j\ell}) = 0\,.$$

Since the communication graph $\mathbb{G}$ is connected, this equation holds if and only if $\gamma_{\mathrm{i}\ell} = \gamma_{j\ell}$ for all $\mathrm{i}, j \in \{1, \dots, n\}$.

We may therefore take $\gamma_\ell^* = \gamma_{n\ell} > 0$ in statement (i) of the theorem. We conclude that the primal feasibility condition (4.3) is satisfied, the complementary slackness condition (4.5b) is satisfied, and the multipliers γ_ℓ^* are dual feasible. *Case III:* Now assume both sets S and R are non-empty. Assume first that the line ℓ is *not* congested, meaning that $I_\ell - I_\ell^{\max} \leq 0$. From (4.14a)–(4.14b) it holds that

$$\begin{aligned}
(I_\ell - I_\ell^{\max}) &\leq -\frac{1}{\mu_{\mathrm{i}}^1} k_{\mathrm{i}}^3 \gamma_{\mathrm{i}\ell}\,, \qquad \mathrm{i} \in R\,,\\
(I_\ell - I_\ell^{\max}) &> -\frac{1}{\mu_{\mathrm{i}}^1} k_{\mathrm{i}}^3 \gamma_{\mathrm{i}\ell}\,, \qquad \mathrm{i} \in S\,.
\end{aligned}$$

Assuming that $k_{\mathrm{i}}^3/\mu_{\mathrm{i}}^1 = \kappa > 0$ for all $\mathrm{i} \in \{1, \dots, n\}$, the above inequalities immediately imply that

$$\gamma_{\mathrm{i}\ell} > \gamma_{j\ell}\,, \qquad \mathrm{i} \in S\,, \quad j \in R\,. \tag{4.16}$$

Equation (4.15b) implies that

$$\sum\nolimits_{j\in\mathcal{N}(\mathrm{i})} a_{\mathrm{i}j}(\gamma_{\mathrm{i}\ell} - \gamma_{j\ell}) \leq 0\,, \quad \mathrm{i} \in S\,.$$

Since $a_{\mathrm{i}j} > 0$ for $j \in \mathcal{N}(\mathrm{i})$, this inequality implies that

$$\text{for all } \mathrm{i} \in S \text{ there exists } j \in \mathcal{N}(\mathrm{i}) \text{ s.t. } \gamma_{j\ell} \geq \gamma_{\mathrm{i}\ell}\,. \tag{4.17}$$

Now let $\overline{\gamma}_S = \max_{\mathrm{i}\in S} \gamma_{\mathrm{i}\ell}$ and let $\mathcal{I}^* \subseteq S$ be the set of indices for which the maximum is achieved. We claim that there exists an $\mathrm{i}^* \in \mathcal{I}^*$ such that i^* has a neighbour in the set R. To see that this is true, suppose that there was no such neighbour, which means that $\mathcal{N}(\mathrm{i}^*) \subset S$ for all $\mathrm{i}^* \in \mathcal{I}^*$. Then (4.17) implies that $\gamma_{j\ell} = \overline{\gamma}_S$ for all $j \in \mathcal{N}(\mathrm{i}^*)$, and therefore that $\mathcal{N}(\mathrm{i}^*) \subset \mathcal{I}^*$. Since the graph $\mathbb{G}$ is connected and R is non-empty, this argument can be repeated a finite number of times until we find an index $\mathrm{i}^* \in \mathcal{I}^*$ with a neighbour in R. For this index, (4.17) implies that there exists a $j \in \mathcal{N}(\mathrm{i}^*) \cap R$ such that $\gamma_{j\ell} \geq \overline{\gamma}_S$. However, this directly contradicts (4.16).

A similar contradiction argument can be applied in the case when the line is congested, meaning $I_\ell > I_\ell^{\max}$. We conclude that the assumption that the sets S and R are both non-empty was invalid, and therefore one set must always be empty, and we reduce to Case I or Case II.

4.7 Simulation Results

In order to validate the proposed distributed control strategy, its performance is assessed in a case study using the microgrid configuration shown in Figure 4.4. The microgrid is composed of five DG units, six distribution lines and four distributed loads. The characteristics of DG units and network parameters are given in Table 4.1 and Table 4.2, respectively.

The generation cost functions of DG unit are assumed quadratic ($C_i = \alpha_i P_i^2 + \vartheta_i P_i + \psi_i$), with parameters shown in Table 4.3 [118]. The communications network is represented by dashed lines in Figure 4.4. The control scheme shown in Figure 4.1 is implemented in each DG unit, together with the proposed distributed control described by equations (4.7) and (4.8).

The simulation was performed using the software PLECS [119], considering current measurements from each line, and local measurements of frequency, real power injection, output current, and voltage.

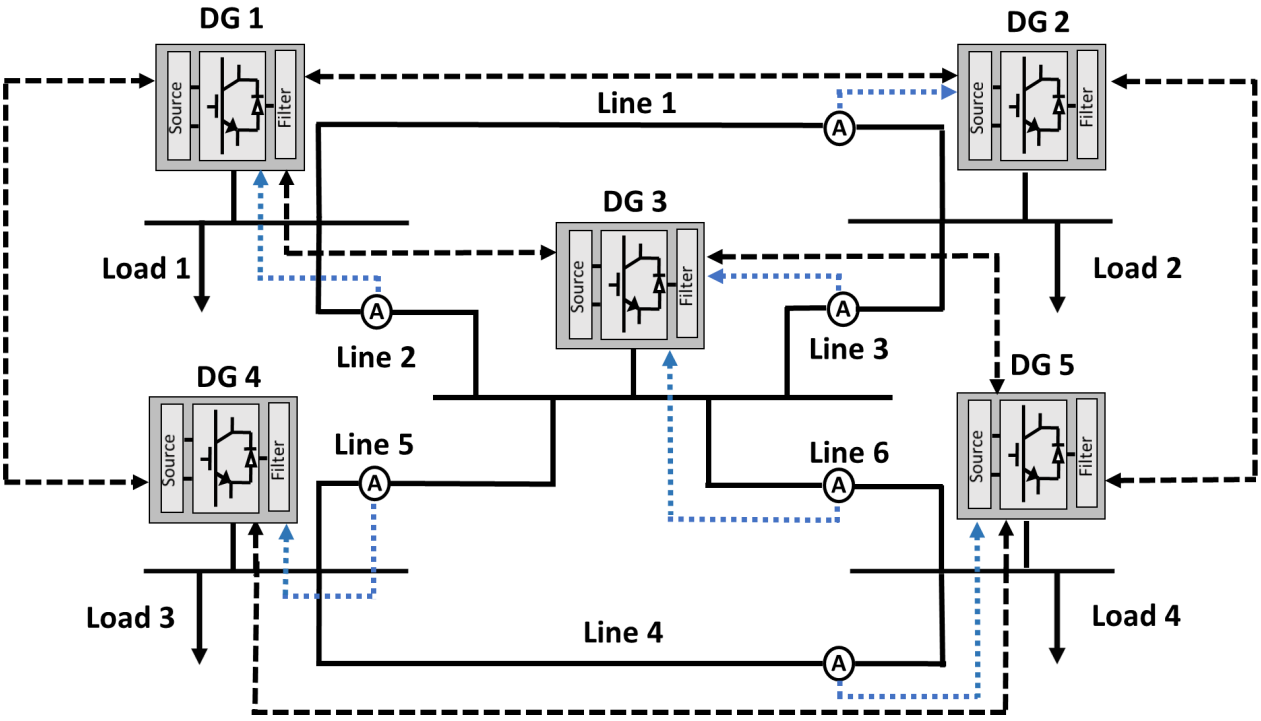

Figure 4.4: Microgrid study case

For voltage regulation purpose, DAPI voltage-regulation and reactive-power-sharing controllers are implemented based on [32]. The droop voltage E_i is defined by (4.18), where n_i represents the Q-E droop coefficient, E^* is the nominal voltage of the microgrid, Q_i is the reactive power injection, and e_i is the control action for voltage regulation, obtained from equation (4.19); e_i establishes a trade-off between voltage regulation and reactive power sharing, where Q_i^* is the reactive power rating of unit i. The consensus approach is used in order to achieve proportional reactive power sharing, where the normalized reactive power

injection $\frac{Q_j}{Q_j^*}$ of each DG is transmitted through the communications network shown in Figure 4.2. The terms β_i and k_i are positive gains, and $b_{\mathrm{i}j}$ is an element of the adjacency matrix of the bidirectional communications network.

$$E_\mathrm{i} = E^* - n_\mathrm{i} Q_\mathrm{i} + \mathrm{e_i} \tag{4.18}$$

$$\mathbf{k_i}\dot{\mathrm{e}}_\mathrm{i} = -\beta_\mathrm{i}\left(E_\mathrm{i} - E^*\right) - \sum\nolimits_{j\in\mathcal{N}(\mathrm{i})} b_{\mathrm{i}j}\left(\frac{Q_\mathrm{i}}{Q_\mathrm{i}^*} - \frac{Q_j}{Q_j^*}\right) \tag{4.19}$$

Table 4.1: DG characteristics

Parameter	**Symbol**	**DG1-DG5**
Maximum Active Power	P_i^{max}	2kW
Minimum Active Power	P_i^{min}	0kW
P-W Droop Coefficient	m_i	0.0025
Q-E Droop Coefficient	n_i	0.0015
Frequency Control Gain	k_i	0.5
Congestion Control Gain 1	k_i^1	0.5
Congestion Control Gain 2	k_i^2	0.25
Congestion Control Gain 4	k_i^4	0.1
Congestion Control Gain 6	k_i^6	0.1
Congestion Control Gain 7	$k_\mathrm{i}^3/\mu_\mathrm{i}^1 = \kappa$	10
Voltage Control Gain	$\mathbf{k_i}$	1

Table 4.2: Microgrid parameters

Parameter	Symbol	Value
Nominal Frequency	$\omega^*/2\pi$	50 Hz
Nominal Voltage	E^*	230 Vrms
Filter Capacitance	C	25μF
Filter Inductance	L_f	1.8mH
Output Impedance	L_o	1.8mH
Line Impedance 1	R,L	0.7Ω, 1.9mH
Line Impedance 2	R,L	0.7Ω, 1.9mH
Line Impedance 3	R,L	0.7Ω, 1.9mH
Line Impedance 4	R,L	0.7Ω, 1.9mH
Line Impedance 5	R,L	0.7Ω, 1.9mH
Line Impedance 6	R,L	0.7Ω, 1.9mH

4.7.1 Simulation Setup

Simulations for the dynamic performance of the controllers were carried out using a time-frame of 55 seconds. At 10 seconds, a 34% incremental step-change is applied to loads 1 and 3, and a 5% incremental step-change is applied to loads 2 and 4, producing the congestion

Table 4.3: DG Cost parameters

Parameter	**DG1**	**DG2**	**DG3**	**DG4**	**DG5**
α_{i} [\$/kW^2]	0.264	0.444	0.4	0.5	0.25
ϑ_{i} [\$/kW]	0.067	0.111	0.1	0.125	0.063
ϕ_{i} [\$]	0	0	0	0	0

of line 5. At 25 seconds, another 12% incremental step-change is applied to loads 1 and 3, and a 39% incremental step-change is applied to loads 2 and 4, yielding an overload of lines 2 and 3 of the microgrid. Finally, at 40 seconds, an 18% decremental step-change is applied to all loads.

The controller gains were tuned using a heuristic approach, where a first approximation of the gains was obtained using the root locus method applied to a condition where all the controllers are active (i.e., all the *max* operators take the value of the first argument). Then, several simulations were carried out for different operating points in order to fine-tune the gains, with satisfactory results. A more precise tuning of the controller could be performed using meta-heuristic optimization techniques; however, this is not addressed in the present work.

4.7.2 Simulation Results

In this section, the dynamic performance of the proposed controller (4.7), (4.8) is illustrated and discussed. It can be observed from Figure 4.5a and Figure 4.5b that the controller is able to successfully restore frequency and resolve congestion after each load perturbation. In specific, Figure 4.5a shows how the controller is able to restore the frequency of all DG units to their nominal value, after a transient of limited excursion.

Likewise, Figure 4.5b illustrates that thanks to the correct performance of the controller (4.7c)-(4.7f), (4.8), the congestion is quickly eliminated by driving line currents within limits. Figure 4.5b shows that before the first step-change in load all line currents are below their maximum limit, whereas Figure 4.5c shows that the load's real power is shared unevenly among the 5 DG units, due to their different cost functions. At 10 seconds, the first step-change occurs and line 5 becomes overloaded; however, the distributed congestion controller removes the overloading in less than 3 seconds, which is fast enough to avoid the activation of thermal protections in distribution lines. At 25 seconds, a second step-change in load is applied, resulting in an overloading of lines 2 and 3. Once again, the congestion control is able to resolve the congestion within a few seconds, as shown in Figure 4.5b (from 25 to 45 seconds).

The real power injected by each DG is shown in Figure 4.5c. When the congestion control action is zero (from 0 to 10 seconds and 40 to 55 seconds), the load's real power is shared among the DG units according to their operating cost (Table 4.3). However, when a control action is required to resolve a congestion (from 10 to 40 seconds), the real power injections of DG units are redistributed in order to remove the line overloading based on their different cost functions and participation factors.

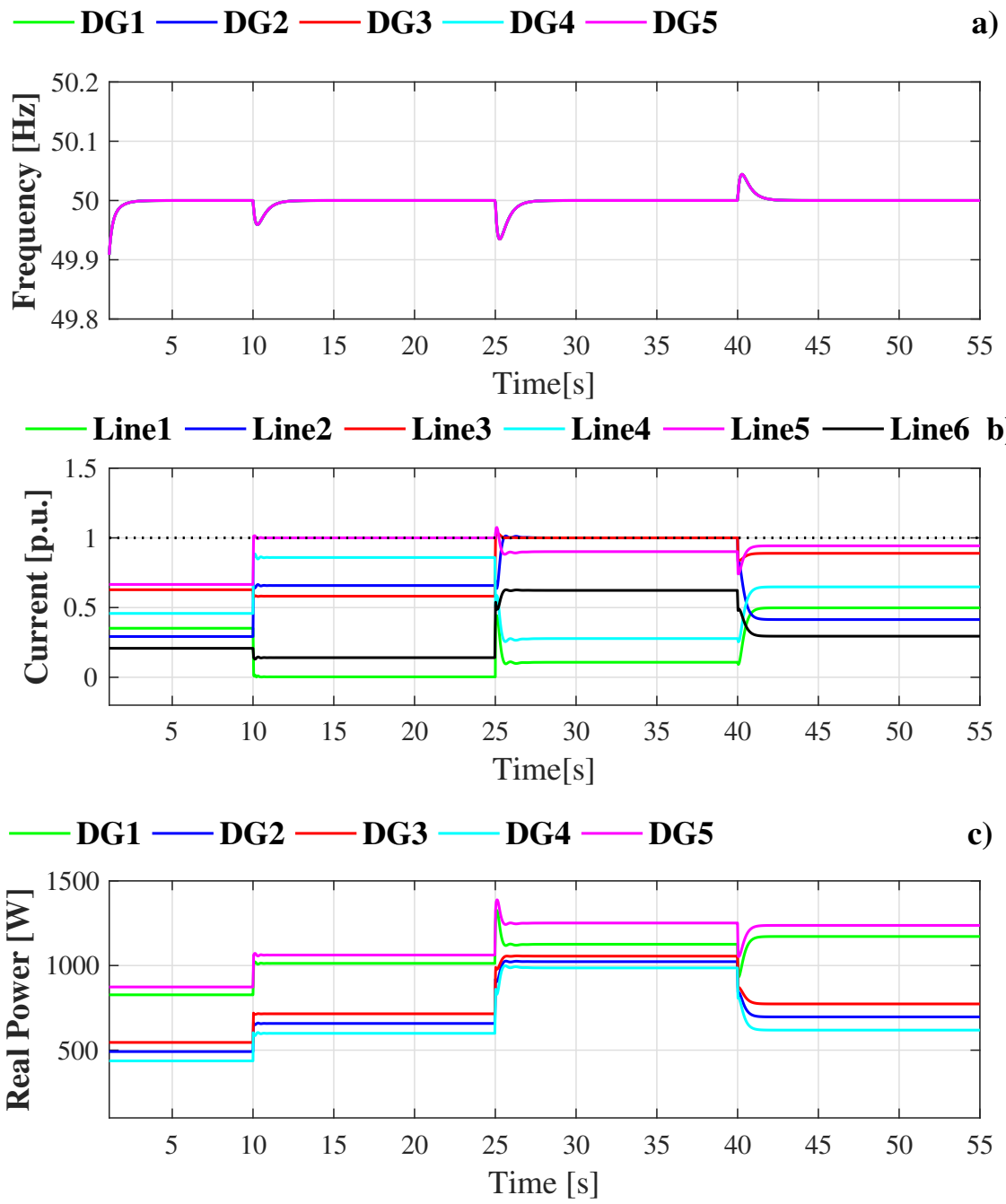

Figure 4.5: Distributed congestion control response a) Frequency at each DG, b) Current from the lines, c) Real power injection for each DG

The frequency restoration is driven by the control actions Ω_i in each DG unit, which are shown in Figure 4.6a. It can be observed that the actions converge to a unique value for all units that restores nominal frequency. Figures 4.6b, 4.6c, and 4.6d show the control actions $\gamma_{i\ell}$ used to remove the congestion in each line, respectively. On the other hand, Figure 4.6d shows how γ_{i5} are nonzero in the 10 to 25 seconds time-window in order to resolve the congestion in line 5. Likewise, in Figure 4.6b and Figure 4.6c the 25 to 40 seconds

time-window, both γ_{i2} and γ_{i3} control actions are required.

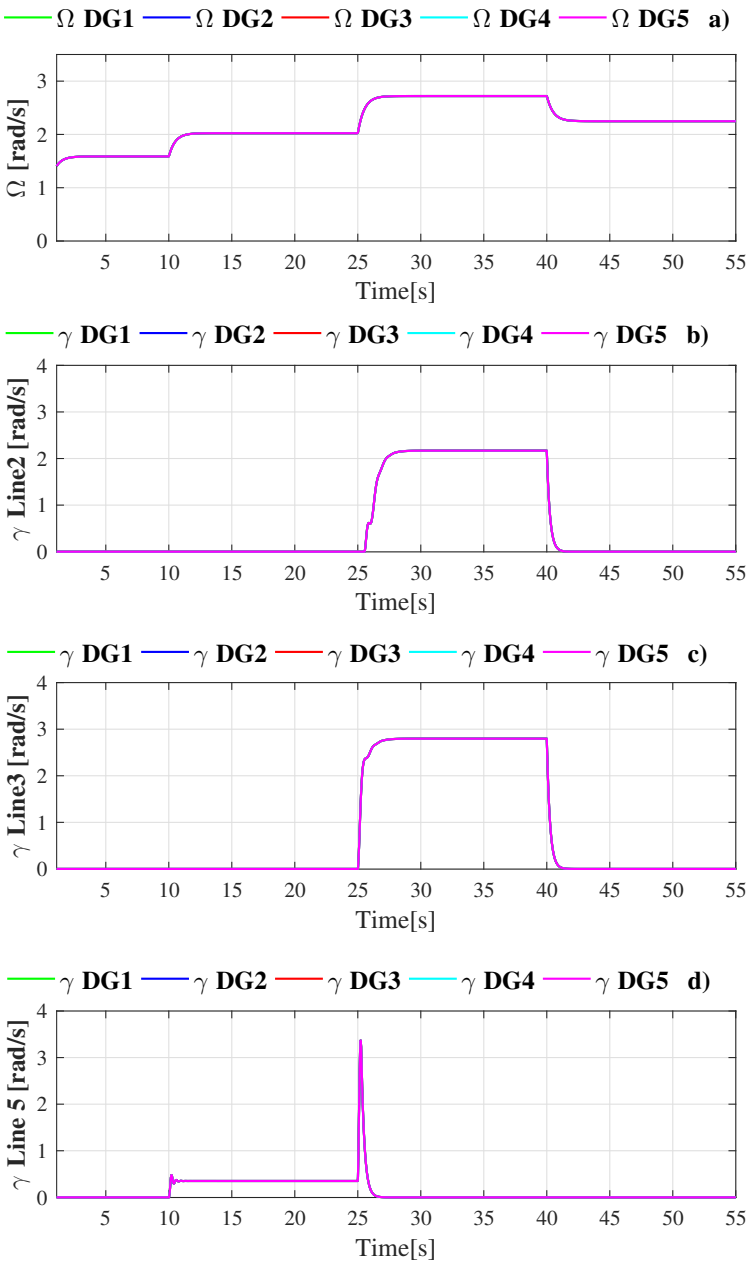

Figure 4.6: a) Control action for frequency regulation, b) Congestion control action for line 2, c) Congestion control action for line 3, d) Congestion control action for line 5

Figure 4.7 shows the λ_i of each DG unit. It can be observed that, in steady-state the values of λ_i converge to a unique value for all units, which then corresponds to the dual variable associated with the demand-supply balance equation in the centralized optimal dispatch problem.

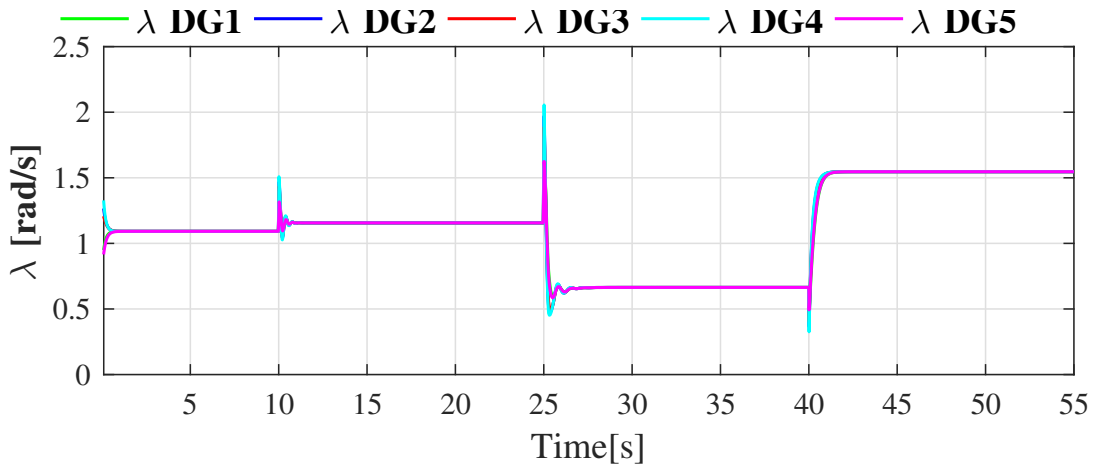

Figure 4.7: Lagrange multiplier λ

In order to analyze the performance of the controller against the sudden loss of a DG unit, a 34% incremental step-change is simulated in loads 1 and 3, and a 5% incremental step-change in loads 2 and 4 at 10 seconds, and the sudden loss of unit DG2 at 20 seconds, with both frequency regulation and congestion controllers activated. The simulation results are shown in Figure 4.8. Figure 4.8a shows that after the disconnection of DG2, frequency is restored to its nominal value within 2-3 seconds; moreover, Figure 4.8b shows that the congestion in line 4 produced by the the disconnection of DG2 is eliminated by the congestion controller (from 20 to 40 seconds). Figure 4.8c shows that at 20 seconds the real power of unit DG2 is drops to zero, and the remaining units increase their real power injections in order to satisfy the microgrid's demand, which remains unchanged, and considering the operating cost.

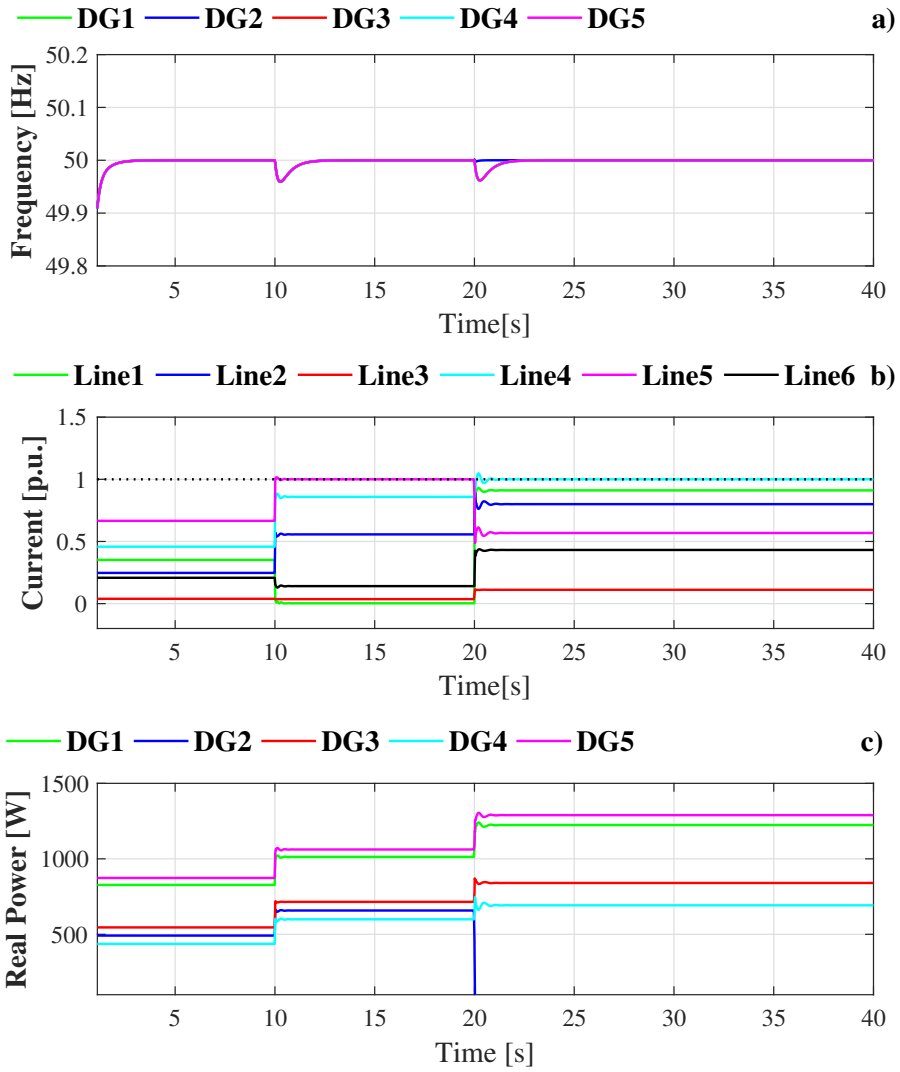

Figure 4.8: Distributed congestion control response test by disconnecting DG2 a) Frequency in each DG, b) Current from the lines, c) Real power injections for each DG

In order to analyze the performance of the controller against communication link failures we simulate a 34% incremental step-change in loads 1 and 3, and a 5% incremental step-change in loads 2 and 4 at 10 seconds, followed by the simultaneous failure of the communication links between units DG1 and DG2, and units DG3 and DG5 at 20 seconds, illustrated in Figure 4.9. Finally, a decremental step-change in loads is applied at 30 seconds to restore the initial loading of the microgrid. The simulation results are shown in Figure 4.10. It is observed that the proposed controller does not suffer noticeable deterioration in its performance against the loss of the communication links. Noteworthy, this results assume that the units have a dynamic adjacency matrix, which is instantly updated upon loss of communication links.

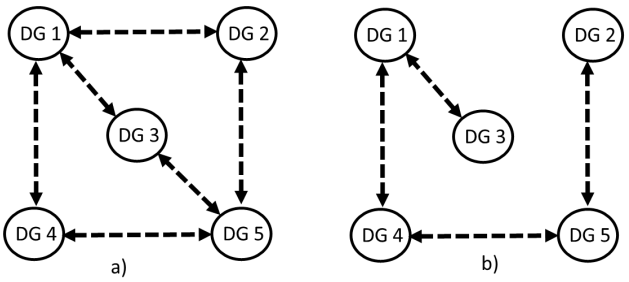

Figure 4.9: Microgrid communication topology a) Original topology, b) Topology with communication links failure

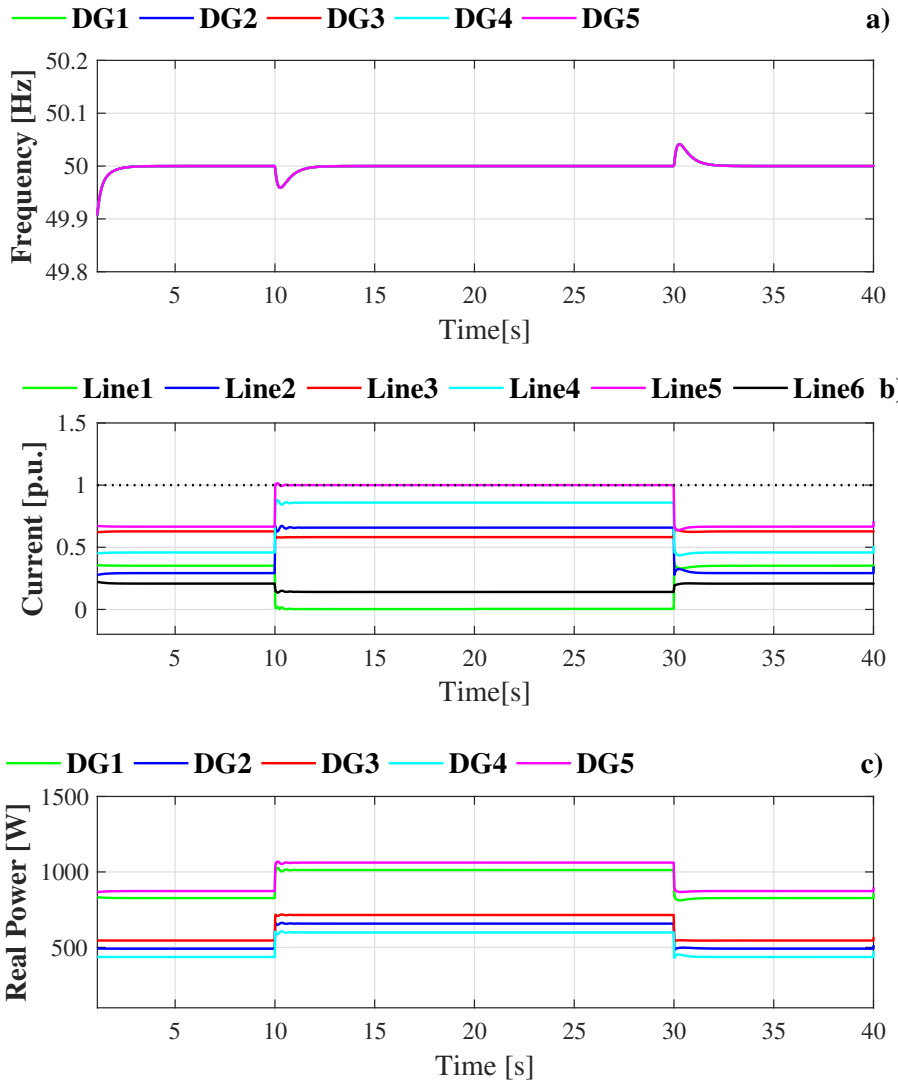

Figure 4.10: Distributed congestion control response test by communication link failure between (DG1 and DG2), and (DG3 and DG5) a) Frequency in each DG, b) Current from the lines, c) Real power injections for each DG

In order to analyze the performance of the controller against communication delays, we introduce constant delays τ_{i} in the consensus terms of the controller, as shown in equations (4.20). We simulate a 34% incremental step-change in loads 1 and 3, and a 5% incremental step-change in loads 2 and 4 at 30 seconds, and the performance of the controller is analyzed for two cases: a) small time-delays ($\tau_{\mathrm{i}} = 0.05s$), and b) large time-delays ($\tau_{\mathrm{i}} = 1s$).

$$k_{\mathrm{i}}\dot{\Omega}_{\mathrm{i}} = -(\omega_{\mathrm{i}} - \omega^*) - \sum\nolimits_{j\in\mathcal{N}(\mathrm{i})} a_{\mathrm{i}j}(\Omega_{\mathrm{i}} - \Omega_j(t-\tau_{\mathrm{i}})) \tag{4.20a}$$

$$k_{\mathrm{i}}^1\dot{\rho}_{\mathrm{i}} = -\sum\nolimits_{j\in\mathcal{N}(\mathrm{i})} a_{\mathrm{i}j}(\lambda_{\mathrm{i}} - \lambda_j(t-\tau_{\mathrm{i}})) \tag{4.20b}$$

$$\begin{aligned} k_{\mathrm{i}}^2\dot{\gamma}_{\mathrm{i}\ell} = &-\sum\nolimits_{j\in\mathcal{N}(\mathrm{i})} a_{\mathrm{i}j}(\gamma_{\mathrm{i}\ell} - \gamma_{j\ell}(t-\tau_{\mathrm{i}})) \\ &+ \mu_{\mathrm{i}}^1 \max\left\{ I_\ell(t-\tau_{\mathrm{i}}) + \frac{1}{\mu_{\mathrm{i}}^1}k_{\mathrm{i}}^3\gamma_{\mathrm{i}\ell} - I_\ell^{\max}, 0 \right\} - k_{\mathrm{i}}^3\gamma_{\mathrm{i}\ell}(t-\tau_{\mathrm{i}}) \end{aligned} \tag{4.20c}$$

Figures 4.11a, 4.11b and 4.11c show the frequency of each DG for the cases of no communication delays (i.e., $\tau_{\mathrm{i}} = 0s$), small time-delays ($\tau_{\mathrm{i}} = 0.05s$), and large time-delays ($\tau_{\mathrm{i}} = 1s$), respectively. It is observed that the performance of the controller with small time-delays is very similar to the case with no delays, where the controller is able to restore frequency in the microgrid within 2 seconds of the perturbation; however, in the case of large time-delays the restoration of frequency is achieved in a much larger time, of nearly 15 seconds after the load perturbation. Figure 4.12 shows response of the distributed congestion control in terms of line currents, for the same 3 cases of time-delay. It is observed that the only line that faces congestion is line 5, and the congestion is resolved in all the cases; however, the convergence rate of the currents in the case of large time-delays shown in Figure 4.12c is noticeably slower than the other 2 cases.

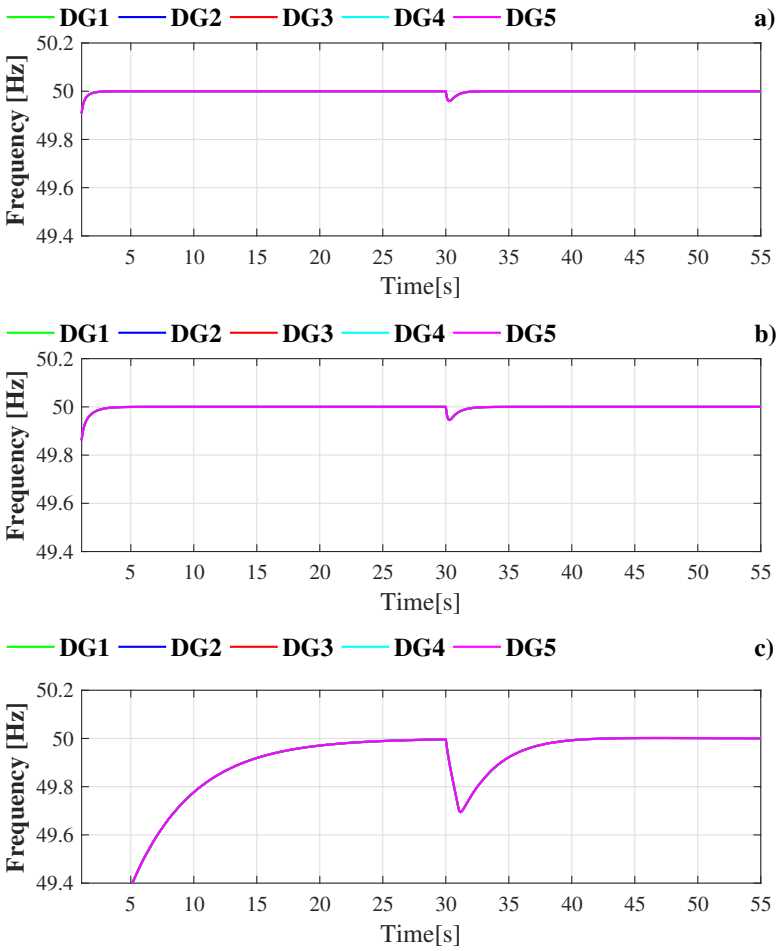

Figure 4.11: Frequency response test with communication delay a) Without time-delay, b) With small time-delays $\tau_{\mathrm{i}} = 0.05s$, c) With large time-delays $\tau_{\mathrm{i}} = 1s$

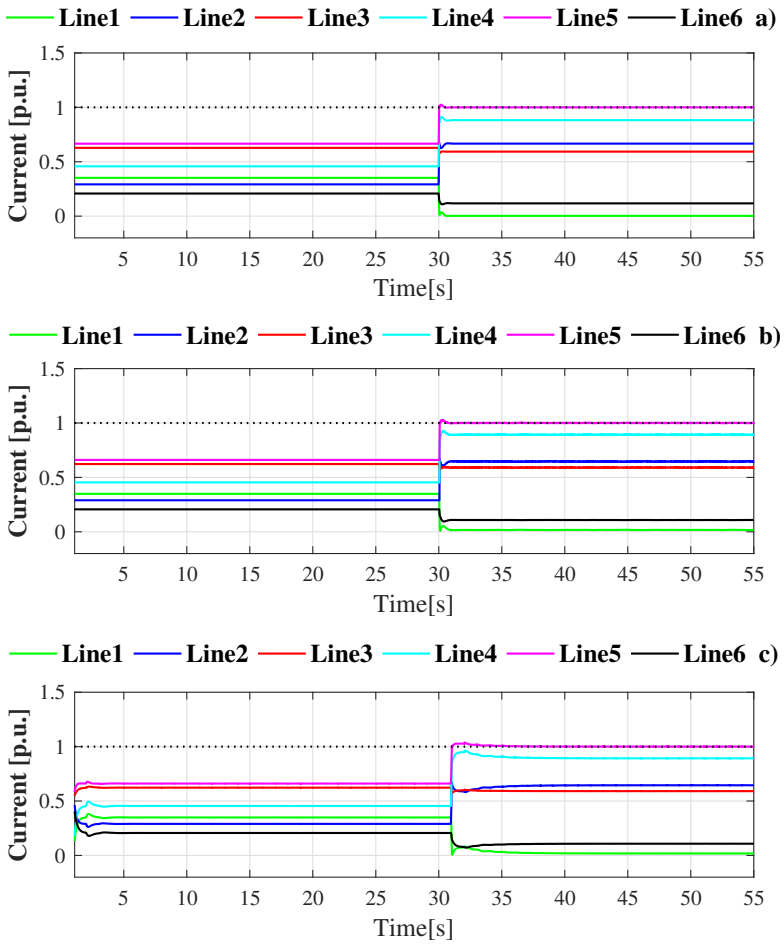

Figure 4.12: Distributed congestion control response test with communication delay a) Without time-delay, b) With small-delays $\tau_{\mathrm{i}} = 0.05s$, c) With large-delays $\tau_{\mathrm{i}} = 1s$

Finally, the impact of estimation errors in $G_{\mathrm{i}\ell}$ factors is analyzed for different levels of error: i) 25% over-estimation in each $G_{\mathrm{i}\ell}$, ii) 25% under-estimation in each $G_{\mathrm{i}\ell}$, and iii) randomly assigned estimation error between -25% and 25% to each factor. The analysis shows that the largest deviation from optimality is obtained in the case of a 25% over-estimation of the factors, where the dispatch deviates a 0.079% from the optimal operation (without estimation errors), which represents a 5.7% of the incremental cost incurred to resolve congestion. Nevertheless, the congestion is resolved regardless of the estimation errors.

4.7.3 Eigenvalue Analysis

Using the proposed distributed congestion control, a linearized model of the closed-loop system (4.10) is derived. The operating point used for the linearization is obtained from a case study where two lines become congested; specifically lines 2 and 3.

Fig. 4.13 shows the eigenvalues obtained for the aforementioned operating point, and also illustrates the eigenvalue trajectories for increments in the gains k_{i} in (4.7b), k_{i}^1 in (4.7c), and k_{i}^2 in (4.7d)). It is observed that the system is stable for the nominal values of the gains,

which are presented in Table 4.1. Critical values of the gains k_{i}, k_{i}^1 and k_{i}^2 were identified in order to obtain stable limits for the controller gains.

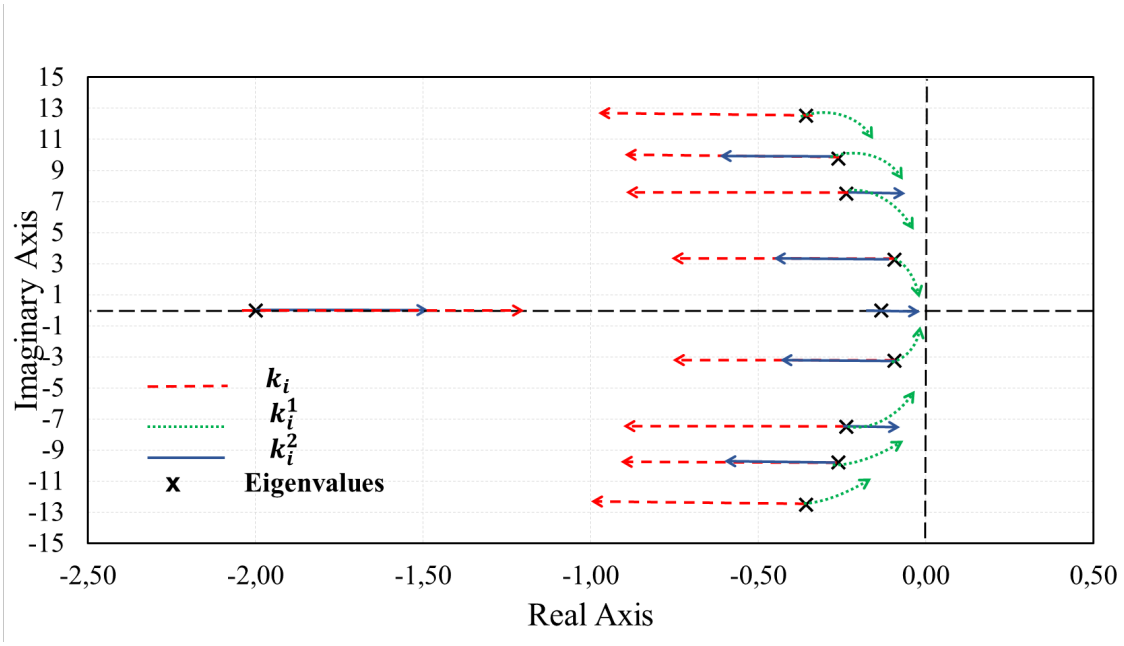

Figure 4.13: Eigenvalue traces of closed-loop system (4.10) as controller gains are varied. (Arrows indicate the direction of increasing gain. Black crosses indicate eigenvalues for the nominal gain of (4.7) in the microgrid study case (Fig. 4.4). The most important eigenvalues have been considered.)

This work does not include any theoretical stability analysis of the closed-loop system; nevertheless, formal linearization provides some qualitative insights into the system behavior.

Given the nonlinearity of the closed-loop system introduced by the *max* functions, the proposed controller necessitates a Lyapunov-based stability analysis. This could be performed using the theory of integral quadratic constraints [120, 121]; however, such analysis is outside the scope of this work.

4.8 Experimental Results

In order to validate the proposed controllers, experimental tests were performed in the Laboratory of Microgrids Control at the University of Chile shown in Figure 4.14. The microgrid topology is composed of three converters, three local loads and three power lines.

The characteristics of DG units and network parameters are given in Table 4.4 and Table 4.5, respectively. Ethernet communication network is implemented to share information among DGs, as is shown at left side of Figure 4.14, and it is able to emulate a communication failure. The topologies, as well as the adjacency matrix A, with and without failure, are shown in Figure 4.15.

Table 4.4: DG characteristics

Parameter	Symbol	DG1-DG3
Max Active Power	P_{i}^{max}	2kW
Min Active Power	P_{i}^{min}	0kW
P-W Droop Coefficient	m_{i}	$2.5{\cdot}10^{-3}\,\frac{\mathrm{rad}}{\mathrm{W{\cdot}s}}$
Q-E Droop Coefficient	n_{i}	$1.5{\cdot}10^{-3}\,\frac{\mathrm{V}}{\mathrm{var}}$
Frequency Control Gain	k_{i}	0.5s
Voltage Control Gain	$\mathbf{k_i}$	1s
OD Control Gain	k_{i}^{1}	0.5s
Max Power Control Gain	k_{i}^{4}	0.1s
Min Power Control Gain	k_{i}^{6}	0.1s
Return to Zero Gain	$\frac{k_{\mathrm{i}}^{3}}{u_{\mathrm{i}}^{1}}, \frac{k_{\mathrm{i}}^{5}}{u_{\mathrm{i}}^{2}}, \frac{k_{\mathrm{i}}^{7}}{u_{\mathrm{i}}^{3}}$	0.01s
Congestion Control Gain	k_{i}^{2}	0.1s

The distributed controller proposed in (4.7) and (4.8) is implemented in each DG unit, as it can be see in Figure 4.1. The gains of the distributed controller implemented are shown in Table 4.4. In this work different operating costs of each DG are considered, DG 2 has the lowest operating cost and DG 3 is the more expensive, the generating cost function (4.21) of each DG unit is assumed quadratic, the parameters used in this work are shown in Table 4.6 [118].

$$C_{\mathrm{i}}(P_{\mathrm{i}}) = \mathrm{a_i}P_{\mathrm{i}}^2 + \mathrm{b_i}P_{\mathrm{i}} + \mathrm{c_i} \tag{4.21}$$

Three operating scenarios are evaluated. i) Performance of the controller against sudden changes in the load, and congested lines. ii) Controller performance against availability of DGs in the microgrid, where the DG 3 is disconnected of the microgrid. iii) Communication links failures scenario, where a failure of the communication link between DG 1 and DG 3 is produced (See Figure 4.15b).

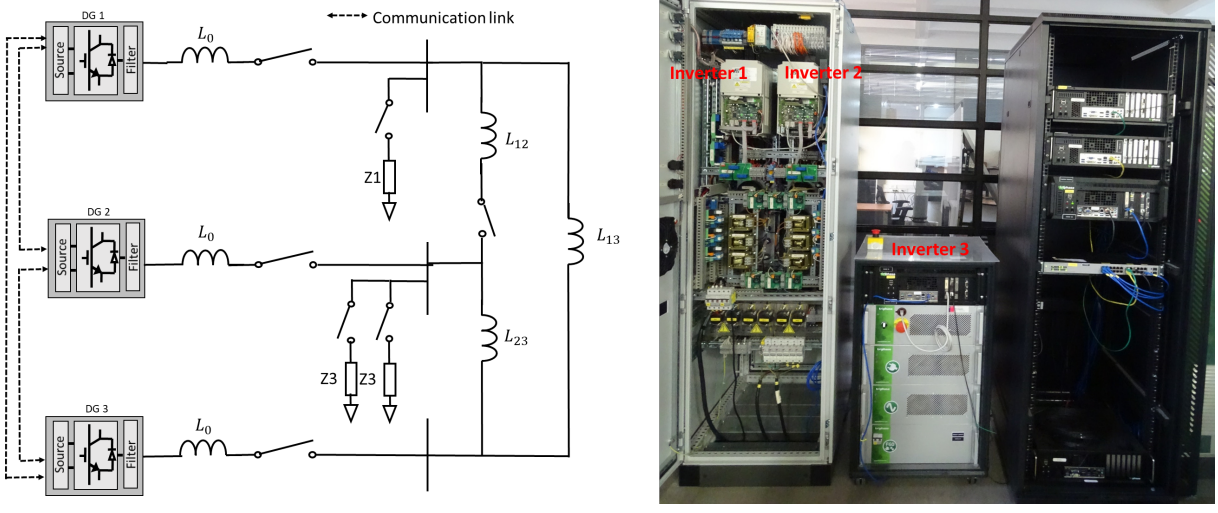

Figure 4.14: Microgrid experimental setup

Table 4.5: Microgrid parameterCong

Parameter	Symbol	Value
Nominal Frequency	$\omega^*/2\pi$	50 Hz
Nominal Voltage	E^*	150 V
Filter Capacitance	C	25μF
Filter Inductance	L_f	1.8mH
Coupling Inductance	L_o	2.5mH
Sampling Period	T_{SP}	1/16E2 S
Load 1	L_1	22Ω
Load 2	L_2	22Ω
Load 3	L_2	15Ω
Line Impedance	$L_{\mathrm{i}}j$	2.5mH
Cutoff f−Droop filter	ω_c	1*2π rad/S

Table 4.6: DG Cost parameters

Parameter	DG1	DG2	DG3
$\mathrm{a_i}$ [\$/kW^2]	0.444	0.264	0.5
$\mathrm{b_i}$ [\$/kW]	0.111	0.067	0.125
$\mathrm{c_i}$ [\$]	0	0	0

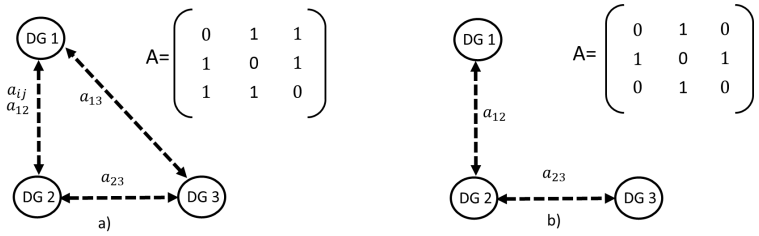

Figure 4.15: Microgrid communication topology a) Original topology b) Topology with communication links failure

4.8.1 Dynamic Performance

In this section, the experimental dynamic performance of the proposed controller (4.7) and (4.8) is illustrated and discussed.

At time-frame 1, the load 1 and the droop control is activated. The droop control is defined by $\omega_{\mathrm{i}} = \omega^* - m_{\mathrm{i}}(P_{\mathrm{i}})$. At time-frame 2, the distributed proposed controller for economic dispatch considering congestion control is activated ((4.7)a to (4.7)f, and (4.8)). At time-frame 3 the load 2 is added, where the congestion from the line 1 is produced as it can be seen in Figure 4.16. At time-frame 4 the load 3 is added, where the lines are not congested. Finally, at time-frame 5 the load 3 is removed, and the line 1 is congested again. It can be observed from Figure 4.16 that the controller is able to successfully resolve congestion after each load perturbation. In the 3 and 5 time-frame, the congestion is quickly eliminated by

driving line currents within limits.

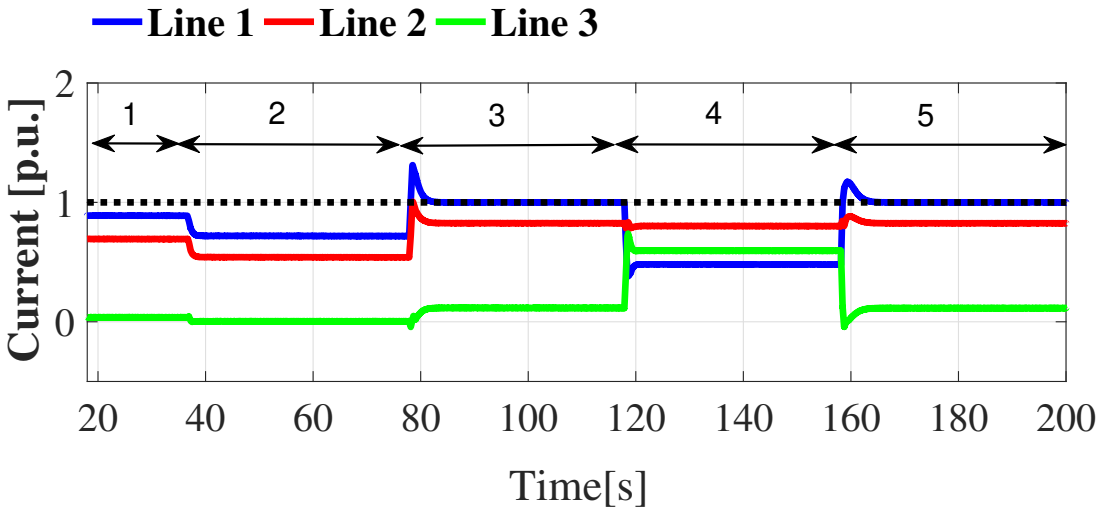

Figure 4.16: Current from the lines

It can be observed from Figure 4.17a and Figure 4.17b that the controller is able to successfully restore frequency and resolve congestion after each load perturbation. In specific, Figure 4.17a shows how the controller is able to restore the frequency of all DG units to their nominal value (See Figure 4.17a time-frame 2-5), when the controller is not activated the frequency does not achieve to the nominal value (See Figure 4.17a time-frame 1). Likewise, Figure 4.17b illustrates that thanks to the correct performance of the controller (4.7a)-(4.7f), (4.8), the congestion is quickly eliminated by driving line currents within limits (See Figure 4.17b time-frame 3 and time-frame 5). At time-frame 3, the step-change occurs and line 1 becomes overloaded; however, the distributed congestion controller removes the overloading in less than 3 seconds, which is fast enough to avoid the activation of thermal protections in distribution lines. At time-frame 3, a step-change in load is applied, resulting in an overloading of lines 1. Once again, the congestion control is able to resolve the congestion within a few seconds, as shown in Figure 4.17b in time-frame 3 and time-frame 5.

Figure 4.17c shows the real power generated by each DG unit, at time-frame 1 the real power is sharing by the units because only the droop control is activated, also the power injected to the microgrid is equal in all DG units because their characteristics are the same (See Figure 4.17c time-frame 1). At time-frame 1 and 2 the load does not change, as it can be seen at time-frame 2 the DG units are re-dispatched considering the operating cost of each unit shown in the Table 4.6 in order to archive the economic dispatch of the microgrid, the DG 2 generates more real power than the other units because its operating cost is the lowest, while DG 3 injects less real power than the other DG units because this is more expensive (See Figure 4.17c time-frame 2). The same performance is shown in the time-frame 4, where the lines are not congested. However, when a control action is required to resolve a congestion (time-frame 2 and time-frame 5), the real power injections of DG units are redistributed in order to remove the line overloading based on their different cost functions and participation factors, as can be see, the DG 2 generates more real power than the other units because its

operating cost is the lowest (See Figure 4.17c time-frame 3 and time-frame 5). The good performance of the proposed controller is shown with an increment and decrement of load at time-frame 3 to time-frame 5.

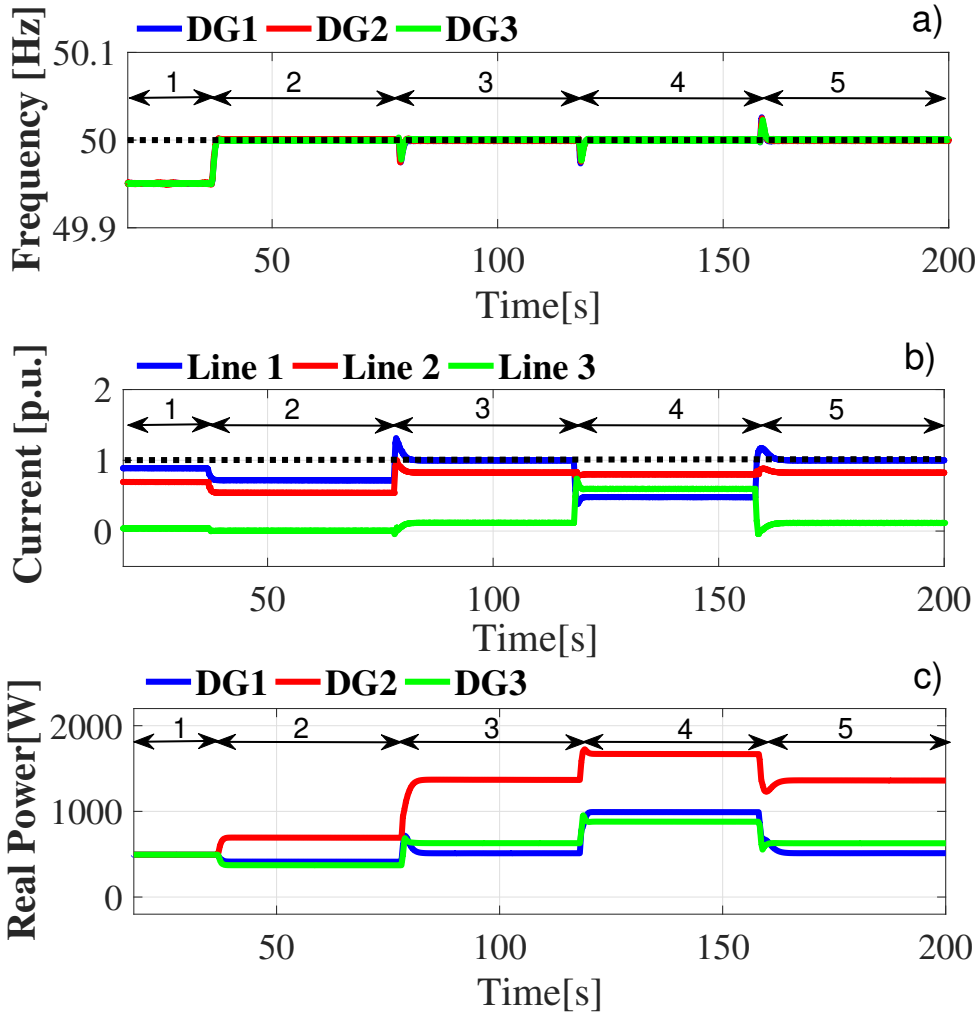

Figure 4.17: Distributed congestion control response a) Frequency at each DG, b) Current from the lines, c) Real power injection for each DG

Figures 4.18 shows the control actions $\gamma_{i\ell}$ used to remove the congestion in each line. On the other hand, Figure 4.18a shows how γ_{i1} (line 1) are nonzero in the time-frame 3 and time-frame 5 in order to resolve the congestion in line 1. The other control actions γ_{i2} and γ_{i3} are equal to zero because the 2 and 3 lines are not congested.

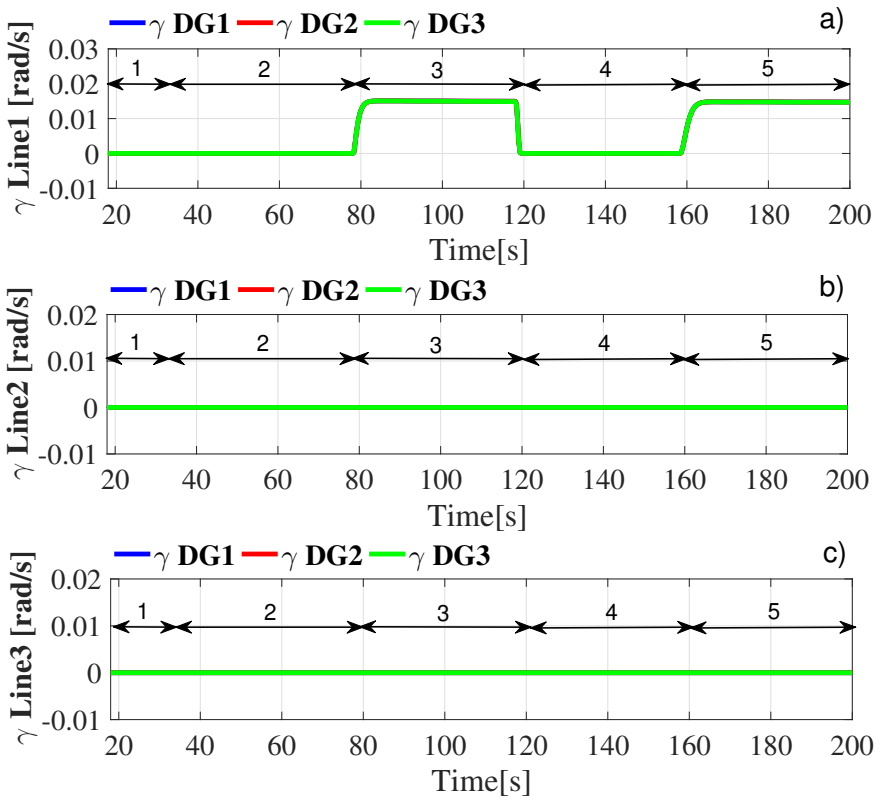

Figure 4.18: a) Congestion control action for line 1, b) Congestion control action for line 2, c) Congestion control action for line 3

Fig. 4.19 shows the λ_i of each DG unit. It can be observed that, in steady-state the values of λ_i converge to a unique value for all units (See 4.19 time-frame 2 to time-frame 5), which then corresponds to the dual variable associated with the demand-supply balance equation in the centralized optimal dispatch problem. In the time-frame 1 lambda is different in all DG units because the controller proposed is not activated.

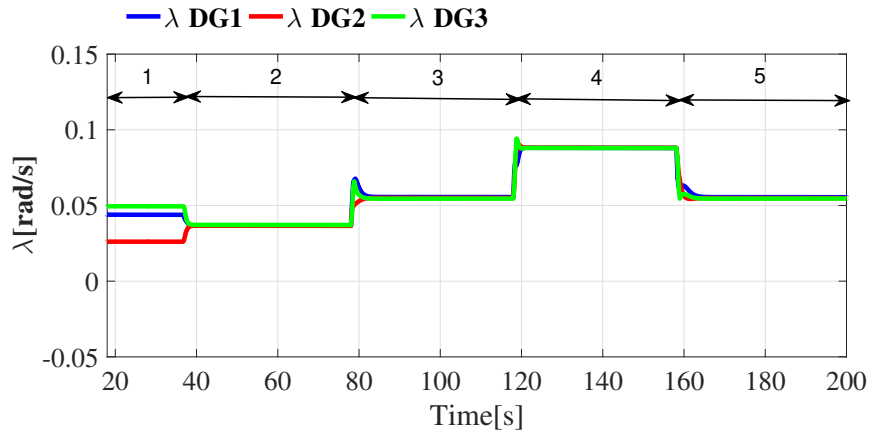

Figure 4.19: Lagrange multiplier λ

4.8.2 Performance Against the Sudden Loss of a DG Unit

In order to analyze the performance of the controller against the sudden loss of a DG unit. In this scenario the DG 3 is disconnected, the results are shown in Figure 4.20, in time-frame 4.

At time-frame 1, the load 1 and the droop control is activated. The droop control is defined by $\omega_i = \omega^* - m_i(P_i)$. At time-frame 2, the distributed proposed controller for economic dispatch considering congestion control is activated ((4.7)a to (4.7)f, and (4.8)). At time-frame 3 the load 2 is added, where the congestion from the line 1 is produced as it can be seen in Figure 4.16b. Finally, at time-frame 4 the DG 3 is disconnected.

In Figure 4.20a the frequency are restored to the nominal value when the disconnection of DG 3 is produced (time-frame 4). Figure 4.20b shows that the congestion in line 1 produced by the the disconnection of DG3 is eliminated by the congestion controller (See Figure 4.20b time-frame 4). Figure 4.20c shows the results of the real power injected, at time-frame 4 when the DG 3 is disconnected the real power is re-dispatched considering the operating cost of each DG, thus the DG 2 supplies more real power than DG 1 because the operating cost of DG 2 unit is lower.At time-frame 4 the real power of unit DG2 is drops to zero because it is descanted.

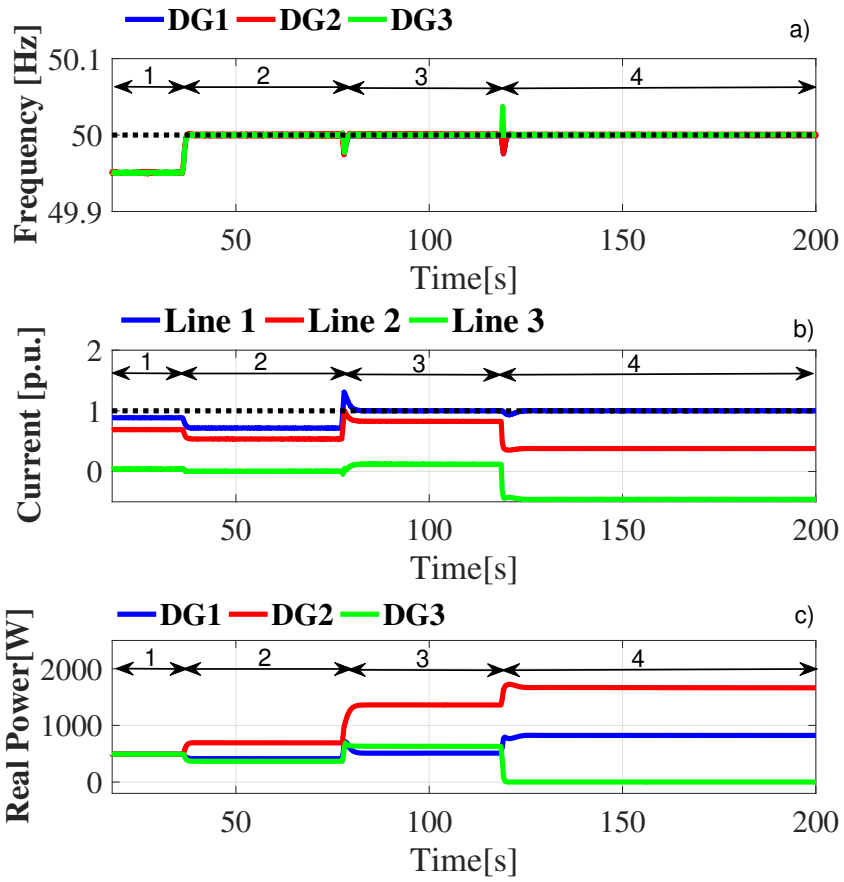

Figure 4.20: Distributed congestion control response test by disconnecting DG3 a) Frequency in each DG, b) Current from the lines, c) Real power injections for each DG

Figures 4.21 shows the control actions $\gamma_{i\ell}$ used to remove the congestion in each line. Figure 4.21a shows how γ_{i1} (line 1) are nonzero in the time-frame 3 in order to solve the congestion in the line 1. When the DG 3 is disconnected, the γ_{11} and γ_{21} have a new value in order to solve the congestion in the line 1. It can be see that the γ_{31} of the DG 3 is zero because the unit is discounted. The other control actions γ_{i2} (Figure 4.21b) and γ_{i3} (Figure 4.21c) are equal to zero because the 2 and 3 lines are not congested.

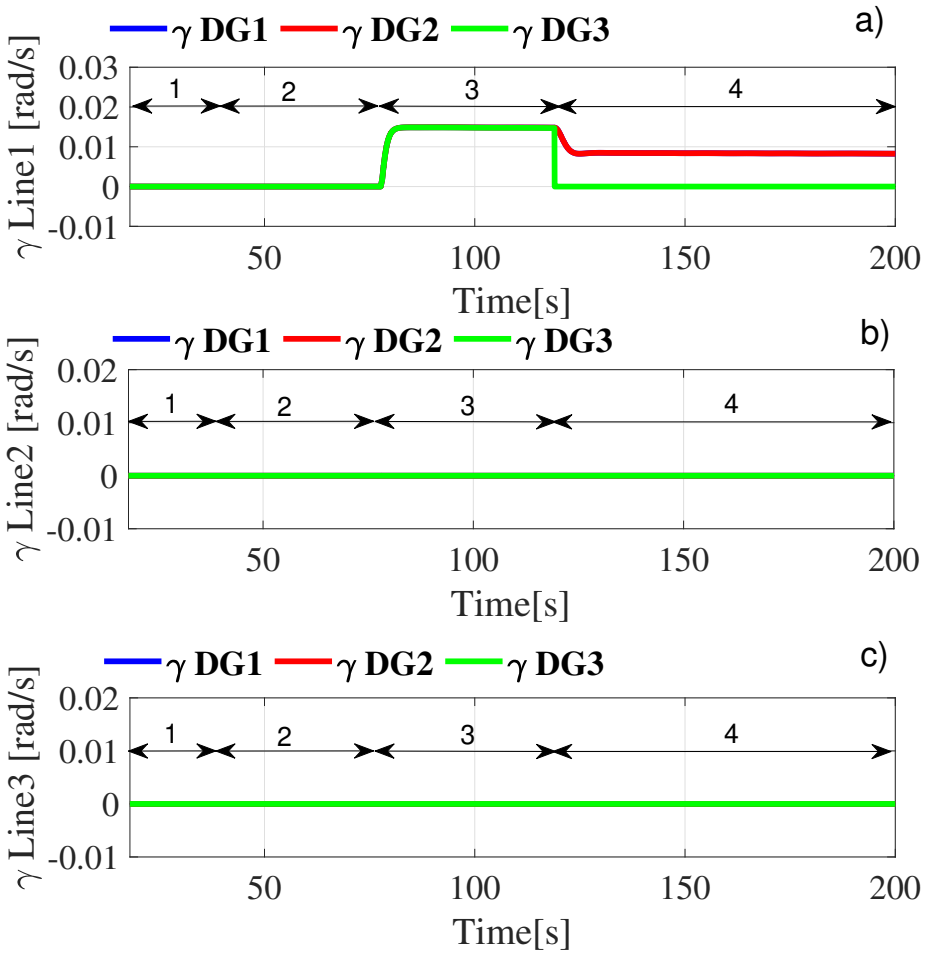

Figure 4.21: a) Congestion control action for line 1, b) Congestion control action for line 2, c) Congestion control action for line 3

Fig. 4.22 shows the λ_i of each DG unit. It can be observed that, in steady-state the values of λ_i converge to a unique value for all units (See Figure 4.22, time-frame 2 to time-frame 4). When the DG 3 unit is disconnected, $\lambda 3$ is equal to zero. In the time-frame 1 lambda is different in all DG units because the controller proposed is not activated.

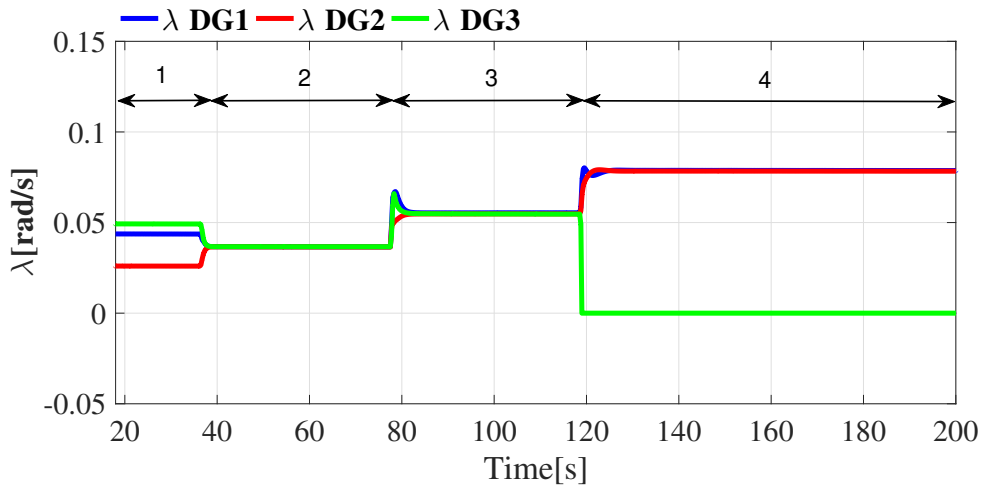

Figure 4.22: Lagrange multiplier λ by disconnecting DG3

4.8.3 Performance Against Communication Link Failures

Figure 4.23 shows the performance of the proposed distributed controller when a communication link failure occurs.

At time-frame 1, the load 1 and the droop control is activated. At time-frame 2, the distributed proposed controller for economic dispatch considering congestion control is activated ((4.7)a to (4.7)f, and (4.8)). At time-frame 3 the load 2 is added, where the congestion from the line 1. At time-frame 4 the communication link between DG 1 and DG 2 fails (Figure 4.15b). Finally at time-frame 5 an incremental of load is produced (load 3).

The experimental results are shown in Figure 4.23. It is observed that the proposed controller does not suffer noticeable deterioration in its performance against the loss of the communication links. Noteworthy, this results assume that the units have a dynamic adjacency matrix, which is instantly updated upon loss of communication links.

As it can be seen the frequency (Figure 4.23a) remain in the nominal value when the communication link failure is produced. The congestion is solved when the communication link failure between (DG1 and DG2) is produced (See Figure 4.23b, time-frame 4).

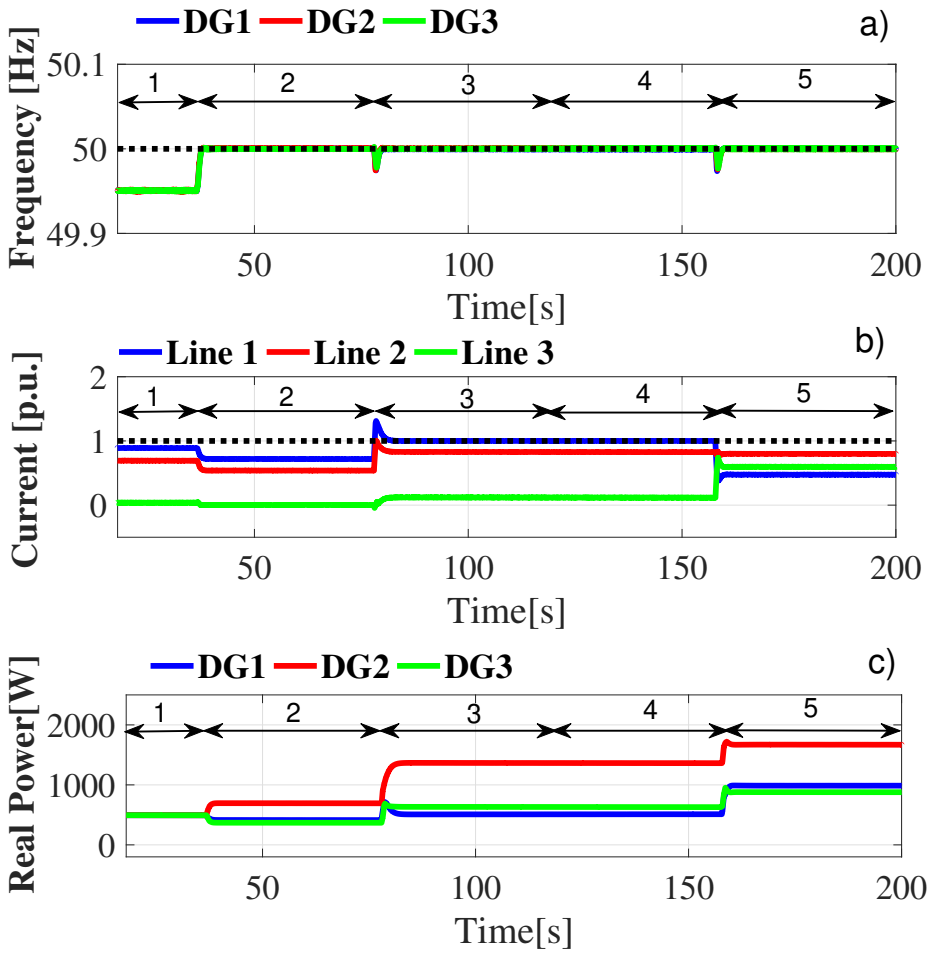

Figure 4.23: Distributed congestion control response test by communication link failure between (DG1 and DG2), a) Frequency in each DG, b) Current from the lines, c) Real power injections for each DG

4.9 Analysis and Discussion

This chapter presented a novel distributed control strategy for frequency control, optimal operation, and congestion management of isolated microgrids. The proposed controller is capable of obtaining optimal microgrid operation while considering output limits of DGs and thermal limits of distribution lines by using real-time measurements. The equivalence between the closed-loop steady-state conditions of the controller and the KKT conditions of a linear OPF formulation is mathematically demonstrated. The capabilities and good dynamic performance of the controller are demonstrated and discussed using several simulations and experimental tests.

The controller proposed in this section considers the following technical and economic tasks: minimum operating cost considering limits of power of DG units, frequency restoration, and congestion management in a distributed approach. Unlike the controller designed in the previous chapter, in this chapter, a novel controller is proposed, which includes conges-

tion management. The proposed congestion control changes the reference of the frequency droop controllers to maintain the frequency at its nominal value, remove the overloading of distribution lines, and induce the system to an optimal dispatch achieve these objectives, local DG controllers minimize the terms of the Lagrangian function associated with their local variables for given values of Lagrangian multipliers. Then, by using a distributed averaging strategy, the controllers converge to unique global values of such multipliers. The exchange of information between local DG controllers occurs through the communication network. The proposal does not rely on the microgrid topology, an external online estimator in order to calculate the participation factor of the unit in the current of line.

The design and operation of the proposed distributed controller rely on the following assumptions:

- A communication network does not include delays, packet loss, connect network, and high bandwidth.
- Each DG in the microgrid is able to communicate ω_{i}, λ_{i}, $\gamma_{i\ell}$, i_{ℓ} to neighboring DGs through a connected and bidirectional communication network.
- Each DG has information about γ_{il} for all distribution lines of the microgrid, and each line subject to congestion has at least one DG with non-zero participation factor associated.
- Current measurements of all distribution lines are available to the local controllers of all DGs in the microgrid.
- Participation factors $G_{\mathrm{i}l}$ are calculated with reasonable accuracy by an external online estimator and are available to each DG.
- Reactive power is only used for voltage control, and it is not available for solving overloading problems.

The contributions of this proposal, shown in this chapter, are as follows:

- The optimal dispatch and frequency restoration are considered at the same time scale in order to achieve the optimal dispatch when fast disturbances occur.
- The KKT optimality conditions of the linear centralized OPF problem are satisfied.
- Microgrid topology is not required to achieve the optimal dispatch.

Chapter 5

Conclusions

In this thesis, a comprehensive review of tertiary control in a distributed control approach was performed. The distributed tertiary control in AC, DC, and hybrid microgrids was studied, and the most important issues were identified. As noted in Chapter 2, the research to date has not included the maximum and minimum limits of power in the controller formulation. Furthermore, the congestion that can be produced from the lines of the microgrid has not been considered in recent research. In this context two strategies for distributed economic dispatch are proposed in this thesis.

Distributed control strategy for frequency restoration and optimal dispatch of an isolated microgrid

A distributed economic dispatch control is proposed to achieve the minimum operating cost at the same time that the frequency and voltage are restored. The control algorithm includes the maximum and minimum limits of power of the DG units in the formulation. The controller of each DG uses its local measurements and information exchanged among neighboring DG units through a communication network. The proposal does not require knowledge of the microgrid topology.

Good performance of the proposed distributed control strategy for frequency and optimal dispatch proposed was validated. Experimental results also validated the good performance of the proposed distributed controller against sudden changes in the load, failures in the communications links, as well as plug-and-play operation of DG units.

The contributions of proposed distributed economic dispatch control are as follows: i) The optimal dispatch and frequency restoration are considered in the same time scale in order to achieve the optimal dispatch when fast disturbances occur. ii) The KKT optimality conditions of the linear centralized OPF problem are satisfied. iii) The microgrid topology is not required for achieving the optimal dispatch. iv) The proposed controller was successfully tested in an experimental microgrid.

Distributed control strategy for frequency restoration, optimal dispatch, and congestion management of an isolated microgrid

An extension of the previously described distributed economic dispatch is presented. This case includes the management of congestion from the electrical lines in an isolated microgrid. The proposed strategy drives the distributed generators within the microgrid to a dispatch that complies with the Karush-Kuhn-Tucker (KKT) conditions of a linear optimal power flow (OPF) formulation. The controller relies on local power and frequency measurements, information from neighboring DGs, and line-flow measurements transmitted through a communications network. The proposed controller is capable of driving the microgrid to its optimal operation while considering output limits of DGs and thermal limits of distribution lines by using real-time measurements.

The simulation and experimental results obtained in this thesis show good performance of the distributed control strategy for frequency restoration, optimal dispatch, and congestion management in the same time-scale. Moreover, the equivalence of the controller steady-state and KKT conditions of a linear OPF formulation is demonstrated. The mathematical proof shows that any equilibrium of the closed-loop microgrid yields a solution of the KKT condition. The equivalence between the closed-loop steady-state conditions of the controller and the KKT conditions of a linear OPF formulation is also mathematically demonstrated.

The contributions of the distributed economic dispatch considering congestion proposed are as follows: (i) A novel distributed control architecture for frequency control, congestion management, and optimal operation of the microgrid is proposed. (ii) The proposed control strategy solves KKT conditions of a linear OPF formulation based on real system measurements, without requiring a mathematical power flow model. (iii) The strong evidence via experiments and simulations that the controller is able to restore the optimal operation of the microgrid in the time-scale of the secondary frequency control is provided. iv) The equivalence between the closed-loop steady-state conditions of the controller and the KKT conditions of a linear OPF formulation is mathematically demonstrated.

The proposals in this thesis improve performance in terms of robustness under communication fails and reliability during plug-and-play operation

5.1 Future Work

Participation factors

It would be useful to consider other more accurate techniques for the estimation of participation factors. This estimator could be based on computational intelligence.

Congestion Management

Future research will consider the integration of distributed voltage/reactive power control in the proposed strategy.

Unbalances Control

Interesting extensions of this work include the application of the proposed controller to the sharing of power unbalances and harmonics, among others.

Losses in the Microgrid

Future research will consider the losses in the microgrid using the same approach, and a distributed optimal dispatch considering loss in the microgrid will be proposed.

Communication Technologies

Future research will consider the latency and packet loss to evaluate distributed control considering different communication technologies.

Appendices

A1 List of Acronyms

DG	Distributed Generation
DER	Distributed Energy Resources
RE	Renewable Energy
DES	Distributed Energy Storage
PCC	Point of Common Coupling
WT	Wind Turbines
PV	Photovoltaic Power
ESS	Energy Storage Systems
AC	Alternate Current
DC	Direct Current
ED	Economic Dispatch
OD	Optimal Dispatch
DSM	Demand Side Management
MG	Microgrid
KKT	Karush-Kuhn-Tucker
BIC	Bidirectional Interlinking Converters
MAS	Multi-Agent System
EMS	Energy Management System
DSM	Demand Side Management
VSI	Voltage Source Inverters
MPC	Model Predictive Control
PI	Proportional Integral Control
BESS	Battery Energy Storage Systems
DAPI	Distributed-average-proportion-integral Control
ED	Economic Dispatch

IC	Incremental Cost
ICC	Incremental Cost Consensus
OPF	Optimal Power Flow
FACTS	Flexible Alternating Current Transmission System
HVDC	High Voltage Direct Current
DSO	Distribution System Operators

Bibliography

[1] S. Parhizi, H. Lotfi, A. Khodaei, and S. Bahramirad. State of the Art in Research on Microgrids: A Review. *IEEE Access*, 3:890–925, June 2015.

[2] R. H. Lasseter. Microgrids and distributed generation. *Journal of Energy Engineering*, 133(3):144–149, April 2007.

[3] R. H. Lasseter. Smart distribution: Coupled microgrids. *Proceedings of the IEEE*, 99(6):1074–1082, June 2011.

[4] J. C. Vasquez, J. M. Guerrero, J. Miret, M. Castilla, and L. Garcia de Vicuna. Hierarchical control of intelligent microgrids. *IEEE Industrial Electronics Magazine*, 4(4):23–29, Dec 2010.

[5] D. E. Olivares, A. Mehrizi-Sani, A. H. Etemadi, C. A. Cañizares, R. Iravani, M. Kazerani, A. H. Hajimiragha, O. Gomis-Bellmunt, M. Saeedifard, R. Palma-Behnke, G. A. Jiménez-Estévez, and N. D. Hatziargyriou. Trends in Microgrid Control. *IEEE Transactions on Smart Grid*, 5(4):1905–1919, July 2014.

[6] Department of Energy office of Electricity Delivery and Energy Reliability. Summary Report : 2012 DOE Microgrid Workshop. Technical report, Office of Electricity Delivery and Energy Reliability Smart Grid R&D Program, 2012.

[7] B. M. Eid, N. A. Rahim, J. Selvaraj, and A. H. El Khateb. Control methods and objectives for electronically coupled distributed energy resources in microgrids: A review. *IEEE Systems Journal*, 10(2):446–458, June 2016.

[8] Ortiz-Villalba D.and Silva C. Jiménez-Estévez G., Palma-Behnke R. It takes a village: Social scada and approaches to community engagement in isolated microgrids. *IEEE Power and Energy Magazine*, 12(4):60–69, June 2014.

[9] Ye G. Nguyen P. Haque A., Nijhuis M. and Slootweg J. G. Integrating direct and indirect load control for congestion management in lv networks. *IEEE Transactions on Smart Grid*, 10(1):741–751, October 2017.

[10] J.C. Vasquez Li C., Savaghebi M. and Guerrero J.M. Multiagent based distributed control for operation cost minimization of droop controlled ac microgrid using incremental cost consensus. In *2015 17th European Conference on Power Electronics and*

Applications Exposition: Geneva, Switzerland, page 1109–1119, Aug 2015.

[11] Yinliang Xu and Zhicheng Li. Distributed optimal resource management based on the consensus algorithm in a microgrid. *IEEE Trans. Ind. Electron.*, 62(4):2584–2592, September 2015.

[12] Matas J. Garcia L. Guerrero J., Vasquez J and Castilla M. Hierarchical control of droop-controlled ac and dc microgrids a general approach toward standardization. *IEEE Transactions on Industrial Electronics*, 58(2):1158–172, April 2011.

[13] Reza L. Katiraei F., Iravani M. and Peter W. Micro-grid autonomous operation during and subsequent to islanding process. *IEEE Transactions on power delivery*, 20(1):248–257, February 2005.

[14] Shuai Z.and Luo A. Shen X., Tan D. Control techniques for bidirectional interlinking converters in hybrid microgrids: Leveraging the advantages of both ac and dc. *IEEE Power Electronics Magazine*, 6(3):39–47, September 2019.

[15] Adam Hirsch, Yael Parag, and Josep Guerrero. Microgrids: A review of technologies, key drivers, and outstanding issues. *Renewable and Sustainable Energy Reviews*, 90(1):402–411, July 2018.

[16] Bidram A. and Davoudi A. Hierarchical structure of microgrids control system. *IEEE Transactions on Smart Grid*, 3(4):1963–1976, May 2012.

[17] Nikos Hatziargyriou. *Microgrids: architectures and control*. John Wiley & Sons, 2014.

[18] Mehrdad Yazdanian and Ali Mehrizi-Sani. Distributed control techniques in microgrids. *IEEE Trans. Smart Grid*, 5(6):2901–2909, August 2014.

[19] Tianqiao Zhao and Zhengtao Ding. Distributed agent consensus-based optimal resource management for microgrids. *IEEE Transactions on Sustainable Energy*, 9(1):443–452, August 2018.

[20] Surendra SD Thukaram. Network congestion management by fuzzy inference using virtual flows. In *2011 International Conference on Power and Energy Systems*, pages 1–6. IEEE, 2011.

[21] D Bao Nguyen, Jacquelien MA Scherpen, and Frits Bliek. Distributed optimal control of smart electricity grids with congestion management. *IEEE Transactions on Automation Science and Engineering*, 14(2):494–504, January 2017.

[22] TH Vo, ANMM Haque, PH Nguyen, IG Kamphuis, M Eijgelaar, and I Bouwman. A study of congestion management in smart distribution networks based on demand flexibility. In *2017 IEEE Manchester PowerTech*, pages 1–6. IEEE, 2017.

[23] M. Shahidehpour S. Huang, Q. Wu and Z. liu. Dynamic power tariff for congestion management in distribution networks. 10(2):2148–2157, January 2018.

[24] Guoxing Yu, Huihui Song, Rui Hou, Yanbin Qu, and HM Kim. Distributed frequency control strategy for islanded microgrid with consideration of transmission congestion. *Int. J. Smart Home*, 10(6):309–320, June 2016.

[25] Farid Katiraei, Reza Iravani, Nikos Hatziargyriou, and Aris Dimeas. Microgrids management. *IEEE power and energy magazine*, 6(3):54–65, May 2008.

[26] J. M. Guerrero, M. Chandorkar, T. L. Lee, and P. C. Loh. Advanced Control Architectures for Intelligent Microgrids—Part I: Decentralized and Hierarchical Control. *IEEE Trans. Ind. Electron.*, 60(4):1254–1262, April 2013.

[27] Omid Palizban and Kimmo Kauhaniemi. Hierarchical control structure in microgrids with distributed generation: Island and grid-connected mode. *Renewable and Sustainable Energy Reviews*, 44:797–813, April 2015.

[28] Yang F. Feng X., Shekhar A. and Bauer P. Comparison of hierarchical control and distributed control for microgrid. *Electric Power Components and Systems*, 55(10):1043–1056, Jul 2017.

[29] Joan Rocabert, Alvaro Luna, Frede Blaabjerg, and Pedro Rodriguez. Control of power converters in ac microgrids. *IEEE transactions on power electronics*, 27(11):4734–4749, October 2012.

[30] Xiaoxiao Yu, Ashwin M Khambadkone, Huanhuan Wang, and Siew Tuck Sing Terence. Control of parallel-connected power converters for low-voltage microgrid—part i: A hybrid control architecture. *IEEE Transactions on Power Electronics*, 25(12):2962–2970, June 2010.

[31] Huanhuan Wang, Ashwin M Khambadkone, and Xiaoxiao Yu. Control of parallel connected power converters for low voltage microgrid—part ii: Dynamic electrothermal modeling. *IEEE Transactions on Power electronics*, 25(12):2971–2980, October 2010.

[32] John W Simpson-Porco, Qobad Shafiee, Florian Dörfler, Juan C Vasquez, Josep M Guerrero, and Francesco Bullo. Secondary frequency and voltage control of islanded microgrids via distributed averaging. *IEEE Trans. Ind. Electron.*, 62(11):7025–7038, May 2015.

[33] Johannes Schiffer, Romeo Ortega, Alessandro Astolfi, Jörg Raisch, and Tevfik Sezi. Conditions for stability of droop-controlled inverter-based microgrids. *Automatica*, 50(10):2457–2469, October 2014.

[34] D. E. Olivares, C. A. Cañizares, and M. Kazerani. A Centralized Energy Management System for Isolated Microgrids. *IEEE Transactions on Smart Grid*, 5(4):1864–1875, July 2014.

[35] M. Brandstetter, A. Schirrer, M. Miletić, S. Henein, M. Kozek, and F. Kupzog. Hierarchical Predictive Load Control in Smart Grids. *IEEE Transactions on Smart Grid*, 8(1):190–199, January 2017.

[36] L. Valverde, C. Bordons, and F. Rosa. Integration of Fuel Cell Technologies in Renewable-Energy-Based Microgrids Optimizing Operational Costs and Durability. *IEEE Transactions on Industrial Electronics*, 63(1):167–177, January 2016.

[37] Rodrigo Palma-Behnke, Carlos Benavides, Fernando Lanas, Bernardo Severino, Lorenzo Reyes, Jacqueline Llanos, and Doris Sáez. A microgrid energy management system based on the rolling horizon strategy. *IEEE Transactions on smart grid*, 4(2):996–1006, January 2013.

[38] Rodrigo Palma-Behnke, Carlos Benavides, E Aranda, Jacqueline Llanos, and Doris Saez. Energy management system for a renewable based microgrid with a demand side management mechanism. In *2011 IEEE symposium on computational intelligence applications in smart grid (CIASG)*, pages 1–8. IEEE, 2011.

[39] A. Fazeli, M. Sumner, M. C. Johnson, and E. Christopher. Real-time deterministic power flow control through dispatch of distributed energy resources. *IET Generation, Transmission Distribution*, 9(16):2724–2735, September 2015.

[40] R. H. Lasseter. MicroGrids. In *2002 IEEE Power Engineering Society Winter Meeting. Conference Proceedings (Cat. No.02CH37309)*, volume 1, pages 305–308 vol.1, 2002.

[41] Mehmet H Cintuglu, Tarek Youssef, and Osama A Mohammed. Development and application of a real-time testbed for multiagent system interoperability: A case study on hierarchical microgrid control. *IEEE Transactions on Smart Grid*, 9(3):1759–1768, August 2018.

[42] Yang Han, Ke Zhang, Hong Li, Ernane Antônio Alves Coelho, and Josep M Guerrero. Mas-based distributed coordinated control and optimization in microgrid and microgrid clusters: A comprehensive overview. *IEEE Transactions on Power Electronics*, 33(8):6488–6508, January 2018.

[43] Natarajan Prabaharan, Amalorpavaraj Rini Ann Jerin, Ehsan Najafi, and Kaliannan Palanisamy. An overview of control techniques and technical challenge for inverters in micro grid. In *Hybrid-Renewable Energy Systems in Microgrids*, pages 97–107. Elsevier, 2018.

[44] Mahmoud Saleh, Yusef Esa, Mohamed El Hariri, and Ahmed Mohamed. Impact of information and communication technology limitations on microgrid operation. *Energies*, 12(15):2926, October 2019.

[45] Vahidreza Nasirian, Ali Davoudi, Frank L Lewis, and Josep M Guerrero. Distributed adaptive droop control for dc distribution systems. *IEEE Transactions on Energy Conversion*, 29(4):944–956, January 2014.

[46] Vahidreza Nasirian, Qobad Shafiee, Josep M Guerrero, Frank L Lewis, and Ali Davoudi. Droop-free team-oriented control for ac distribution systems. In *2015 IEEE Applied Power Electronics Conference and Exposition (APEC)*, pages 2911–2918. IEEE, 2015.

[47] Josep M Guerrero, Luis Garcia De Vicuna, José Matas, Miguel Castilla, and Jaume

Miret. Output impedance design of parallel-connected ups inverters with wireless load-sharing control. *IEEE Transactions on industrial electronics*, 52(4):1126–1135, April 2005.

[48] Fanghong Guo, Changyun Wen, and Yong-Duan Song. *Distributed control and optimization technologies in smart grid systems*. CRC Press, 2017.

[49] Chen G. and Feng E. Distributed secondary control and optimal power sharing in microgrids. *IEEE/CAA Journal of Automatica Sinica*, 2(3):304– 312, January 2015.

[50] Fanghong Guo, Changyun Wen, Jianfeng Mao, and Yong-Duan Song. Distributed economic dispatch for smart grids with random wind power. *IEEE Transactions on Smart Grid*, 7(3):1572–1583, October 2015.

[51] Florian Dörfler, John W Simpson-Porco, and Francesco Bullo. Breaking the hierarchy: Distributed control and economic optimality in microgrids. *IEEE Transactions on Control of Network Systems*, 3(3):241–253, April 2015.

[52] Jacqueline Llanos, Juan Gomez, Doris Saez, Daniel Olivares, and John Simpson-Porco. Economic dispatch by secondary distributed control in microgrids. In *2019 21st European Conference on Power Electronics and Applications (EPE'19 ECCE Europe)*, pages P–1. IEEE, 2019.

[53] Jeff Shamma. *Coperative Control of Distributed Multi-Agent Systems*. Wiley & Sons, September 2007.

[54] Frank L Lewis, Hongwei Zhang, Kristian Hengster-Movric, and Abhijit Das. *Cooperative control of multi-agent systems: optimal and adaptive design approaches*. Springer Science & Business Media, February 2013.

[55] F. Bullo. *Lectures on Network Systems*. Kindle Direct Publishing, 2019. With contributions by J. Cortes, F. Dorfler, and S. Martinez.

[56] Lin Xiao, Stephen Boyd, and Sanjay Lall. A scheme for robust distributed sensor fusion based on average consensus. In *IPSN 2005. Fourth International Symposium on Information Processing in Sensor Networks, 2005.*, pages 63–70. IEEE, 2005.

[57] Wei Ren, Randal W Beard, and Ella M Atkins. Information consensus in multivehicle cooperative control. *IEEE Control Systems*, 27(2):71–82, January 2007.

[58] Guerrero J. Shafiee Q. and Vasquez J. Distributed secondary control for islanded microgrids a novel approach. *IEEE Transactions on Power Electronics*, 29(2):1018–1031, January 2014.

[59] Constanza Ahumada, Roberto Cárdenas, Doris Saez, and Josep M Guerrero. Secondary control strategies for frequency restoration in islanded microgrids with consideration of communication delays. *IEEE Transactions on Smart Grid*, 7(3):1430–1441, January 2015.

[60] Yang Han, Hong Li, Pan Shen, Ernane Antônio Alves Coelho, and Josep M Guerrero. Review of active and reactive power sharing strategies in hierarchical controlled microgrids. *IEEE Transactions on Power Electronics*, 32(3):2427–2451, November 2016.

[61] Alfredo Vaccaro, Giovanni Velotto, and Ahmed F Zobaa. A decentralized and cooperative architecture for optimal voltage regulation in smart grids. *IEEE Transactions on Industrial Electronics*, 58(10):4593–4602, October 2011.

[62] Erik Weitenberg, Yan Jiang, Changhong Zhao, Enrique Mallada, Claudio De Persis, and Florian Dörfler. Robust decentralized secondary frequency control in power systems: Merits and tradeoffs. *IEEE Transactions on Automatic Control*, 64(10):3967–3982, July 2018.

[63] Qobad Shafiee, Vahidreza Nasirian, Juan C Vasquez, Josep M Guerrero, and Ali Davoudi. A multi-functional fully distributed control framework for ac microgrids. *IEEE Transactions on Smart Grid*, 9(4):3247–3258, October 2016.

[64] John W Simpson-Porco, Florian Dörfler, and Francesco Bullo. Synchronization and power sharing for droop-controlled inverters in islanded microgrids. *Automatica*, 49(9):2603–2611, October 2013.

[65] John W Simpson-Porco, Florian Dörfler, Francesco Bullo, Qobad Shafiee, and Josep M Guerrero. Stability, power sharing,& distributed secondary control in droop-controlled microgrids. In *2013 IEEE International Conference on Smart Grid Communications (SmartGridComm)*, pages 672–677. IEEE, 2013.

[66] Fanghong Guo, Changyun Wen, Jianfeng Mao, and Yong-Duan Song. Distributed secondary voltage and frequency restoration control of droop-controlled inverter-based microgrids. *IEEE Transactions on industrial Electronics*, 62(7):4355–4364, October 2014.

[67] Yinliang Xu, Hongbin Sun, Wei Gu, Yan Xu, and Zhengshuo Li. Optimal distributed control for secondary frequency and voltage regulation in an islanded microgrid. *IEEE Transactions on Industrial Informatics*, 15(1):225–235, May 2018.

[68] Guannan Lou, Wei Gu, Yinliang Xu, Ming Cheng, and Wei Liu. Distributed mpc-based secondary voltage control scheme for autonomous droop-controlled microgrids. *IEEE transactions on sustainable energy*, 8(2):792–804, February 2016.

[69] Guo Zhuoyu, Li Shaoyuan, and Zheng Yi. Distributed model predictive control for secondary voltage of the inverter-based microgrid. In *2017 36th Chinese Control Conference (CCC)*, pages 4630–4634. IEEE, 2017.

[70] Meng Chen, Xiangning Xiao, and Josep M Guerrero. Secondary restoration control of islanded microgrids with a decentralized event-triggered strategy. *IEEE Transactions on Industrial Informatics*, 14(9):3870–3880, 2017.

[71] Inam Ullah Nutkani, Poh Chiang Loh, and Frede Blaabjerg. Droop scheme with consideration of operating costs. *IEEE Transaction on Power Electronics*, 29(3):54–65,

March 2014.

[72] Inam Ullah Nutkani, Poh Chiang Loh, and Frede Blaabjerg. Cost-based droop scheme with lower generation costs for microgrids. *IET Power Electronics*, 7(5):1171–1180, March 2014.

[73] Inam Ullah Nutkani, Poh Chiang Loh, Peng Wang, and Frede Blaabjerg. Linear decentralized power sharing schemes for economic operation of ac microgrids. *IEEE Transactions on Industrial Electronics*, 63(1):225–234, March 2015.

[74] Loh P. C. Nutkani I. U. and Blaabjerg F. Cost-prioritized droop schemes for autonomous ac microgrids. *IEEE Trans. Power Electron*, 30(2):1109–1119, March 2015.

[75] Inam Ullah Nutkani, Poh Chiang Loh, Peng Wang, and Frede Blaabjerg. Decentralized economic dispatch scheme with online power reserve for microgrids. *IEEE Transactions on Smart Grid*, 8(1):139–148, March 2015.

[76] R. Olfati-Saber, J. Fax, and R. M. Murray. Consensus and Cooperation in Networked Multi-Agent Systems. In *Proceedings of the IEEE*, volume 95, pages 215 – 233, 2007.

[77] P. Lin, C. Jin, J. Xiao, X. Li, D. Shi, Y. Tang, and P. Wang. A distributed control architecture for global system economic operation in autonomous hybrid ac/dc microgrids. *IEEE Transactions on Smart Grid*, 10(3):2603–2617, May 2019.

[78] Chengcheng Zhao, Jianping He, Peng Cheng, and Jiming Chen. Consensus-based energy management in smart grid with transmission losses and directed communication. *IEEE Trans. Smart Grid*, 8(5):2049–2061, August 2017.

[79] W. Zhang, W. Liu, X. Wang, L. Liu, and F. Ferrese. Online optimal generation control based on constrained distributed gradient algorithm. *IEEE Transactions on Power Systems*, 30(1):35–45, January 2015.

[80] Giulio Binetti, Ali Davoudi, Frank L Lewis, David Naso, and Biagio Turchiano. Distributed consensus-based economic dispatch with transmission losses. *IEEE Trans. Power Syst.*, 29(4):1711–1720, January 2014.

[81] T. Yang, D. Wu, Y. Sun, and J. Lian. Minimum-time consensus-based approach for power system applications. *IEEE Transactions on Industrial Electronics*, 63(2):1318 – 1328, February 2016.

[82] T. Xu, W. Wu, S. Hongbin, and L.Wang. Fully distributed multi-area dynamic economic dispatch method with second-order convergence for active distribution networks. *IET Generation, Transmission and Distribution*, 11(16):3955–3965, May 2017.

[83] R. Wang, Q. Li, B. Zhang, and L. Wang. Distributed consensus based algorithm for economic dispatch in a microgrid. *IEEE Transactions on Smart Grid*, 10(4):3630–3640, July 2019.

[84] C. LI, J. Vasquez, and J. Guerrero. Convergence analysis of distributed control for

operation cost minimization of droop controlled dc microgrid based on multiagent. In *European Conference on Power Electronics and Applications (EPE'15 ECCE-Europe)*, pages 3459–3464, 2016.

[85] Z. Cheng, Z. Li, J. Liang, J. Gao, J. Si, and S. Li. Distributed economic power dispatch and bus voltage control for droop-controlled dc microgrids. *Energies*, 12(12):1–22, April 2019.

[86] Inam Ullah Nutkani, Poh Chiang Loh, Peng Wang, and Frede Blaabjerg. Autonomous droop scheme with reduced generation cost. *IEEE Transactions on Industrial Electronics*, 61(12):6803–6811, March 2014.

[87] G. Chen, J. Ren, and E. Feng. Distributed finite-time economic dispatch of a network of energy resources. *IEEE Transactions on Smart Grid*, 8(2):822–832, January 2016.

[88] Z. Zhang and M. Chow. Incremental Cost Consensus Algorithm in a Smart Grid Environment. In *IEEE Power and Energy Society General Meeting*, pages 1–6, August 2011.

[89] G. Chen, F. Lewis, E. Ning Feng, and Y. Song. Distributed optimal active power control of multiple generation systems. *IEEE Transactions on Industrial Electronics*, 62(11):7079 – 7090, May 2015.

[90] Z. Zhang and Mo-Yuen Chow. Convergence analysis of the incremental cost consensus algorithm under different communication network topologies in a smart grid. *IEEE Transactions on Power Systems*, 27(4):1761 – 1768, April 2012.

[91] G. Binetti, A. Davoudi, F. L. Lewis, D. Naso, and B. Turchiano. Delay effects on consensus-based distributed economic dispatch algorithm in microgrid. *IEEE Transactions on Power Systems*, 33(1):602 – 612, January 2018.

[92] Chen G. and Guo Z. Distributed secondary and optimal active power sharing control for islanded microgrids with communication delays. *IEEE Transactions on Smart Grid*, 10(2):2002–2014, May 2019.

[93] Vasquez J.C. Li C. and Guerrero J.M. Convergence analysis of distributed control for operation cost minimization of droop controlled dc microgrid based on multiagent. In *2016 IEEE Applied Power Electronics Conference and Exposition (APEC)*, March 2016.

[94] Zhongguan Wang, Wenchuan Wu, and Boming Zhang. A fully distributed power dispatch method for fast frequency recovery and minimal generation cost in autonomous microgrids. *IEEE Trans. Smart Grid*, 7(1):19–31, October 2016.

[95] M. Zaery, E. M. Ahmed, M. Orabi, and M. Youssef. Operational cost reduction based on distributed adaptive droop control technique in dc microgrids. In *IEEE Energy Conversion Congress and Exposition (ECCE)*, pages 2638–2644, 2017.

[96] J. Hu, J. Duan, H. Ma, and M. Chow. Distributed adaptive droop control for optimal

power dispatch in dc microgrid. *IEEE Transactions on Industrial Electronics*, 65(1):778 – 789, Junuary 2018.

[97] S. Moayedi and A. Davoudi. Unifying distributed dynamic optimization and control of islanded dc microgrids. *IEEE Transactions on Power Electronics*, 32(3):2329–2346, March 2016.

[98] H. Han, H. Wang, Y. Sun, J. Yang, and Z. Liu. Distributed control scheme on cost optimisation under communication delays for dc microgrids. *IET Generation, Transmission and Distribution*, 11(17):4193–4201, November 2017.

[99] Z. Wang, W. Wu, and B. Zhang. A distributed control method with minimum generation cost for dc microgrids. *IEEE Transactions on Energy Conversion*, 31(4):1462–1470, December 2016.

[100] V.H. Bui A. Hussain and H.M. Kim. Robust optimal operation of ac/dc hybrid microgrids under market price uncertainties. *IEEE Access*, 6:2654–2667, December 2017.

[101] A. Maulik and D. Debapriya. Optimal power dispatch considering load and renewable generation uncertainties in an ac-dc hybrid microgrid. *IET Generation, Transmission and distribution*, 13(7):1164–1176, April 2019.

[102] B. Zhao, H. Qiu, X. Zhang, W. Gu, and C. Wang. Robust optimal dispatch of ac/dc hybrid microgrids considering generation and load uncertainties and energy storage loss. *IEEE Transactions on Power Systems*, 33:5945 – 5957, May 2087.

[103] Tine L Vandoorn, Jan Van de Vyver, Louis Gevaert, Lieven Degroote, and Lieven Vandevelde. Congestion control algorithm in distribution feeders: integration in a distribution management system. *Energies*, 8(6):6013–6032, October 2015.

[104] Giovanni De Carne, Marco Liserre, Konstantina Christakou, and Mario Paolone. Integrated voltage control and line congestion management in active distribution networks by means of smart transformers. In *2014 IEEE 23rd International Symposium on Industrial Electronics (ISIE)*, pages 2613–2619. IEEE, 2014.

[105] Shaojun Huang, Qiuwei Wu, Zhaoxi Liu, and Arne Hejde Nielsen. Review of congestion management methods for distribution networks with high penetration of distributed energy resources. In *IEEE PES Innovative Smart Grid Technologies, Europe*, pages 1–6. IEEE, 2014.

[106] Nathan Ainsworth and Santiago Grijalva. A line weighted frequency droop controller for decentralized enforcement of transmission line power flow constraints in inverter-based networks. In *2013 IEEE Power & Energy Society General Meeting*, pages 1–5. IEEE, 2013.

[107] Changhong Zhao, Enrique Mallada, Steven Low, and Janusz Bialek. A unified framework for frequency control and congestion management. In *2016 Power Systems Computation Conference (PSCC)*, pages 1–7. IEEE, 2016.

[108] Chen G. and Zhao Z. Distributed optimal active power control in microgrid with communication delays. In *35th Chinese Control Conference*, Jule 2016.

[109] Ren J. Gang C. and Feng N. E. Distributed finite-time economic dispatch of a network of energy resources. *IEEE Transactions on Smart Grid*, 8(2):822–832, April 2017.

[110] Peng C. Chengcheng Z., Jianping H. and Jiming C. Consensus-based energy management in smart grid with transmission losses and directed communication. *IEEE Transactions on Smart Grid*, 8(5):2049–2061, May 2017.

[111] Zhongguan Wang, Wenchuan Wu, and Boming Zhang. A fully distributed power dispatch method for fast frequency recovery and minimal generation cost in autonomous microgrids. *IEEE Trans. Smart Grid*, 7(1):19–31, August 2016.

[112] Spiteri-Staines C. Micallef A., Apap M., Guerrero J., and Vasquez J. Reactive power sharing and voltage harmonic distortion compensation of droop controlled single phase islanded microgrids. *IEEE Transactions on Smart Grid*, 5(3):1149–1158, February 2014.

[113] Zhaojian Wang, Feng Liu, Steven H Low, Changhong Zhao, and Shengwei Mei. Distributed frequency control with operational constraints, part i: Per-node power balance. *IEEE Trans. Smart Grid*, 10(1):40–52, July 2019.

[114] Zhaojian Wang, Feng Liu, Steven H Low, Changhong Zhao, and Shengwei Mei. Distributed frequency control with operational constraints, part ii: Network power balance. *IEEE Trans. Smart Grid*, 10(1):53–64, July 2019.

[115] Peng Yi, Yiguang Hong, and Feng Liu. Distributed gradient algorithm for constrained optimization with application to load sharing in power systems. *Syst. Control Lett.*, 83:45–52, August 2015.

[116] Changhong Zhao, Enrique Mallada, Steven Low, and Janusz Bialek. A unified framework for frequency control and congestion management. In *2016 Power Systems Computation Conference (PSCC)*, pages 1–7. IEEE, 2016.

[117] Masoud Farivar, Russell Neal, Christopher Clarke, and Steven Low. Optimal inverter var control in distribution systems with high pv penetration. In *IEEE-PES GM*, pages 1–7, 2012.

[118] Pedro Vergara, Juan Rey, Hamid Shaker, Josep Guerrero, Bo Jørgensen, and Luiz da Silva. Distributed strategy for optimal dispatch of unbalanced three-phase islanded microgrids. *IEEE Trans. Smart Grid*, October 2018.

[119] Plexim. Plecs software for power electronics. web address: http://www.plexim.com, 2010.

[120] Mikael Johansson and Anders Rantzer. Computation of piecewise quadratic lyapunov functions for hybrid systems. *IEEE Trans. on Automatic Control*, 43(4):555 – 559, September 1998.

[121] Jorge M Gonçalves, Alexandre Megretski, and Munther A Dahleh. Global analysis of piecewise linear systems using impact maps and surface lyapunov functions. *IEEE Trans. on Automatic Control*, 48(12):2089–2106, October 2003.